

IN THIS JOURNAL

Minimum Energy
Expenditure

Strains of Lactic Acid
Bacteria

Soil Arthropods in Major
Plantation

Study of Existence in the
Philosophy



Great Britain
Journals Press



London Journal of
Research in Science: Natural & Formal

Volume 25 | Issue 14 | Compilation 1.0

journalspress.com

Print ISSN: 2631-8490
Online ISSN: 2631-8504
DOI: 10.17472/LJRS



London Journal of Research in Science: Natural and Formal

Volume 25 | Issue 14 | Compilation 1.0

PUBLISHER

Great Britain Journals Press
1210th, Waterside Dr, Opposite Arlington Building, Theale, Reading
Phone:+444 0118 965 4033 Pin: RG7-4TY United Kingdom

SUBSCRIPTION

Frequency: Quarterly

Print subscription

\$280USD for 1 year

\$500USD for 2 year

(color copies including taxes and international shipping with TSA approved)

Find more details at <https://journalspress.com/journals/subscription>

ENVIRONMENT

Great Britain Journals Press is intended about Protecting the environment. This journal is printed using led free environmental friendly ink and acid-free papers that are 100% recyclable.

Copyright ©2025 by Great Britain Journals Press

All rights reserved. No part of this publication may be reproduced, distributed, or transmitted in any form or by any means, including photocopying, recording, or other electronic or mechanical methods, without the prior written permission of the publisher, except in the case of brief quotations embodied in critical reviews and certain other noncommercial uses permitted by copyright law. For permission requests, write to the publisher, addressed “Attention: Permissions Coordinator,” at the address below. Great Britain Journals Press holds all the content copyright of this issue. Great Britain Journals Press does not hold any responsibility for any thought or content published in this journal; they belong to author's research solely. Visit <https://journalspress.com/journals/privacy-policy> to know more about our policies.

Great Britain Journals Press Headquaters

1210th, Waterside Dr,
Opposite Arlington
Building, Theale, Reading
Phone:+444 0118 965 4033
Pin: RG7-4TY
United Kingdom

Reselling this copy is prohibited.

Available for purchase at www.journalspress.com for \$50USD / £40GBP (tax and shipping included)

Featured Blog Posts

blog.journalspress.com



They were leaders in building the early foundation of modern programming and unveiled the structure of DNA. Their work inspired environmental movements and led to the discovery of new genes. They've gone to space and back, taught us about the natural world, dug up the earth and discovered the origins of our species. They broke the sound barrier and gender barriers along the way. The world of research wouldn't be the same without the pioneering efforts of famous research works made by these women. Be inspired by these explorers and early adopters - the women in research who helped to shape our society. We invite you to sit with their stories and enter new areas of understanding. This list is by no means a complete record of women to whom we are indebted for their research work, but here are of history's greatest research contributions made by...

Read complete here:
<https://goo.gl/1vQ3lS>

Women In Research



Computing in the cloud!

Cloud Computing is computing as a Service and not just as a Product. Under Cloud Computing...

Read complete here:
<https://goo.gl/VvHC72>



Writing great research...

Prepare yourself before you start. Before you start writing your paper or you start reading other...

Read complete here:
<https://goo.gl/np73jP>

Journal Content

In this Issue



Great Britain
Journals Press

- i.** Journal introduction and copyrights
- ii.** Featured blogs and online content
- iii.** Journal content
- iv.** Editorial Board Members

- 1. Advances in Cyclometalated Iridium (III) Complexes: Emerging Strategies and Applications in Anticancer Therapy. **1-61**
- 2. From Infinity (Wuji 无极) to Taiji (太极), Yin-Yang (阴阳) to Heaven-Earth (Qiankun 乾坤: A Yin-Yang (阴阳) Philosophical Exploration of Existence and Cosmic Origins. **63-82**
- 3. Concept of the "Minimum Energy Expenditure" Principle. **83-90**
- 4. Effect of Temperature, PH, and Salt on Bacteriocin Activity Produced from Different Strains of Lactic Acid Bacteria (LAB). **91-101**
- 5. Species Richness and Diversity of Soil Arthropods in Major Plantation Crops under Different Farming Practices. **103-109**

- V.** Great Britain Journals Press Membership

Editorial Board

Curated board members



Dr. Abdelkader Zarrouk

Faculty of Sciences, Dept. of Chemistry
Laboratory Applied Chemistry and Environment
Mohammed First University Ph.D.,
Mohammed First University Oujda, Morocco

Prof. Tai-Yin Huang

Associate Professor of Physics,
Pennsylvania State University,
Penn State Lehigh Valley, Ph.D.,
Physics, University Of Cincinnati,
President of the Lehigh Valley,
Taiwanese Women Association

Prof. Dr. Ahmed Asaad Ibrahim Khalil

National Institute for Laser Enhanced Sciences,
NILES Cairo University, Giza,
Egypt Ph.D., Experimental Physics V Institute
Engineering Application of Lasers
University Bochum, Germany

Dr. Mohamed Salem Badawi

Department of Physics,
Awarded Junior Radiation Physics Medal,
7th Radiation Physics and Protection
Conference, Ismailia, Egypt

Prof. Marie-Christine Record

Department of Chemistry,
Aix-Marseille University Ph.D.,
Materials Sciences, Montpellier University,
France

Prof. Hakan Arslan

Mersin University Ph.D.,
Chemistry Nigde University
Turkey

Prof. Wanyang Dai

Department of Mathematics,
Nanjing University, China
Ph.D., Applied Mathematics,
Georgia Institute of Technology, USA

Dr. Hyongki Lee

Assistant Professor,
University of Houston
Ph.D. in Geodetic Science,
Ohio State University, USA

Nicola Mastronardi

Consiglio Nazionale delle Ricerche,
Ph.D. Applied Mathematics Katholieke
Universiteit Leuven
Belgium

Dr. Indranil Sen Gupta

Ph.D., Mathematics
Texas A & M University
Department of Mathematics
North Dakota State University
North Dakota, USA

Dr. Arvind Chhabra

University of Connecticut Health Center
USA Ph.D., Biotechnology Central
Drug Research Institute

Dr. Vladimir Burtman

Research Scientist
The University of Utah
Geophysics
Frederick Albert Sutton Building
115 S 1460 E Room 383
Salt Lake City, UT 84112, US

Dr. Xianghong Qi

University of Tennessee
Oak Ridge National Laboratory
Center for Molecular Biophysics
Oak Ridge National Laboratory
Knoxville, TN 37922
United States

Dr. Arshak Poghossian

Ph.D. Solid-State Physics
Leningrad Electrotechnical Institute, Russia
Institute of Nano and Biotechnologies
Aachen University of Applied Sciences, Germany

Dr. Bingyun Li

Ph.D. Fellow, IAES
Guest Researcher, NIOSH, CDC, Morgantown, WV
Institute of Nano and Biotechnologies
West Virginia University, US

Dr. Maria Gullo

Ph.D., Food Science, and Technology
University of Catania
Department of Agricultural and Food Sciences
University of Modena and Reggio Emilia, Italy

Dr. A. Heidari

Ph.D., D.Sc
Faculty of Chemistry
California South University (CSU), United States

Dr. Alicia Esther Ares

Ph.D. in Science and Technology,
University of General San Martin, Argentina
State University of Misiones, US

Research papers and articles

Volume 25 | Issue 14 | Compilation 1.0



Scan to know paper details and
author's profile

Advances in Cyclometalated Iridium (III) Complexes: Emerging Strategies and Applications in Anticancer Therapy

Irena Kostova

Medical University

ABSTRACT

Recently, organometallic iridium(III) complexes have attracted considerable attention in the development of new metal-based antineoplastic drugs, and this area of research has been intensively explored. Their diverse mechanisms of antitumor action are distinct from those of classical metal complexes approved for clinical use, which makes them particularly worthy of detailed investigation. A typical organometallic anticancer Ir(III) complex consists of an iridium(III) center coordinated to two cyclometalated C^N ligands and one N^N ancillary ligand. Modification of the cyclometalated ligands plays a dominant role in controlling the photophysical properties, whereas alteration of the ancillary ligand allows functionalization for targeted imaging or therapeutic applications.

This review discusses and analyzes cyclometalated iridium complexes that exhibit significant anticancer activity and exceptional photophysical characteristics. Unlike platinum-based anticancer drugs, these iridium(III) complexes primarily act by damaging various intracellular organelles (such as mitochondria and lysosomes), although the reported results remain scattered and systematic structure–activity relationships are still underdeveloped.

Keywords: organometallic Ir(III) complexes, cyclometalated ligands, N^N ancillary ligands, antitumor agents, photodynamic therapy, reactive oxygen species, theranostic agents, mitochondrial targeting, ligand modification, metal-based chemotherapy.

Classification: LCC Code: QD411, RS431.C45, RC271.C5

Language: English



Great Britain
Journals Press

LJP Copyright ID: 925614

Print ISSN: 2631-8490

Online ISSN: 2631-8504

London Journal of Research in Science: Natural & Formal

Volume 25 | Issue 14 | Compilation 1.0



Advances in Cyclometalated Iridium (III) Complexes: Emerging Strategies and Applications in Anticancer Therapy

Irena Kostova

ABSTRACT

Recently, organometallic iridium(III) complexes have attracted considerable attention in the development of new metal-based antineoplastic drugs, and this area of research has been intensively explored. Their diverse mechanisms of antitumor action are distinct from those of classical metal complexes approved for clinical use, which makes them particularly worthy of detailed investigation. A typical organometallic anticancer Ir(III) complex consists of an iridium(III) center coordinated to two cyclometalated C^N ligands and one N^N ancillary ligand. Modification of the cyclometalated ligands plays a dominant role in controlling the photophysical properties, whereas alteration of the ancillary ligand allows functionalization for targeted imaging or therapeutic applications.

This review discusses and analyzes cyclometalated iridium complexes that exhibit significant anticancer activity and exceptional photophysical characteristics. Unlike platinum-based anticancer drugs, these iridium(III) complexes primarily act by damaging various intracellular organelles (such as mitochondria and lysosomes), although the reported results remain scattered and systematic structure–activity relationships are still underdeveloped.

Furthermore, organometallic Ir (III)-based complexes can overcome several limitations associated with Pt-based chemotherapeutic agents. Although they have only recently gained substantial attention, Ir(III) complexes display a range of properties that make them highly promising as prospective antineoplastic agents. Their chemical reactivity and binding behavior depend largely on their coordination geometry and the nature of the ligands employed.

The biological profiles and cellular uptake of metal-based antitumor agents are determined by the structure of the complex—specifically, the metal center, the biologically active auxiliary ligands, and their spatial arrangement. Among the various Ir(III) complexes evaluated for pharmacological activity, cyclometalated iridium complexes are particularly interesting due to their favorable photochemical and photophysical properties, including high stability under physiological conditions, luminescence across the visible to near-infrared (NIR) spectrum, and ability to participate in redox processes. Consequently, these highly luminescent organometallic complexes have been extensively investigated for various photophysical applications, especially as promising photosensitizers or phosphorescent agents in biosensing and biological imaging.

Overall, this review provides new insights into the development of cyclometalated iridium complexes and perspectives on enhancing their properties for improved therapeutic applications and synergy with existing treatment strategies.

Keywords: organometallic Ir(III) complexes, cyclometalated ligands, N^N ancillary ligands, antitumor agents, photodynamic therapy, reactive oxygen species, theranostic agents, mitochondrial targeting, ligand modification, metal-based chemotherapy.

Author: Department of Chemistry, Faculty of Pharmacy, Medical University, 2 Dunav St., Sofia 1000, Bulgaria.
email: irenakostova@yahoo.com

I. INTRODUCTION

Over the past several decades, classical metal-based antitumor agents have represented an indispensable class of chemotherapeutic drugs; however, their clinical use remains constrained by significant functional and physiological limitations. Conventional platinum- and ruthenium-based compounds, such as cisplatin, carboplatin, and NAMI-A, while therapeutically effective, suffer from several drawbacks including severe systemic toxicity, poor selectivity toward malignant cells, the emergence of multidrug resistance, insufficient cellular uptake, and limited pharmacological efficacy [1–4]. These disadvantages collectively highlight the urgent necessity of designing and developing new generations of metal-containing antineoplastic agents that could overcome the limitations inherent to traditional metallodrugs.

The induction of cell death represents a fundamental strategy in anticancer therapy, whereby the successful accumulation of a cytotoxic agent within tumor cells triggers irreversible molecular and biochemical alterations leading to cellular demise. Cell death can proceed through several mechanistically distinct pathways, not all of which are therapeutically favorable. Among the best characterized are: (i) apoptosis, or programmed cell death, which is generally regarded as the most desirable anticancer mechanism; (ii) necrosis, an uncontrolled and often inflammatory form of cell death; and (iii) autophagy, a self-degradative process essential for cellular homeostasis. Other less common, yet biologically relevant, pathways include (iv) ferroptosis, (v) oncosis, (vi) paraptosis, and (vii) pyroptosis. The ability of metal-based agents to selectively modulate these death pathways constitutes a critical determinant of their pharmacological effectiveness and therapeutic index.

In recent years, non-platinum metal complexes have emerged as a diverse and promising class of antineoplastic agents exhibiting mechanisms of action distinct from those of classical Pt(II)-based drugs. The structural diversity and redox versatility of transition metals allow for unique modes of biomolecular interaction, including DNA intercalation, protein binding, enzyme inhibition, and the generation of reactive oxygen species (ROS). Advances in coordination and medicinal chemistry have facilitated the design of various metal-based scaffolds with notable biological activity, including complexes of Ru(III) [5], Pd(II) [6], Pt(II) and Pt(IV) [7,8], Rh(III) [9], and numerous other metallodrugs under active investigation.

Among these systems, iridium-based complexes have attracted growing attention due to their remarkable structural, chemical, and photophysical properties. Iridium exhibits a wide range of accessible coordination numbers and oxidation states under physiological conditions, a rich variety of coordination geometries, and exceptional photochemical stability [10,11]. In particular, Ir(III) complexes possess highly tunable photophysical and electrochemical characteristics, including strong spin-orbit coupling, long-lived excited states, and efficient phosphorescence—all of which contribute to their potential for both therapeutic and diagnostic (theranostic) applications. Chloroiridium(III) complexes have been reviewed elsewhere [12] and are therefore beyond the scope of this discussion.

Cyclometalated iridium(III) complexes, in particular, have demonstrated distinctive intracellular localization patterns, including accumulation within the cytoplasm, nucleus, lysosomes, endosomes, mitochondria, and endoplasmic reticulum [10–13]. In contrast to conventional platinum-based drugs, which primarily target nuclear DNA, iridium complexes often preferentially accumulate in mitochondria or lysosomes, where they can actively participate in intracellular redox processes, induce oxidative stress through ROS generation, and ultimately promote apoptotic cell death [13]. This subcellular targeting confers additional advantages such as enhanced selectivity and reduced off-target toxicity.

Cyclometalated Ir(III) species also represent promising analogues to their isoelectronic ruthenium(II) counterparts, offering a broader range of tunable photophysical characteristics and higher ligand-field stabilization energies. The versatile photochemical behavior of Ir(III) complexes has led to their application across multiple therapeutic modalities, including photothermal therapy (PTT), photoactivated chemotherapy (PACT), and sonodynamic therapy (SDT). Of particular note is their utilization in photodynamic therapy (PDT)—a minimally invasive therapeutic strategy that leverages light-activated photosensitizers to generate cytotoxic singlet oxygen and other reactive species [13,14]. These unique photoresponsive properties render iridium(III) complexes valuable platforms for the development of multifunctional agents capable of simultaneous imaging and targeted therapy.

Structurally, cyclometalated compounds are organometallic complexes containing metallacycles characterized by a D–M–C σ -bond framework, where D denotes a donor atom (typically from group VA or VIA elements), M represents the metal center, and C is a carbon atom in either sp^2 or sp^3 hybridization. A prototypical organometallic Ir(III) complex can be represented by the general formula $[Ir(C^N_2(N^N)]^+$, where C^N denotes a bidentate cyclometalating ligand and N^N represents an ancillary diimine ligand. Typical examples include 2-phenylpyridinate (ppy) as the C^N ligand and 2,2'-bipyridine (bpy) as the N^N ligand. Although most complexes are monocationic and stabilized by counterions such as Cl^- or PF_6^- , variations incorporating monodentate ligands are also well documented.

Over the past decade, a substantial number of polypyridyl Ir(III) complexes have been synthesised and systematically investigated, revealing pronounced biological activity, particularly in the context of anticancer activity [15–17]. The inherent modularity of these complexes—stemming from their chemically modifiable ligand frameworks—enables fine-tuning of key physicochemical parameters, including lipophilicity, solubility, redox potential, and photochemical responsiveness. This molecular flexibility facilitates the rational optimization of pharmacological and optical properties, establishing cyclometalated Ir(III) complexes as one of the most promising classes of next-generation metallodrugs for targeted and multifunctional cancer therapy.

Investigating the ligands (monodentate or bidentate) and the leaving groups can effectively modulate the activity of the resulting complexes. Currently, the activity regulations are primarily focusing on the study of different bidentate ligands, including N^N ligands (bipyridine, phenanthroline, etc.), N^C ligands (phenylpyridine, β -carboline, etc.), in some cases N^O ligands (hydrazone derivatives, picolinic acid, amino acids), N^S (thiocarbazones), O^O (β -diketonato derivatives), which have been proven to display improved activity. Among all these ligands, the most studied for the ascertainment of their anticancer mode of action were N^N and N^C ligands, presented in detail in the current review. The design of the C^N ligands is critical to regulate the extension of emission wavelengths of Ir(III) complexes. While the alteration of the ancillary N^N ligand largely determines the strength and functionalization with biological targets for imaging or therapy purposes [18–20]. Given the versatility of the ligands employed, it is unsurprising that numerous iridium(III) complexes have been extensively investigated for a variety of applications [21–23].

The current broad overview, based on recently published reports, focuses on the anticancer activity of this interesting class of organometallic compounds, which offers advantages in the development of new metallodrugs. The reported work, which presents results from cytotoxicity screenings against various cancer cell lines as well as studies on cellular internalization mechanisms, will be reviewed and discussed.

II. CYCLOMETALATED Ir(III) COMPLEXES WITH 2-PHENYL PYRIDINE (PPY) AS A C^N LIGAND

2-Phenylpyridine (ppy) is the prototypical and most widely used cyclometalating ligand. The cyclometalated iridium complexes with 2-phenylpyridine as a C^N ligand have been widely investigated for their potential application as anticancer therapeutic agents. They have exhibited notable antiproliferative activity against various cancer cell lines [24] and demonstrated good selectivity, making them promising candidates for inhibiting the invasion of malignant cells into surrounding tissues. Cyclometalated Ir(III) complexes bearing 2-phenylpyridine derivatives can efficiently sensitize ground-state oxygen ³O₂ to generate cytotoxic singlet oxygen ¹O₂, thus serving as highly promising photosensitizers. Moreover, numerous cyclometalated iridium(III) complexes have exhibited desirable two-photon absorption (TPA) features [25]. The general formula of the complexes can be expressed as [Ir(ppy)₂(biPy)]PF₆, where ppy is 2-phenylpyridine or its derivatives, and with easy adjustment of ligands, the luminescence and pharmacological properties of these complexes can also be readily modified [26]. 2-Phenylpyridine is a C^N chelating ligand and bipyridine or its derivatives (biPy) is a N^N chelating ligand. The combination of potential antineoplastic activity and luminescent properties of cyclometalated Ir(III) complexes makes them promising candidates for the development of novel theranostic systems. These complexes exhibit unique biologically favorable photophysical characteristics, including high quantum yields, excellent resistance to photobleaching and cell bleaching, which render them effective bioimaging agents [27]. Their large ligand-field splitting energy and strong spin-orbit coupling arise from the pronounced σ -donating nature of the cyclometalating ligands, the high positive charge of the Ir(III) center, and the extensive spatial distribution of the 5d orbitals. In addition, they possess long luminescence lifetimes, large Stokes shifts [28], tunable energy levels [29], as well as good cell permeability and photostability [30]. Cyclometalated iridium complexes are primarily investigated as potential anticancer agents [31]. In addition, phosphorescent cyclometalated Ir(III) complexes serve as excellent biosensing probes due to their high photostability and resistance to photobleaching. These properties enable them to selectively target various subcellular organelles and inhibit specific protein activities [32].

2.1. Tris-Cyclometalated Iridium Complexes with 2-Phenylpyridine

The tris-cyclometalated iridium complexes holding three cyclometalating C^N ligands are neutral. These complexes have been used far less extensively in cellular imaging compared to iridium(III) bis-cyclometalated complexes. Meksawangwong *et al.* reported a photoactive tris-cyclometalated Ir(III) complex bearing a quaternary ammonium moiety and investigated its photophysical properties as a potential probe for cellular imaging, Fig. 1, [28]. The complex has possessed outstanding features, enabling it to be used as a cellular stain in fluorescence microscopy. Cytotoxicity was assessed using mouse skin fibroblasts (NIH-3T3) and human prostate adenocarcinoma (PC3) cell lines by fluorescence and laser scanning confocal microscopy. Studies have demonstrated that the complex was less toxic than its precursor amine complex and had lysosomal localisation [28].

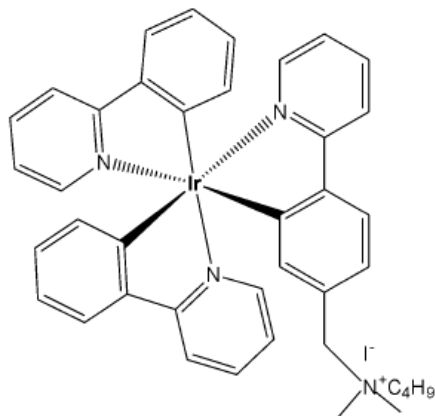


Fig. (1): Structure of $[\text{Ir}(\text{ppy})_2(\text{ppy}-\text{Me}_2\text{N}^+\text{C}_4\text{H}_9)\text{I}^-]$.

Similarly, a series of iridium(III) mono-, bis, and tris-amino acid complexes, Fig. 2, exhibited varying degrees of cellular uptake [33]. The authors have synthesised a series of nine neutral luminescent cyclometalated octahedral iridium(III) tris(2-phenylpyridine) complexes, functionalized with three different amino acids (glycine, alanine, and lysine), on one, two, or all three of the 2-phenylpyridine ligands. It has been revealed that the monosubstituted complexes in this series exhibit significantly higher cellular uptake compared to the bis- and tris-substituted compounds, with the lysine complexes showing greater uptake than their glycine and alanine analogues [33]. All compounds were comprehensively characterized using one- and two-dimensional NMR spectroscopy, and photophysical data were collected for the mono-, bis-, and tris-substituted Ir(III) complexes. Cellular uptake and localisation have been studied with flow cytometry and confocal microscopy, respectively. Confocal experiments have demonstrated that all nine substituted Ir(III) complexes showed variable uptake in the cancer cells. Among the tested compounds, the monosubstituted complexes demonstrated the highest levels of cellular uptake, whereas the lysine derivatives displayed the highest cytotoxicity. This systematic study of amino acid-functionalized $\text{Ir}(\text{ppy})_3$ complexes provides guidelines for further functionalization and possible implementation of luminescent iridium complexes, for example, in (automated) peptide synthesis or biomarker specific targeting [33].

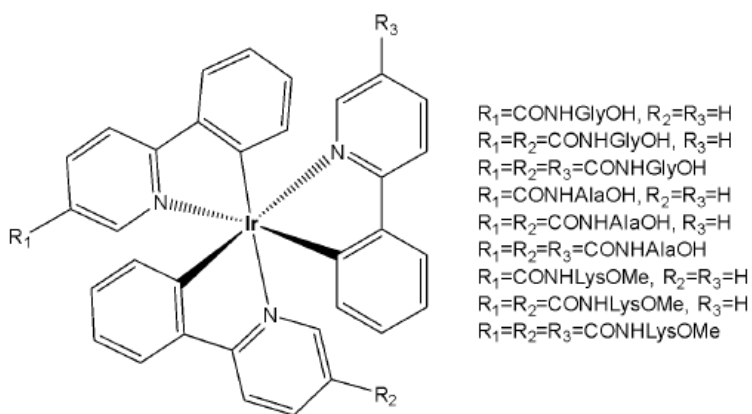


Fig. (2): Ir(III) tris(2-phenylpyridine) complexes, functionalized with amino acids.

Berkers *et al.* established methods using fluorescent reporters to profile proteasome activity across different mouse tissues while carefully avoiding post-lysis artefacts, demonstrating that proteasome subunit activity is regulated in an organ-specific manner [34]. The techniques described could be used to study the pharmacological properties of proteasome inhibitors *in vivo*. The monosubstituted complexes exhibited a remarkable 20-fold increase in cellular uptake in 4T1 cells (at 10 μM

concentration for one h incubation), which was attributed to the higher lipophilicity of the probes. This result has been supported by the theoretical lipophilicity (ClogP), which showed a distribution coefficient between 2.05 and 3.18, in comparison to the negative values of ClogP for the di- and trisubstituted complexes. Flow cytometry analysis revealed a significant reduction in cell viability following treatment with the lysine derivatives, indicating increased toxicity. The cellular distribution of the studied complexes varied depending on the number of residues, showing nuclear localisation for mono-compounds, endosomal localisation for bis-compounds, and lysosomal localisation for tris-compounds [33].

Moromizato *et al.* developed a neutral iridium(III) probe, Fig. 3, that functions as both a luminescent pH sensor and a pH-dependent photosensitizer in live cells [35]. In this study, the design and synthesis of a new pH-sensitive cyclometalated Ir(III) complex *fac*-Ir(deatpy)₃, containing 2-(5'-N,N-diethylamino-4'-tolyl)pyridine (deatpy) ligand with three amino groups at the 5'-positions, Fig. 3a, have been reported. The complex has exhibited a considerable change in emission intensity between neutral and slightly acidic pH (pH 6.5–7.4). Luminescence microscopic studies using HeLa-S3 cells have indicated that the complex could be used to selectively stain lysosomes. Moreover, this complex was capable of generating singlet oxygen in a pH-dependent manner, inducing the death of HeLa-S3 cells upon photoirradiation at 377 or 470 nm. As predicted, the complex localised within the lysosomes of HeLa-S3 cells through a passive transport mechanism. Additionally, photoirradiation of the complex induced necrosis-like death in HeLa-S3 cells, demonstrating the ability of the probe to generate ¹O₂ in a pH-dependent manner.

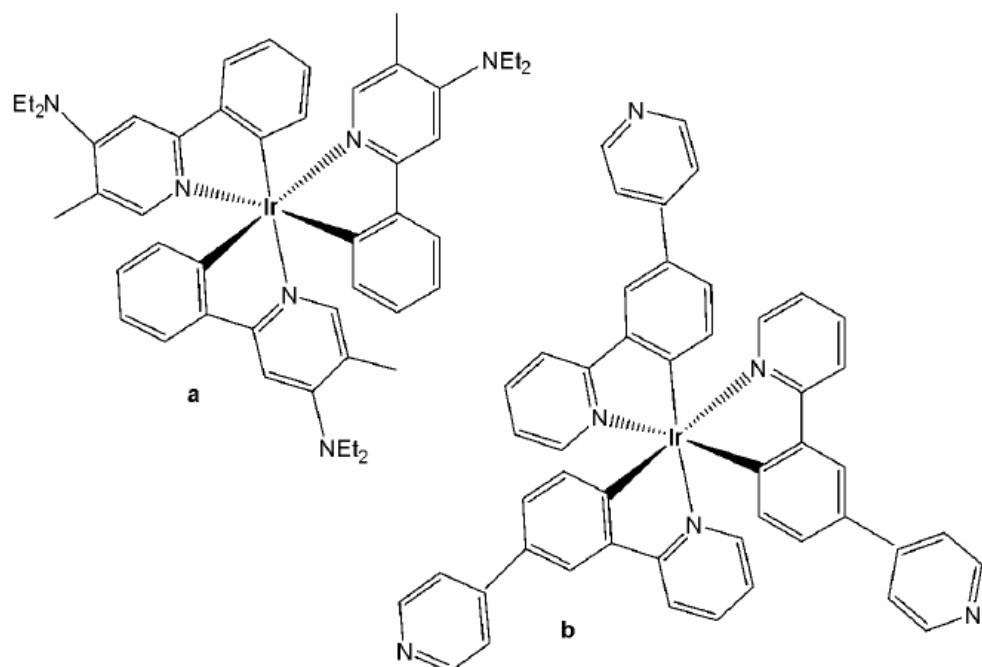


Fig. (3): Ir(III) complexes *fac*-Ir(deatpy)₃ and *fac*-Ir(4pyppy)₃.

Following their previous publication on pH-responsive probes [35], Aoki and co-workers synthesised another neutral iridium(III) analogue, *fac*-Ir(4pyppy)₃, which contains three pyridyl groups at the 4'-position of the phenylpyridine ligands, (Fig. 3b), [36]. The introduction of three pyridyl groups resulted in strong emission (at 500 nm) in dimethylsulfoxide (DMSO). The reversible pH-dependent emission profile of the complex, resulting from the protonation and deprotonation of the pyridine rings, has also been discussed. The generation of singlet oxygen (¹O₂) by the photoirradiation of the Ir(III) complex was evidenced by the decomposition of 1,3-diphenylisobenzofuran (DPBF), the

oxidation of thioanisole, and the oxidation of 2,2,5,5-tetramethyl-3-pyrroline-3-carboxamide (TPC). The induction of necrosis-like cell death of HeLa-S3 cells upon photoirradiation was also reported. Upon incubation in HeLa-S3 cells, the complex (Fig. 3b) has exhibited accumulation within mitochondria, potentially through a passive transport mechanism. Additionally, after photoirradiation at 465 nm for 10 min, the complex in Fig. 3b has generated much more ${}^1\text{O}_2$ in comparison to the Ir(III) complex $\text{fac-}\text{Ir}(\text{deatpy})_3$ [35], thus inducing necrosis-like cell death.

Qiu *et al.* designed a neutral iridium(III) probe (Fig. 4) for long-term lysosome tracking [37]. The water-soluble tris-cyclometalated iridium(III) complex has been functionalized by morpholine moieties, which could be protonated inside the lysosomes and work as a “locker”, allowing the accumulation of the complex, Fig. 4, in these acidic organelles. Additionally, the electron-rich morpholine moiety quenched the iridium(III) phosphorescence via photoinduced electron transfer (PET) under basic conditions. Upon protonation, this process was inhibited, resulting in enhanced emission intensity in acidic lysosomes. The uptake of the complex shown in Fig. 4 occurred via an energy-dependent pathway, and the probe exhibited no toxicity toward HeLa cell lines (at a concentration of 10 μM after 48 h of incubation). Furthermore, the complex in Fig. 4 successfully tracked lysosomes for up to 4 days, enabling imaging and monitoring of various physiological activities of lysosomes during cell migration and apoptosis. The ability to achieve long-term lysosomal tracking is crucial for elucidating lysosomal functions and for evaluating drug and gene delivery systems.

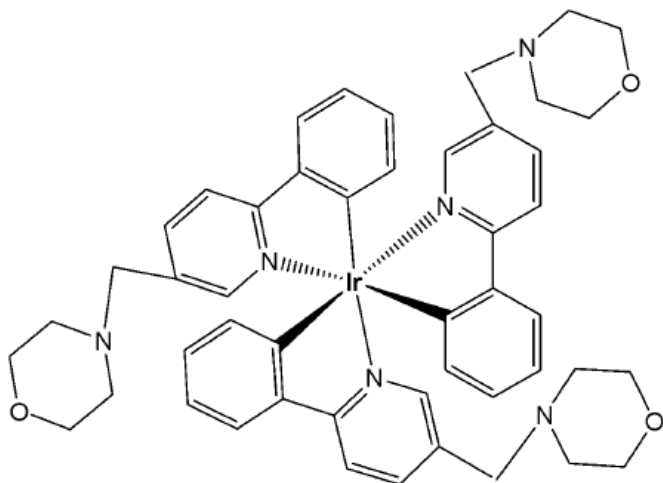


Fig. (4): Tris-cyclometalated iridium(III) complex, functionalized by morpholine moieties.

2.2. Biscyclometalated Iridium(III) Complexes with 2-Phenylpyridine

Biscyclometalated complexes of the type $[\text{Ir}(\text{C}^{\text{N}})^2(\text{N}^{\text{N}})]^+$ present a wide variety of cellular targets depending on the ancillary ligands. Indeed, mitochondria [38-41], lysosomes [42-44], endoplasmic reticulum [45,46], endosomes or nucleus [47,48] have all been recognized as common target organelles for a range of Ir(III) biscyclometalated derivatives.

2.2.1. Biscyclometalated Iridium(III) Complexes of 2-Phenylpyridine with Two Monodentate Ligands

N-monodentate ligands have not been extensively explored in biscyclometalated iridium(III) complexes and limited examples have been reported. The -NH moiety on the ancillary ligands can modulate the overall charge of the complex through acid–base equilibrium, thereby influencing its photophysical properties, cellular uptake, and localisation.

Wu *et al.* have reported three cyclometalated Ir(III) complexes containing monodentate five-membered heterocyclic ligands, shown in Fig. 5(a-c) [49]. These complexes displayed intense absorption bands at approximately 250–300 nm attributed to $\pi-\pi^*$ transitions and relatively weaker bands at 350–450 nm assigned to metal-to-ligand charge transfer absorption. These iridium(III) complexes have been found to generate $^1\text{O}_2$ efficiently. Cytotoxicity studies were conducted using lung cancer using lung cancer (A549, A549R), prostate cancer (PC3), hepatocellular carcinoma (HepG2), and normal liver (LO2) cell lines to evaluate the effects of the compounds. In the dark, the IC_{50} values of these complexes ranged from 8.91 to 38.9 μM ; however, upon light irradiation, the IC_{50} values decreased to below 0.94 μM . Additionally, these complexes have exhibited selectivity towards human cancer cells over non-cancerous cells. The complex, shown in Fig. 5(b), has demonstrated five times lower cytotoxicity against LO2 cells. The complexes in Fig. 5(a–c) not only formed covalent bonds upon light irradiation but were also efficiently internalized by tumor cells, where they were further retained within the cytoplasm. They can be activated by light via dual modes to induce tumor cell death [49]. Upon visible light (425 nm) irradiation, the five-membered heterocyclic ligands would dissociate from the metal centre. Moreover, the complexes in Fig. 5(a–c) could also act as effective singlet oxygen photosensitizers. Thus, the complexes shown in Fig. 5(a–c) may exert their light-mediated anticancer effects through dual mechanisms: ligand exchange reactions and the generation of singlet oxygen ($^1\text{O}_2$) under visible light irradiation. Notably, the complex in Fig. 5(a) has displayed a high phototoxicity index of 61.7 against human cancer cells. Additional studies have demonstrated that the light-mediated antineoplastic effects exerted by the complexes shown in Fig. 5(a–c) occur through the generation of reactive oxygen species (ROS), activation of caspases, and subsequent induction of apoptosis. This study has demonstrated that these complexes can act as novel dual-mode light-mediated antitumor agents.

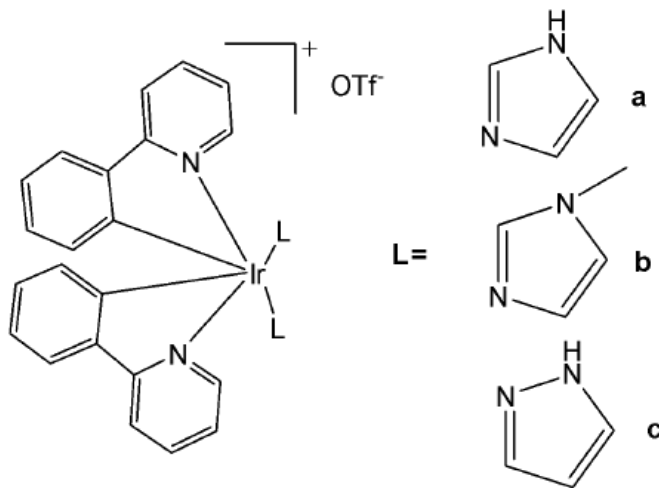


Fig. (5): Cyclometalated Ir(III) complexes with monodentate five-membered heterocyclic ligands.

2.2.2. Biscyclometalated Iridium(III) Complexes of 2-Phenylpyridine with One Bidentate N⁺N Ligand

Liu *et al.* synthesised and characterized four triphenylamine (TPA)-appended cyclometalated iridium complexes of the type $[\text{Ir}(\text{ppy})_2(\text{N}^+\text{N})]\text{PF}_6$, featuring TPA-functionalized bipyridine chelating ligands (N^+N) and phenylpyridine (ppy) ligands, Fig. 6(a-d), [26]. The introduction of TPA units helped to adjust the lipid solubility of complexes and also improved their anticancer and bactericidal activity. The complexes presented in Fig. 6(a, b, d) demonstrated comparable antineoplastic activity. All the complexes have exhibited improved antitumor properties compared to cisplatin against A549 cells. The complex shown in Fig. 6(a) ($\text{IC}_{50} = 4.34 \mu\text{M}$) was nearly five times more potent than cisplatin,

while the complex in Fig. 6(d) exhibited some selectivity toward cancer cells over normal cells. Meanwhile, complexes could effectively prevent the metastasis of cancer cells. These complexes could be transported via serum proteins, followed by a binding mechanism consistent with static quenching. They were observed to disturb the cell cycle at the G₀/G₁ phase and induce apoptosis. The complexes exhibited largely similar photophysical properties, displaying a strong interligand absorption band ($\pi-\pi^*$) at 280 nm and a relatively weaker metal-to-ligand charge transfer (MLCT) transition band in the 350–500 nm range. Cellular uptake occurred via a non-energy-dependent pathway, with effective accumulation in lysosomes. This induced lysosomal damage, which affected mitochondrial membrane potential, ultimately triggering apoptosis and leading to cell death [26]. The study has demonstrated that these complexes could be regarded as potential antitumor agents with dual functions, including metastasis inhibition and lysosomal damage.

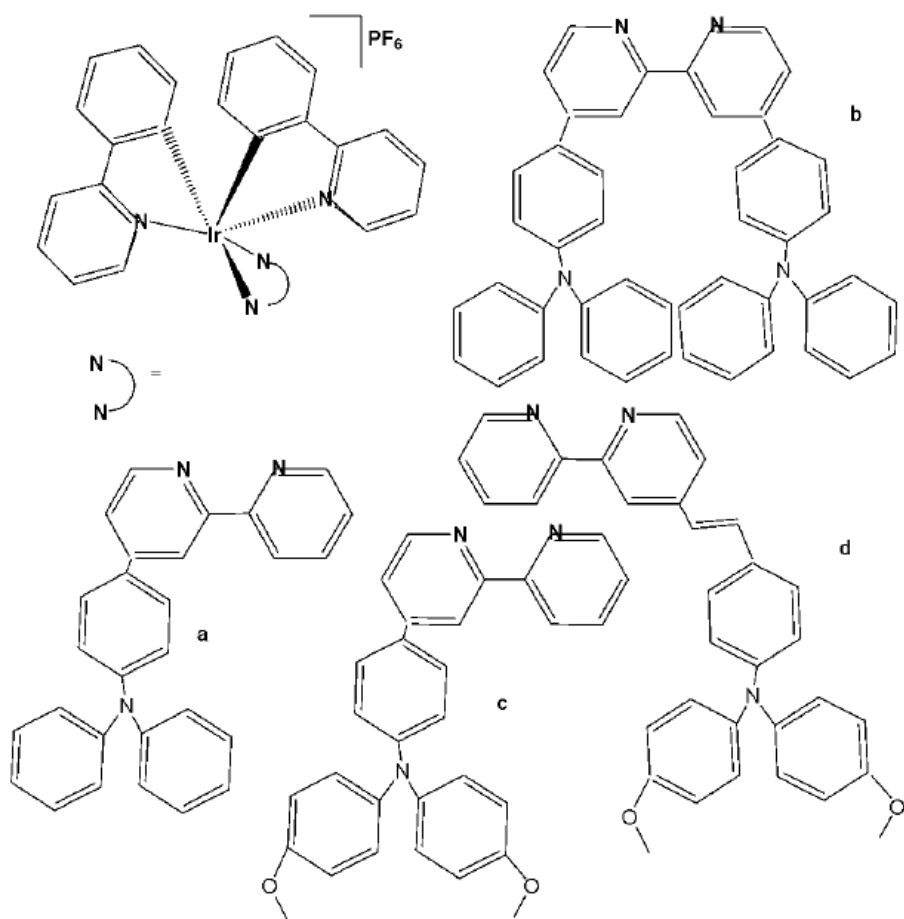


Fig. (6): Iridium(III) complexes with general formula $\text{Ir}(\text{ppy})_2(\text{N}^{\wedge}\text{N})\text{PF}_6$.

Wu *et al.* have synthesised and reported four phosphorescent Ir(III) complexes, Fig. 7(a-d), with the general formula $[\text{Ir}(\text{N}^{\wedge}\text{C})_2(\text{N}^{\wedge}\text{N})](\text{PF}_6)$, where $\text{N}^{\wedge}\text{N} = (2,2'\text{-bipyridine})\text{-}4,4'\text{-diyl}(\text{dimethanol})$, $4,4'\text{-bis}(\text{chloro-methyl})\text{-}2,2'\text{-bipyridine}$; $\text{N}^{\wedge}\text{C} = 2\text{-phenylpyridine}$ or $2\text{-(2,4-difluorophenyl)pyridine}$, examined for anticancer activity by MTT assay [50]. The complexes shown in Fig. 7(b) and Fig. 7(d) exhibited high cytotoxicity against cisplatin-resistant A549, MDA-MB-231, human prostate carcinoma PC3, and HeLa cells. Notably, the complex in Fig. 7(b) demonstrated strong selectivity for cancer cells, effectively reduced intracellular ATP levels, and exerted anticancer effects by repressing metabolism and activating multiple cell death signalling pathways. All the complexes tended to accumulate in the mitochondria, likely due to their lipophilic nature. Owing to the substitution of two reactive chloromethyl units on the $\text{N}^{\wedge}\text{N}$ chelate, complexes in Fig. 7(b) and Fig. 7(d) behaved significantly differently from the other two after subcellular uptake. Complexes in Fig. 7(b) and Fig. 7(d) have

shown much highest cytotoxic activity compared to those in Fig. 7(a) and Fig. 7(c) and these complexes induced cell death by nuclear fragmentation [50]. They were fixed within the mitochondria following nucleophilic substitution with the thiol moieties located in various mitochondrial proteins. The highest cytotoxicity was observed with the most active complexes, which induced caspase-dependent apoptosis. Moreover, mitochondrial damage, ROS elevation and cell cycle arrest for the most potent complexes have been investigated in detail.

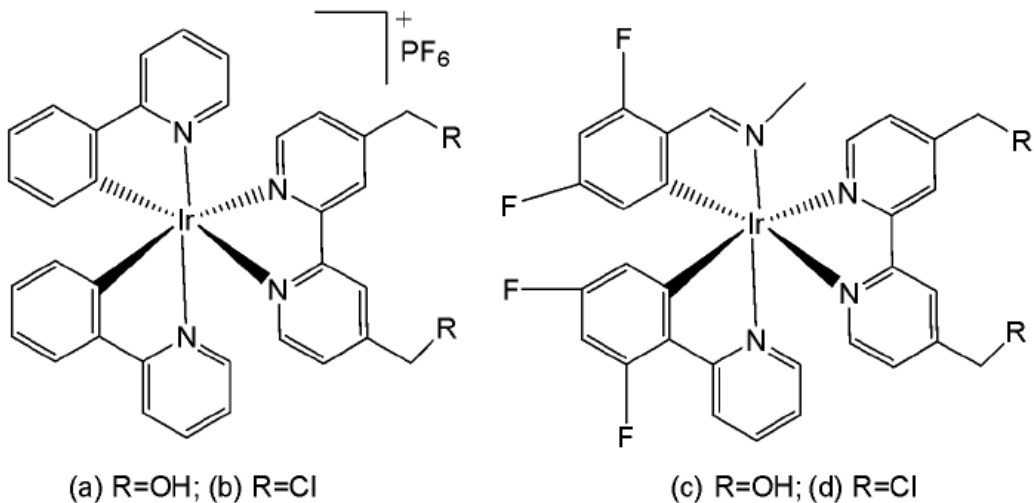


Fig. (7): Structures of Ir(III) complex with the general formula $[\text{Ir}(\text{N}^{\wedge}\text{C})_2(\text{N}^{\wedge}\text{N})](\text{PF}_6)$.

Zhang *et al.* reported the synthesis and anticancer evaluation of a series of iridium(III)-polypyridyl complexes with the formulas $\text{Ir}(\text{ppy})_2(\text{BHIP})$ ($\text{BHIP} = 2\text{-}(3\text{-bromo-4-hydroxy) phenylimidazo}[4.5\text{-f}][1,10]\text{ phenanthroline}$; Fig. 8a) and $\text{Ir}(\text{ppy})_2(\text{HPIP})$ ($\text{ppy} = 2\text{-phenylpyridine; HPIP} = 2\text{-}(4\text{-hydroxy) phenylimidazo}[4,5\text{f}][1,10]\text{phenanthroline}$; Fig. 8b), along with their corresponding liposomal derivatives, Fig. 8(a)-Lipo and Fig. 8(b)-Lipo [51]. The complexes were fully characterized by elemental analysis, IR, ESI-MS, ^1H NMR, and ^{13}C NMR spectroscopy, and their *in vitro* and *in vivo* anticancer activities were systematically evaluated.

The complexes shown in Fig. 8(a) and Fig. 8(b) were tested against several cancer cell lines (MCF-7, HeLa, B16, and SGC-7901) and normal cells using MTT assays. Both complexes exhibited IC_{50} values above 200 μ M against HeLa, A549, B16, MCF-7, SGC-7901, BEL-7402, and LO2 cells, indicating negligible cytotoxic activity. However, their liposomal formulations—prepared via the reverse-phase evaporation method—showed a significant enhancement in cytotoxicity. The IC_{50} values of Fig. 8(a)-Lipo and Fig. 8(b)-Lipo against HeLa and B16 cells demonstrated markedly higher anticancer potency compared with the free complexes. Further mechanistic studies revealed that the liposome-encapsulated complexes induced apoptosis through reactive oxygen species (ROS)-mediated lysosomal–mitochondrial dysfunction and caused cell-cycle arrest at the S phase. DNA fragmentation analyses provided additional evidence of apoptosis [51]. The *in vivo* antitumor efficacy of the complexes in Fig. 8(b) and Fig. 8(b)-Lipo was also evaluated in B16 tumor-bearing mice, focusing on apoptosis induction, ROS generation, mitochondrial membrane potential changes, intracellular Ca^{2+} levels, and cytochrome *c* release.

The observed enhancement in cytotoxic activity upon liposomal encapsulation is a notable finding, although the precise mechanism of improvement has not been fully elucidated. It is likely attributed to enhanced cellular uptake, protection from degradation, and improved bioavailability conferred by liposomal delivery. Overall, the study demonstrated that liposome-encapsulated complexes induced apoptosis in B16 cells via two primary pathways: (1) DNA damage leading to microtubule

polymerization inhibition, cell-cycle arrest at the S phase, and apoptosis; and (2) ROS overproduction resulting in lysosomal–mitochondrial dysfunction, cytochrome *c* release, caspase-3 activation, PARP cleavage, and ultimately apoptosis. The observed ROS levels were within physiologically relevant ranges and comparable to those induced by standard chemotherapeutic agents.

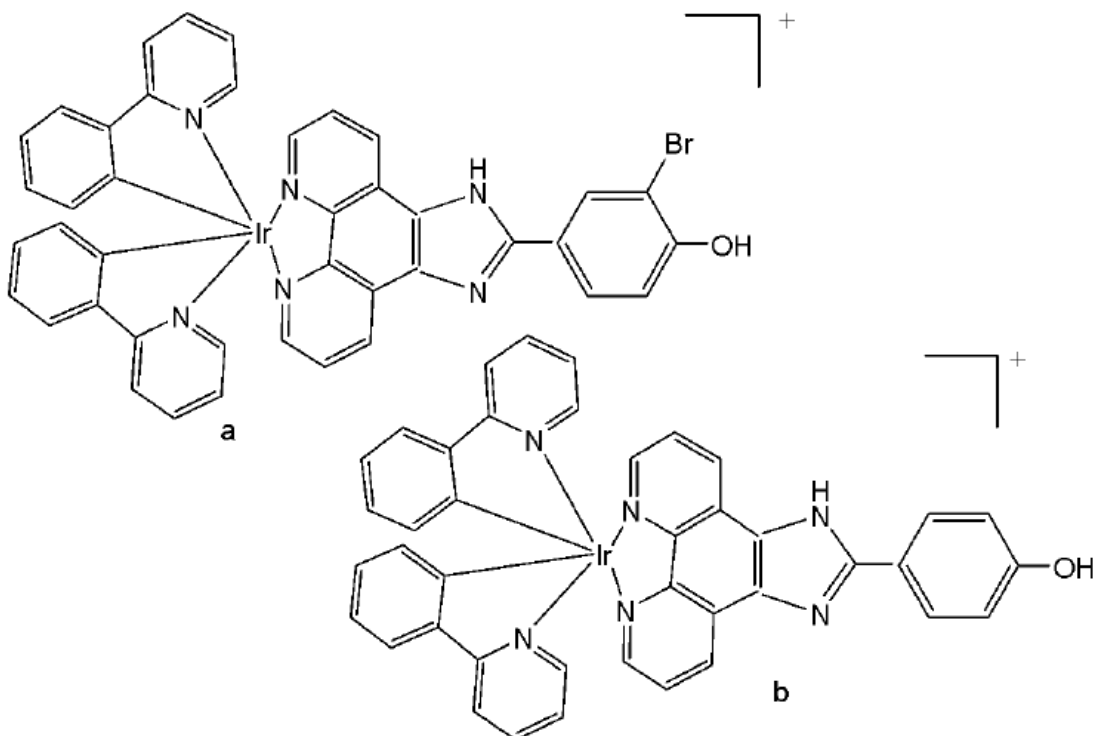


Fig. (8): Structures of iridium-polyppyridyl complexes.

Venkatesh *et al.* reported the preparation of two highly luminescent octahedral cationic Ir(III) complexes (Fig. 9a and Fig. 9b) featuring one or two 4-hydroxy- or amino-2,2,6,6-tetramethylpiperidine-N-oxyl (TEMPO) motif, and their anticancer potency investigation [52]. The antiproliferative activity of the ligands (TEMPO) and their Ir(III) complexes was mainly due to the induction of apoptosis through activation of multiple caspases, and their activity has been demonstrated in various cancer and non-cancer cell lines. Correspondingly, the *in vitro* cytotoxic activities of novel mono- and bis-TEMPO-substituted cyclometalated iridium(III) complexes, along with cisplatin, were evaluated against human prostate cancer cells (A2780, A278ocisR, A549, and PC3) and the human lung fibroblast MRC5 cell line. The results indicated that the presence of the TEMPO radical unit significantly enhanced antiproliferative activity. Notably, the complex shown in Fig. 9b demonstrated a fivefold higher cytotoxicity than cisplatin against A278ocisR cells and an eightfold greater cytotoxicity than cisplatin against PC3 cells. Both the complexes (Fig. 9a and Fig. 9b) were relatively inactive in inhibiting the growth of non-cancerous MRC5 cells, as compared to the tested cancer cell lines. The treatment of both the complexes (Fig. 9a and Fig. 9b) did not display an elevated ROS level in A2780 cells, possibly due to the presence of antioxidant TEMPO unit(s). The luminescence of the complexes allowed studying their subcellular localisation by confocal microscopy. When the complexes (Fig. 9a and Fig. 9b) were expected to preferentially localise in mitochondria, their effects on the mitochondrial membrane potential of drug-treated PC3 cells were examined using flow cytometry with the mitochondria-specific dye JC-10. The color change of JC-10 staining induced by the complexes (Fig. 9a and Fig. 9b) indicated mitochondrial membrane depolarization and a loss of membrane potential in the treated cancer cells. Moreover, these complexes were not cross-resistant with cisplatin in ovarian cancer cells, and the complex (Fig. 9b) was 7 times more active than CDDP

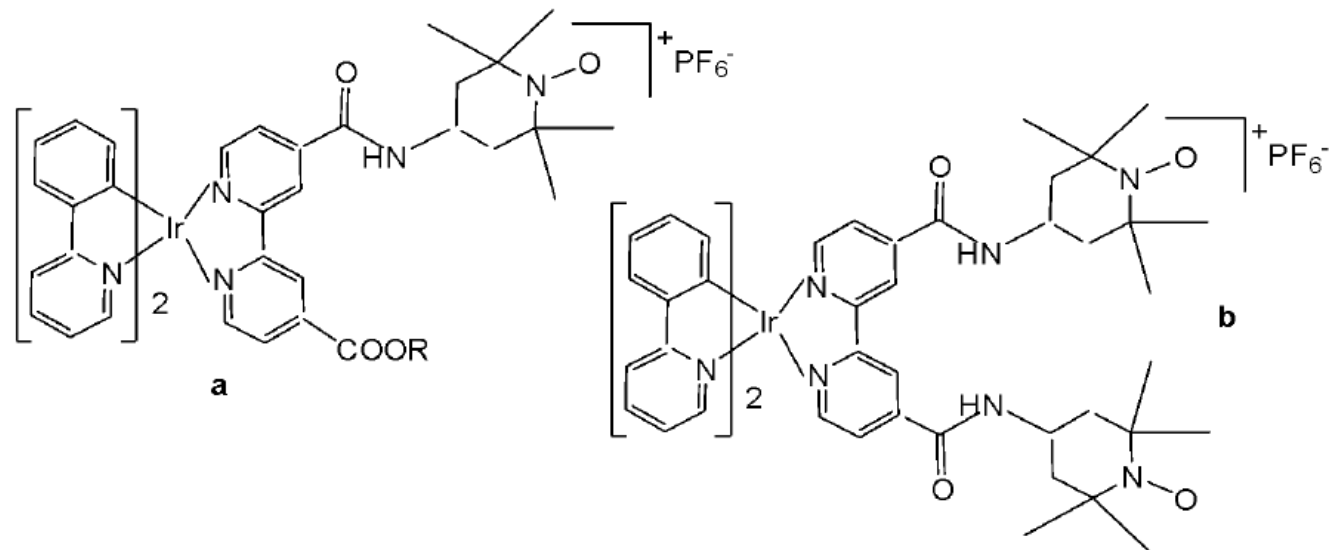


Fig. (9): Ir(III) complexes featuring one or two 4-hydroxy- or amino-2,2,6,6-tetramethylpiperidine-N-oxyl (TEMPO) motif(s).

The use of luminescent Ir(III) compounds in the area of cancer diagnosis and treatment has been recently reported, including modulators in protein–protein interactions, membrane-disruptors or mitochondria-targeted agents [53]. Iridium(III) anticancer agents have acted via targeting non-nucleic acid biomolecules, thereby perturbing cell function, which could be visualised owing to the intrinsic luminescence of the compounds, many of them being located in mitochondria. Photodynamic therapy (PDT) employs photosensitizers (PS) that become cytotoxic only upon light irradiation. Transition-metal complexes are highly promising PS due to long excited-state lifetimes and high photo-stabilities. However, these complexes usually absorb higher-energy UV/Vis light, whereas the optimal tissue transparency is in the lower-energy NIR region. One limitation to the clinical use of metal complexes investigated for PDT has been their absorption of light in the UV/Vis region, as the optimal tissue penetration window is 700–900 nm. Lipophilic cationic Ir(III) species have been reported to have a high affinity to mitochondria, and cyclometalated Ir(III) compounds have been demonstrated to be excellent PDT agents [53], causing dual-mode (oxygen-independent and oxygen-dependent) photodynamic damage in mitochondria and killing cancer cells effectively even under hypoxic conditions.

Iridium(III) organometal compounds absorb high-energy UV/vis light, while the optimal tissue transparency is located in the low-energy NIR spectrum region. Most of the metal complexes applied for PDT utilise UV/Vis light with limited penetration depth. McKenzie *et al.* have reported two photo-stable Ir(III) complexes (Fig. 10) with long-lived triplet excited states as photosensitizers that could be excited under both one- and two-photon light in a number of cancerous cell lines [54]. The new low-molecular-weight, long-lived, and cell-permeable iridium complexes of the $[\text{Ir}(\text{N}^{\text{C}})^2(\text{N}^{\text{N}})]^+$ family, which exhibit strong two-photon absorption, were shown to localize to mitochondria and lysosomal structures in live cells. The compounds feature bisbenzimidazole and

its N, N-dimethylated derivative, respectively, as the N⁺N ligand. The studied Ir(III) biscyclometalated octahedral complexes based on the N-functionalized 2,2'-bibenzo[d]imidazole (Fig. 10) were efficient photosensitizers under 1-photon irradiation (405 nm) with photo-indices greater than 555 [54]. The obtained complexes have been studied against HeLa cells. The non-substituted derivative (R = H) has shown lower cytotoxic activity in the dark, whereas the substituted one (R = Me) has exhibited better cytotoxicity in the dark with a low LD₅₀ value. The reason for the superior cytotoxicity of this compound was the presence of N-CH₃ groups, which greatly affected the interaction with cells, reducing the number of H-bonds. The non-substituted derivative has displayed a photosensitizing effect against A-375, HCT-116, and U2-OS tumour cells, indicating its potential as a photodynamic therapy (PDT) agent. Both the complexes in Fig. 10 were cell-permeable, and the substituted one (R = Me) showed higher dark cytotoxicity, while the non-substituted derivative (R = H) possessed more potent PDT activity. Targeting different subcellular organelles can achieve different antitumour effects and mechanisms. The non-substituted derivative (R = H) sequentially localises in mitochondria and lysosomes over the course of incubation and can disrupt the functions of both organelles, inducing apoptosis upon light irradiation. Additionally, this complex maintained high PDT activity under NIR TPE (760 nm) at low concentrations and light doses [54].

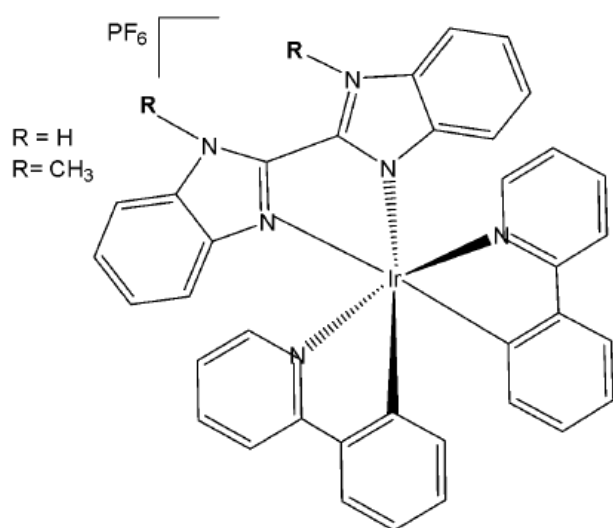


Fig. (10): Ir(III) complexes derived from the N-functionalized 2,2'-bibenzo[d]imidazole.

Murphy *et al.* have published the cyclometalated iridium(III) complex Ir(ppy)₂(pybz) (pybzH = 2-pyridyl-benzimidazole), carrying a 2-pyridylbenzimidazole ligand, and its protonated analogue, Fig. 11, [55]. Photophysical data in dichloromethane solution have shown a structured emission profile in the green region of the spectrum for the non-protonated complex, and an expected red shift for the protonated complex with emission centred around 590 nm. Nevertheless, the emission profiles from CHO cells incubated with the probes at a concentration of 10 μ M for 5 min were essentially identical. In fact, the protonation equilibrium between the two complexes depended on the local pH, with the non-protonated complex predominating in cellular environments maintained at approximately pH 7.4. A shift was observed in acidic lysosomes, as the protonation equilibrium formed the cationic protonated complex. The MTT assay has demonstrated low cytotoxicity of these complexes, with IC₅₀ values >200 μ M for 24 h incubation for both the complexes [55].

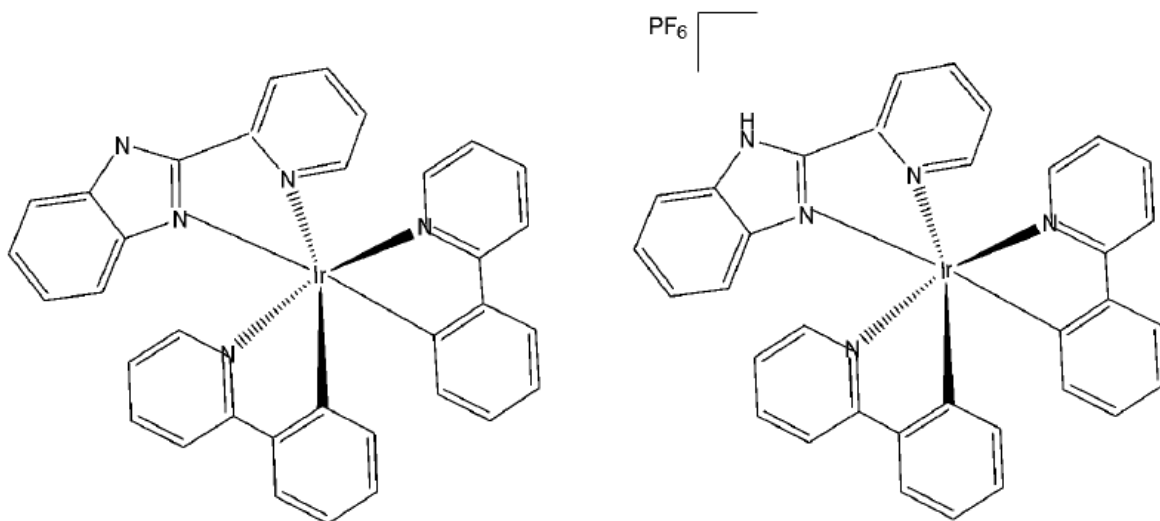


Fig. (11): Iridium(III) non-protonated and protonated complexes $\text{Ir}(\text{ppy})_2(\text{pybz})$.

Wang *et al.* have synthesised and reported anticancer Ir(III) complexes with half-sandwich and cyclometalated (Fig. 12) structures of the functionalized α -lipoic acid ($\text{N}^{\wedge}\text{N-LA}$) as a $\text{N}^{\wedge}\text{N}$ ligand, which is a 2,2-bipyridine derivative [56]. The cyclometalated complex, shown in Fig. 12, possessed the formula $[\text{Ir}(\text{C}^{\wedge}\text{N})_2(\text{N}^{\wedge}\text{N-LA})]\text{PF}_6$, where $\text{C}^{\wedge}\text{N}$ is 2-phenylpyridine. The half-sandwich and cyclometalated complexes were treated with various cancer cell lines. Their antiproliferative activity was determined against human lung carcinoma A549, cisplatin-resistant A549R, human breast carcinoma MCF-7, epithelial ovarian carcinoma A2780, human cervical carcinoma HeLa, and human normal liver LO2 cell lines by MTT assay after 48 h treatment. The iridium(III) half-sandwich complex exhibited no cytotoxicity ($\text{IC}_{50} > 200 \mu\text{M}$), likely due to its poor stability, low lipophilicity limiting cellular uptake, and its susceptibility to hydrolysis and reaction with GSH. The cyclometalated complex (Fig. 12) exhibited excellent cytotoxicity, compared to cisplatin, with IC_{50} values ranging from 3.4 to 6.7 μM . The complex, formed by combining the $\text{N}^{\wedge}\text{N-LA}$ ligand with tripyridine, has shown a positive synergic effect. It also displayed an ability to overcome the cisplatin-resistance in A549R cells. The cyclometalated complex was stable in aqueous solution and had no reaction with GSH, guaranteeing its bioactivity. Furthermore, the excellent photophysical property of the cyclometalated complex provided a more convenient way to study its anticancer mechanism of action through confocal spectroscopy, especially the subcellular localisation. The complex localised and accumulated in the lysosomes of A549 cells, induced the production of a significant amount of ROS, and arrested the cell cycle at the G_0/G_1 phase, which differs from the apoptosis induced by the clinical drug α -lipoic acid itself. The complex (Fig. 12) was hydrophobic in nature, thus having an effect on the cellular uptake due to the lipid bilayer of the cell membrane and the cell death by autophagy [56]. The study has demonstrated the relationship between the anticancer activity and the affiliated structure. This work has also provided insights to clarify the subtle structure-property relationship between the half-sandwich and cyclometalated iridium complexes, and highlighted the importance of the tailored design of metallodrugs according to their future functions.

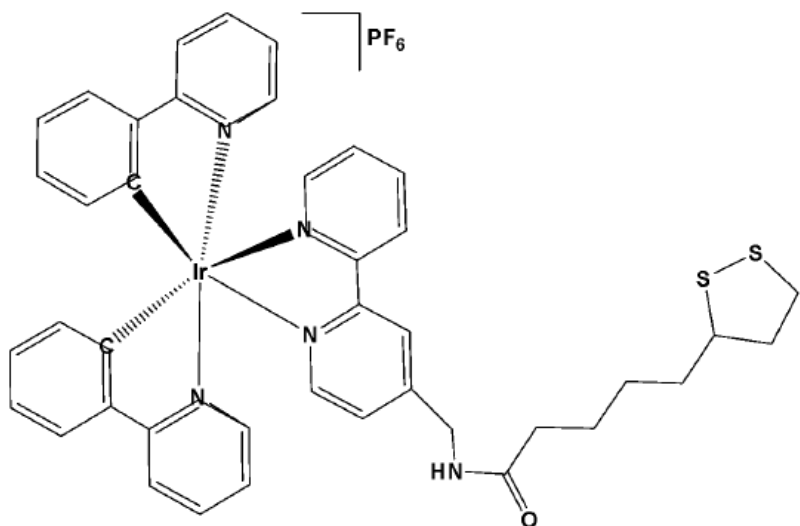


Fig. (12): Structure of $[\text{Ir}(\text{C}^{\wedge}\text{N})_2(\text{N}^{\wedge}\text{N-LA})]\text{PF}_6$ ($\text{C}^{\wedge}\text{N}$ = 2-phenylpyridine).

The biscyclometalated cationic complexes of the type $[\text{Ir}(\text{III})(\text{C}^{\text{N}})^2(-\text{N}^{\text{N}})]\text{Cl}$ (Fig. 13), incorporating thiabendazole and N-benzyl-thiabendazole, have been designed and synthesised to investigate the photophysical and biological effects associated with modifications of the ancillary ligand [57]. These complexes exhibit a diverse range of cellular targets, largely influenced by the nature of the auxiliary ligands, including the nucleus, endosomes, lysosomes, endoplasmic reticulum, mitochondria, and others. In this viewpoint, arylazoles of the N^{N} type are admirable ancillary ligands, because of their structural and biochemical variety. Precisely, the imidazole or benzimidazole ligands can be readily functionalized through the amine bond. In this series of biscyclometalated $\text{Ir}(\text{III})$ complexes, the amine (N-H) group of 4-(1H-benzo [d]imidazol-2-yl)thiazole ligand has been functionalized with a lipophilic benzyl (N-Bn) group [57]. The complexes have been tested against human colon SW480 and human lung A549 adenocarcinoma cell lines. In the dark, the $\text{Ir}(\text{III})$ complex with benzyl group ($\text{R} = \text{Bn}$) was one order more cytotoxic than cisplatin against the tested cell lines. The biological properties were studied further to determine their mechanism of action. These $\text{Ir}(\text{III})$ complexes have interfered with mitochondrial functions, leading to cell apoptosis. In addition, improvement of their effects has been observed after irradiation with visible blue light via photocatalyzing the oxidation of S-containing L-amino acids. It has been demonstrated that the complex with thiabendazole was more active than the complex with N-benzyl-thiabendazole, which provided a reasonable mechanism for their biological action (oxidative stress could be selectively promoted through a photocatalytic action) upon irradiation. This different PDT behaviour depending on the ancillary substituent might be helpful for future rational design of new metal-based photosensitizers.

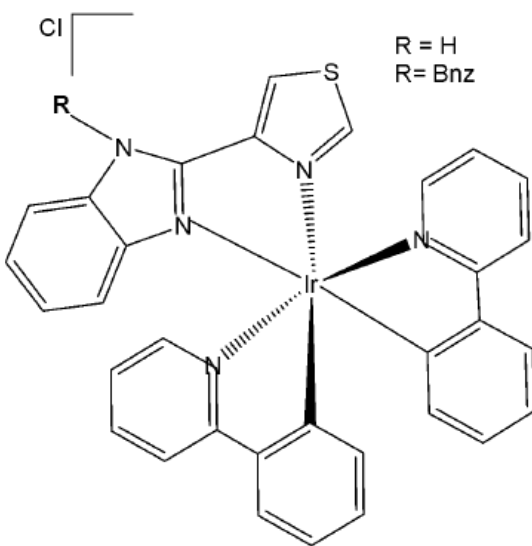


Fig. (13): Iridium compounds with substituted 4-(1H-benzo [d]imidazol-2-yl)thiazole ligand.

The derivatives of guanidine and thiourea are multifunctional compounds widely utilised in medicine. Guanidine derivatives are found in arginine and guanine, whereas thiourea is located in 2-thiouridine of tRNA. As their applications continue to expand across fields such as cancer therapy, sensors, and electronics, their toxicity becomes an important consideration. Iridium(III) complexes with guanidine and thiourea substituents (Fig. 14) have recently been systematically developed [58]. The cytotoxicity of these compounds has been evaluated against three human ovarian cancer (EFO-21, EFO-27 and COLO-704) cell lines and their cisplatin-resistant sub-lines (EFO-21^rCDDP²⁰⁰⁰, EFO-27^rCDDP²⁰⁰⁰ and COLO-704^rCDDP¹⁰⁰⁰). The derivative of guanidine ($IC_{50} = 1.4 \mu M$) was ten times more cytotoxic than the derivative of thiourea ($IC_{50} = 13.5 \mu M$). The cisplatin-resistant sublines are more tolerant to both complexes. The results have confirmed that the guanidine derivative showed cytotoxic activity in the nM range against the tested cell lines. The compounds displayed toxicity trends that were strongly dependent upon S/NH substitution. The patterns of toxicity were illuminated by using the intrinsic luminescence of the complexes as a handle for cellular imaging.

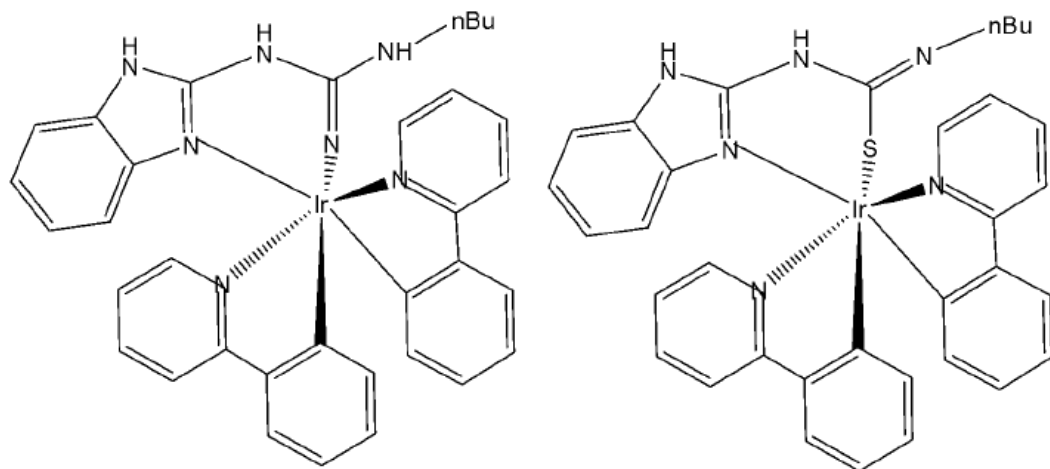


Fig. (14): Iridium(III) complexes with guanidine and thiourea substituents.

The incorporation of Ir(III) complexes with guanidine ligands might improve the efficacy in cancer therapy. Song *et al.* have synthesised three new cyclometalated iridium(III) complexes (Fig. 15), containing guanidine-modified ligands, which were found to exert excellent cytotoxic effects on

different types of cancer cells upon light irradiation at 425 nm [29]. Iridium(III) complexes containing guanidine ligands, Fig. 15(a-c), used in PDT, represented promising non-invasive therapeutic systems with no cumulative toxic effects [29]. Complex in Fig. 15(a) exhibited the lowest cytotoxicity towards cancer cell lines (HeLa, MCF-7, and Hep-G2) while showing the highest phototoxicity index. Complex in Fig. 15(b) demonstrated moderate cytotoxic effects on cancer cell lines with IC_{50} values ranging between 20 and 60 μ M. The mechanisms underlying the antitumour effects of the complex shown in Fig. 15(a), including subcellular localisation, mitochondrial dysfunction, ROS production, cell cycle arrest, and mitochondria-associated apoptotic signalling pathways, have been elucidated. Mechanistic investigations revealed that the complex in Fig. 15(a) could induce apoptosis via the activation of ROS-mediated mitochondria-associated caspase-independent signalling pathways, both in the presence and absence of light irradiation, and also promoted cell cycle arrest at the G₂/M phase. Studies have shown that the complex in Fig. 15(a) induced tumour cell death *in vivo* in HepG2 xenograft-bearing mice under light irradiation and exerted no severe side effects on surrounding organs [29].

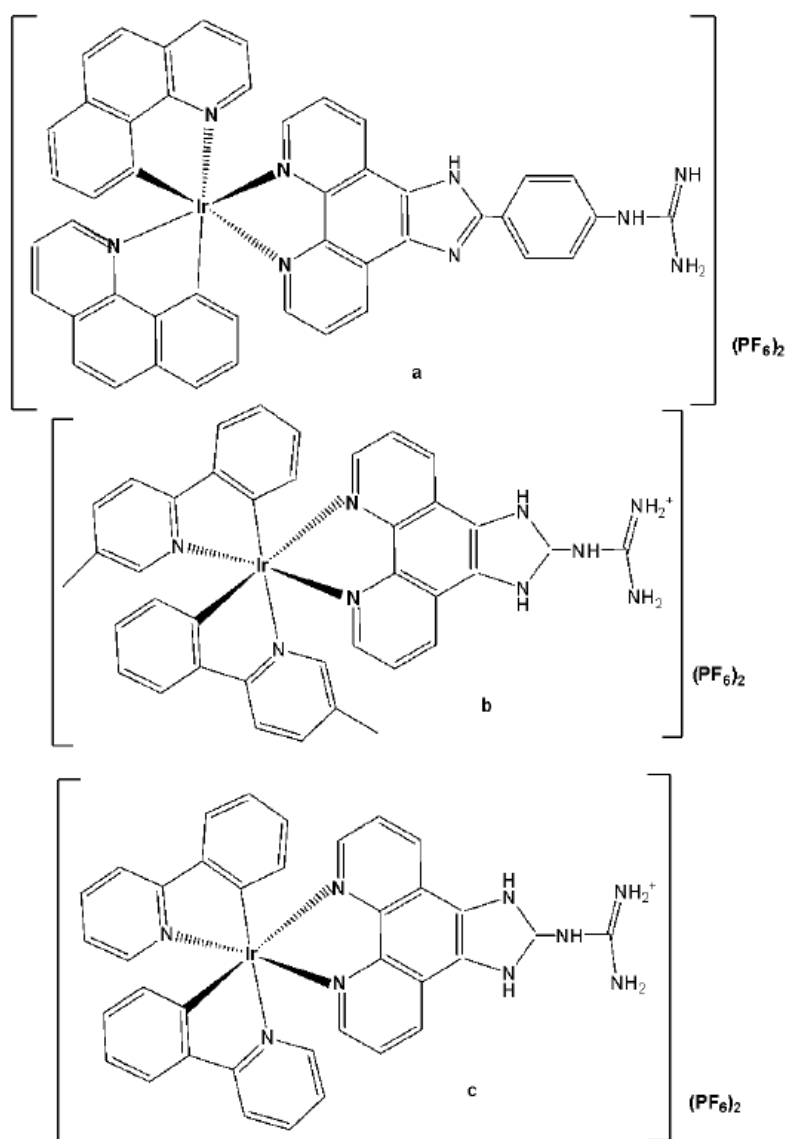


Fig. (15): Structures of Ir(III) complexes with guanidine-modified ligands.

Iridium-based photosensitizers are of great interest in photodynamic therapy (PDT) due to their tunable photophysical and photochemical characteristics and structural flexibility. Zhao et al. synthesised and

reported iridium(III) complexes, as shown in Fig. 16(a–b), highlighting the potential of a nanoplatform based on a long-lived iridium(III)-based photosensitizer for tumor therapy [59]. The iridium-naphthalimide photosensitizer in Fig. 16(a), featuring a long-lived intra-ligand excited state, was specifically designed to achieve significantly enhanced singlet oxygen (${}^1\text{O}_2$) generation efficiency, approximately 45 fold higher than that of the model iridium(III) complex shown in Fig. 16(b) under 460 nm irradiation. To achieve deep tissue penetration, the iridium-naphthalimide complex in Fig. 16(a) was further covalently bonded to the up-conversion nanoparticles (UCNPs). Besides, 1-benzyl-3-(5'-hydroxymethyl-2'-furyl)indazole (YC-1), an effective HIF-1 α inhibitor, was physically adsorbed into the hydrophobic layer at the surface of UCNPs. Upon near-infrared (NIR) irradiation iridium(III)-naphthalimide complex in Fig. 16(a), mediated the toxic ${}^1\text{O}_2$, which was generated for PDT, whose efficient conversion of oxygen to ${}^1\text{O}_2$ during the PDT would exacerbate the hypoxic condition of tumour tissue and lead to the upregulation of HIF-1 α for the following HIF-1 targeting tumour therapy. All of this transforms PDT-induced tumor hypoxia into a therapeutic advantage, thereby opening up new strategies to overcome hypoxia in PDT therapy. These complexes showed slight cytotoxicity in normoxic and hypoxic cells, displaying their low dark toxicity and good biocompatibility [59].

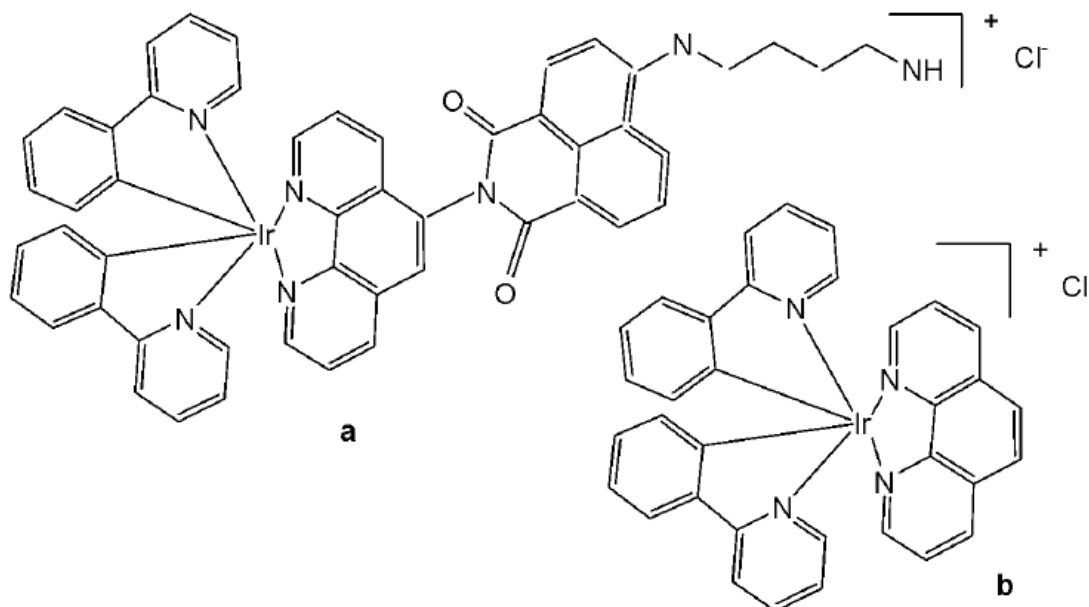


Fig. (16): The iridium-naphthalimide photosensitizer and its model iridium(III) complex.

The combination of the ease of synthesis and the excellent photophysical and biochemical properties makes the biscyclometalated Ir(III) complexes with a formula of $[\text{Ir}(\text{C}^{\wedge}\text{N})_2(\text{N}^{\wedge}\text{N})]^+$ more suitable to be developed as non-platinum antineoplastic drugs. In many papers, phenanthroline and its derivatives as $\text{N}^{\wedge}\text{N}$ chelating ligands have been applied to cyclometalated Ir (III) complexes and acted as effective phototherapy drugs towards different tumour cells. Xue *et al.* have synthesised and characterized phosphorescent cationic iridium complexes using phenanthroline derivatives as $\text{N}^{\wedge}\text{N}$ ligands and 2-phenylpyridine as the $\text{C}^{\wedge}\text{N}$ ligand [60]. Importantly, effective induction of the generation of singlet oxygen ${}^1\text{O}_2$ after irradiation, leading to apoptosis, was observed. The photodynamic therapy effect was further assessed by histological examination and immunohistochemistry.

Hong *et al.* have reported the synthesis of iridium (III) complex with the general formula $[\text{Ir}(\text{ppy})_2(\text{paip})]\text{PF}_6$ (Fig. 17), where ppy and paip are 2-phenylpyridine and 2-(4-aminophenyl) imidazo [4,5-f] [1,10] phenanthroline, respectively. The cytotoxicity studies were carried out by MTT

assay on Bel-740, HeLa, HepG-2 and PC-12 cell lines. The complex showed higher cytotoxic activity than cisplatin towards PC12 cells with $IC_{50}=10.2\text{ }\mu\text{M}$. The intracellular ROS generation and mitochondrial membrane potential (MMP) changes were determined by a fluorescent microscope and flow cytometry. Complex in Fig. 17 demonstrated efficient cellular uptake, accumulating in both the nucleus and mitochondria. It induced apoptosis by elevating ROS levels and decreasing mitochondrial membrane potential, thereby inhibiting cell growth in PC-12 cells at the G_0/G_1 phase [61]. Cell invasion assay has shown that the complex could effectively inhibit the cell invasion and activate caspase 3 and procaspase 7, down-regulated the expression of Bcl-2 and Bcl-x, and up-regulated the expression levels of Bak.

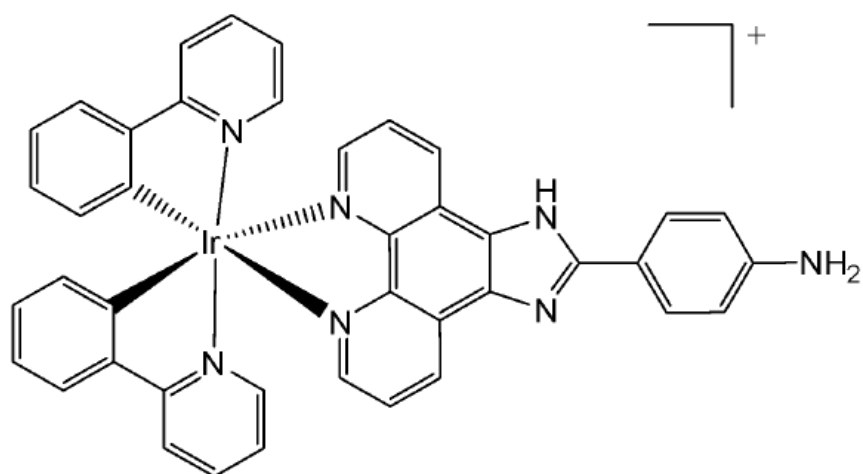


Fig. (17): Iridium(III) complex $[\text{Ir}(\text{ppy})_2(\text{paip})]\text{PF}_6$ of 2-(4-aminophenyl) imidazo[4,5-f][1,10]phenanthroline.

Liang *et al.* have synthesised and reported the complex $[\text{Ir}(\text{ppy})_2(\text{MHPIP})]\text{PF}_6$ (Fig. 18), where ppy = 2-phenylpyridine and MHPIP = 2-(1-methyl-1-H-Pyrazol-3yL)-1H-imidazo[4,5f][1,10]phenanthroline [62]. The *in vitro* cytotoxic activity of the free proligand MHPIP and its complex was evaluated using the MTT assay. The free ligand MHPIP exhibited no cytotoxicity against the tested cell lines. In contrast, the complex showed selective toxicity toward HepG2 cells ($IC_{50} = 39.5\text{ }\mu\text{M}$) while exhibiting no cytotoxic effects on other cancer cell lines, including SGC-7901, HeLa, BEL-7402, A549, or on normal LO2 cells. The level of reactive oxygen species, mitochondrial membrane potential, autophagy, intracellular Ca^{2+} levels and cell invasion were investigated by fluorescence microscopy, and the cell cycle arrest was studied by flow cytometry. These studies demonstrated that the complex effectively induced apoptosis and autophagy in HepG2 cells by causing DNA damage and ROS-mediated mitochondrial dysfunction, as well as by inhibiting the PI3K/AKT/mTOR pathways, thereby promoting autophagy and significantly suppressing cell growth at the G_0/G_1 phase [62].

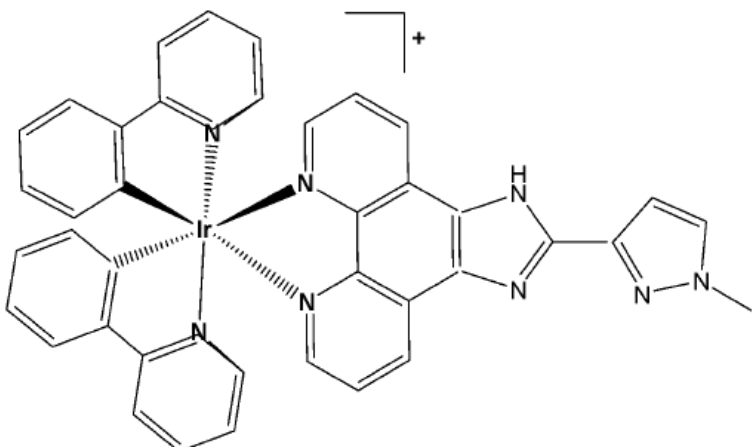


Fig. (18): Structure of Iridium (III) complex with formula $[\text{Ir}(\text{ppy})_2(\text{MHPIP})]\text{PF}_6$.

A charged iridium(III) complex carrying a phenanthroline-based ligand, functionalized with an isothiocyanate group, has been developed to target specific mitochondrial proteins [63]. The cellular properties of the studied luminescent cyclometalated iridium(III) complex $[\text{Ir}(\text{pq})_2(\text{phen-ITC})](\text{PF}_6)$ (Hpq =2-phenylquinoline, phen-ITC=5-isothiocyanato-1,10-phenanthroline), that efficiently and specifically labels mitochondria in living mammalian cells, have been investigated. The isothiocyanate unit allowed the probe to covalently bind to amine-containing biomolecules such as lysine and the N-terminal of proteins, yielding luminescent bioconjugates. The studied complex accumulated only in the mitochondria of living 3T3, HeLa and RPE cells, while a diffuse staining was present with prefixed 3T3 cells, indicating that the process required active cellular metabolism. The binding of the complex to mitochondrial proteins interfered with the function and the morphology of this organelle, as shown by the MTT assay. The viability of 3T3 cells decreased to 60% with a concentration higher than $10 \mu\text{M}$ and an incubation time of 12 h [63]. A family of three luminescent cyclometalated iridium(III) diimine complexes $[\text{Ir}(\text{bsn})_2(\text{N}^{\wedge}\text{N})](\text{PF}_6)$, bound to functionalized 1,10-phenanthroline ligands, where Hbsn = 2-(1-naphthyl)benzothiazole, $\text{N}^{\wedge}\text{N}$ = 5-amino-1, 10-phenanthroline, 5-isothiocyanato-1, 10-phenanthroline, and N-butyl-N'-1, 10-phenanthroline-5-yl thiourea, has been studied by the group of Lo [64]. The photophysical and electrochemical properties of these complexes have been examined. The cytotoxic effects and cellular internalization of the complexes in HeLa cells have been investigated through multiple approaches. The intracellular distribution of the complexes in HeLa cells was the same, with the formation of a luminescent ring surrounding the nucleus. Additionally, cytotoxicity data have shown similar IC_{50} values in the range of $1.0\text{--}4.2 \mu\text{M}$, revealing the high toxicity of these probes. All the complexes have exhibited very efficient cellular uptake properties in a relatively short incubation time, indicating that they represented attractive candidates for developing novel cellular imaging reagents.

Kuang *et al.* have reported iron(III)-activated iridium(III) compounds as pro-drugs for gastric cancer theranostics that were firstly localised in lysosomes and subsequently transferred to mitochondria [65]. The Ir(III) complexes (Fig. 19) have not been toxic to normal LO2 and MCF-10A cell lines; however, they have shown considerable cytotoxicity and selectivity against AGS and MKN-28 gastric cancer cells with low IC_{50} values. When activated by Fe^{3+} , the complexes are hydrolyzed in lysosomes to yield an amino-bipyridyl Ir(III) complex and 2-hydroxybenzochinone, a ROS generator. In addition to exhibiting high cytotoxicity against various tumor cells, the complexes display an intense phosphorescence, making them advantageous for diagnostic applications. Additionally, in the xenograft AGS tumor model, these compounds demonstrated greater activity than the reference drug fluorouracil while exhibiting fewer side effects in murine models. The same research group has also reported a series of iridium(III) complexes with benzothiazole-substituted ligands [66]. Notably, the

compound bearing benzothiazole substituents, $[\text{Ir}(\text{ppy})_2(\text{bbtb})]^+$ (Fig. 19), specifically targeted mitochondria and activated oncosis-related proteins, including porimin and calpain [66]. Ir(III) complexes, shown in Fig. 19, have exhibited high cytotoxic activity against various tumour cell lines, together with cisplatin-resistant cells, showing low IC_{50} values ($\text{IC}_{50} < 10 \mu\text{m}$ for AGS cells) and lower cytotoxicity against normal hepatocytes ($\text{IC}_{50} > 200 \mu\text{m}$ for LO2 cells) [65,66]. An increase in phosphorescence and cytotoxicity, along with the shift of subcellular localisation from lysosomes to mitochondria, can be monitored using confocal microscopy.

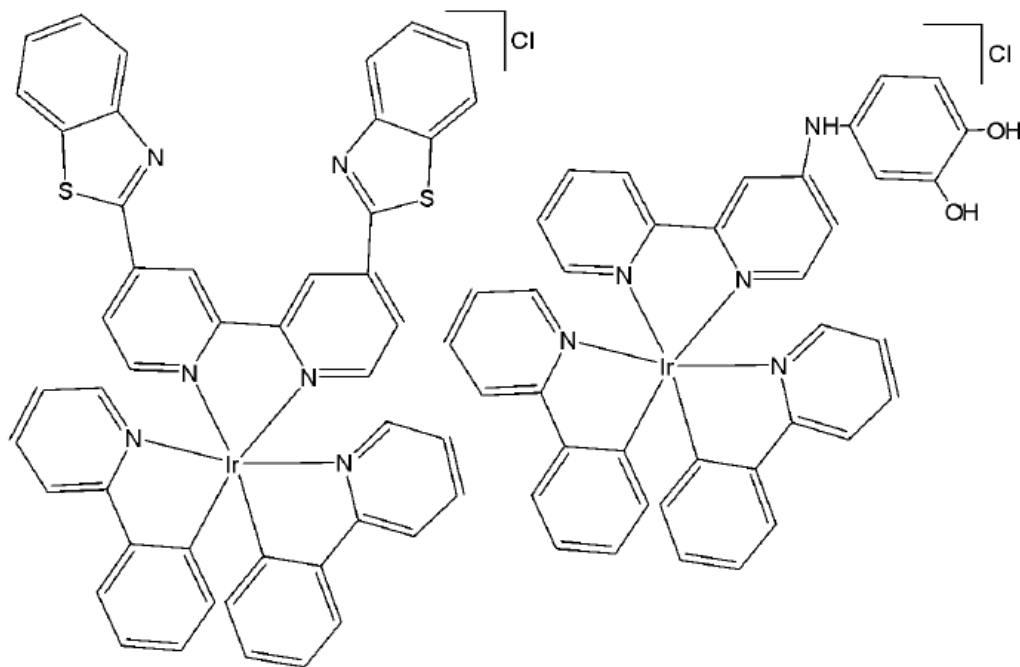


Fig. (19): Oncosis-inducing cyclometalated Ir (III) complexes.

2.3. Biscyclometalated Ir(III) Complexes with Substituted 2-Phenylpyridines as Modified C^N Ligands

The development of multifunctional theranostic agents, which combine tumour targeting, imaging, and therapeutic capabilities, has significantly advanced the clinical diagnostics and treatment of tumours. However, the integration of imaging and therapy functionalities into a unimolecular framework remains a great challenge. Yi *et al.* have synthesised and reported a family of amphiphilic gemini Ir(III) complexes, presented in Fig. 20(a-f) [67]. These complexes contain quaternary ammonium groups (QA) which were employed as hydrophilic functional groups to modify both the C^N ligands and the auxiliary N^N ligands of the hydrophobic iridium(III) complex. This structure gives the complexes adjustable water solubility and excellent self-assembly properties. These complexes can spontaneously form vesicles in aqueous media through self-assembly due to their amphiphilic nature, exhibiting two distinct molecular arrangements in the aggregated vesicles depending on the position of the quaternary ammonium groups.

Spectroscopic and computational results have revealed that introducing quaternary ammonium groups into cyclometalating ligands (C^N ligands), Fig. 20(a-c), endows gemini iridium(III) complexes with adjustable water solubility, excellent self-assembly properties, and the opportunity to overcome the drawback of aggregation-caused emission quenching, ensuring high emission intensity and excellent singlet oxygen ${}^1\text{O}_2$ generation ability of the complexes in aqueous media due to the dipyridyl groups arranged by an edge-to-edge configuration. The efficacy of ${}^1\text{O}_2$ generation of the complexes followed the

order Fig. 20(c) > 20(b) > 20(a) > 20(f) > 20(e) > 20(d), which was consistent with their increasing emission lifetimes.

The potential application of the studied gemini iridium(III) complexes for photodynamic therapy has been assessed toward HepG2 and MCF-7 cells via a MTT assay under dark and irradiation conditions. Under dark condition, the complexes exhibited slight cytotoxicity toward the tested cells ($IC_{50} > 300 \mu M$), which is an important characteristic for the PDT agent. The possible reason is that the heavy atom iridium is wrapped by the aggregated vesicles, which avoid interacting nonspecifically with the proteins. In comparison, the complex in Fig. 20(c), due to its appropriate lipophilicity, became highly phototoxic to HepG2 and MCF-7 cells with IC_{50} values as low as $1.2 \mu M$ (PI = 250.0) and $1.3 \mu M$ (PI = 230.7), where PI is the ratio between the IC_{50} values in the dark upon light irradiation.

With appropriate water solubility and positive charge, the complex in Fig. 20(c) showed higher cellular uptake efficiency by an energy-dependent endocytosis pathway. This complex localized specifically in the mitochondria, exhibited outstanding photostability, low dark cytotoxicity, and an impressive phototoxicity index with satisfactory performance in mitochondria-targeted imaging and photodynamic therapy (PDT) of tumour cells. Due to its excellent photostability the complex in Fig. 20(c) could be used as mitochondria targeted imaging agent.

Furthermore, *in vivo* studies have proven that the complex in Fig. 20(c) was nontoxic to normal organs and possessed exceptional antitumor activity and remarkably inhibited the growth of the HepG2 tumour cells under PDT treatment. Therefore, this work represents a promising strategy for designing potential clinically applicable multifunctional iridium(III) complexes as theranostic agents for mitochondria-targeted imaging and PDT in a single molecular framework [67].

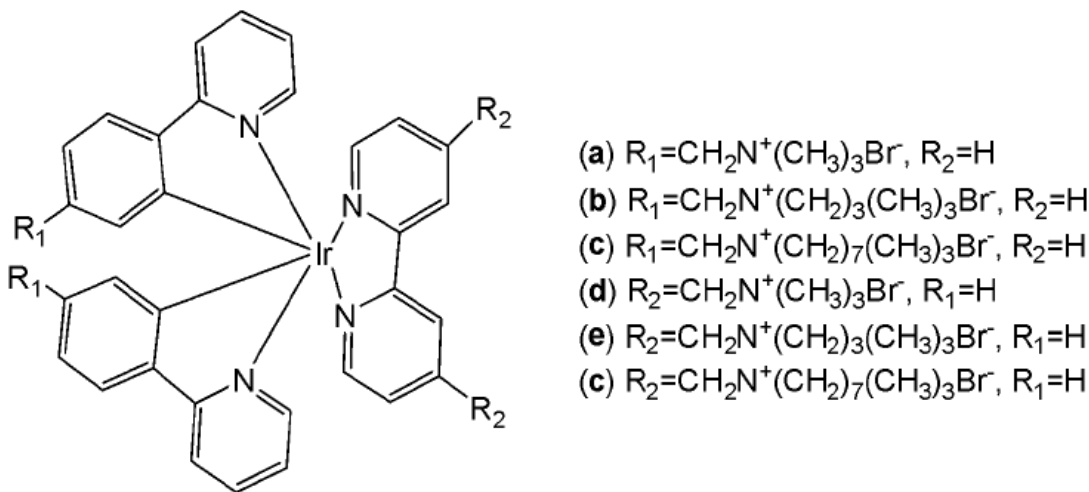


Fig. (20): Ir(III) complexes with quaternary ammonium groups in C^N and N^N ligands.

Cao *et al.* have synthesised six cyclometalated iridium(III) complexes, presented in Fig. 21(a-f), each incorporating a series of extended planar diimine ligands [11]. All complexes exhibited higher cytotoxic activity (IC_{50} varying between 0.1 and $8.4 \mu M$) compared to cisplatin against different cancer cells (A549, A549R, HepG2, PC3 and HLF). The order of cytotoxicity was as follows: Fig. 21(c) > 21(d) > 21(e) > 21(f) > 21(a) > 21(b), and the most active of them, with an IC_{50} around $0.1 \mu M$, were found to be 100-fold times greater than cisplatin against HeLa cells. These complexes were likely to overcome the acquired and intrinsic drug resistance of cisplatin. Among the studied compounds, the complexes with dipyrdo[3,2-*a*:2',3'-*c*]phenazine ligands could bind to DNA tightly *in vitro*, intercalate to mtDNA *in situ*, and induce mtDNA damage. These compounds exhibited a drop in the mitochondrial

membrane potential, disability of adenosine triphosphate generation, disruption of mitochondrial energetic and metabolic status, which subsequently caused protective mitophagy, G₀/G₁ phase cell cycle arrest, and apoptosis (Fig. 21) [11].

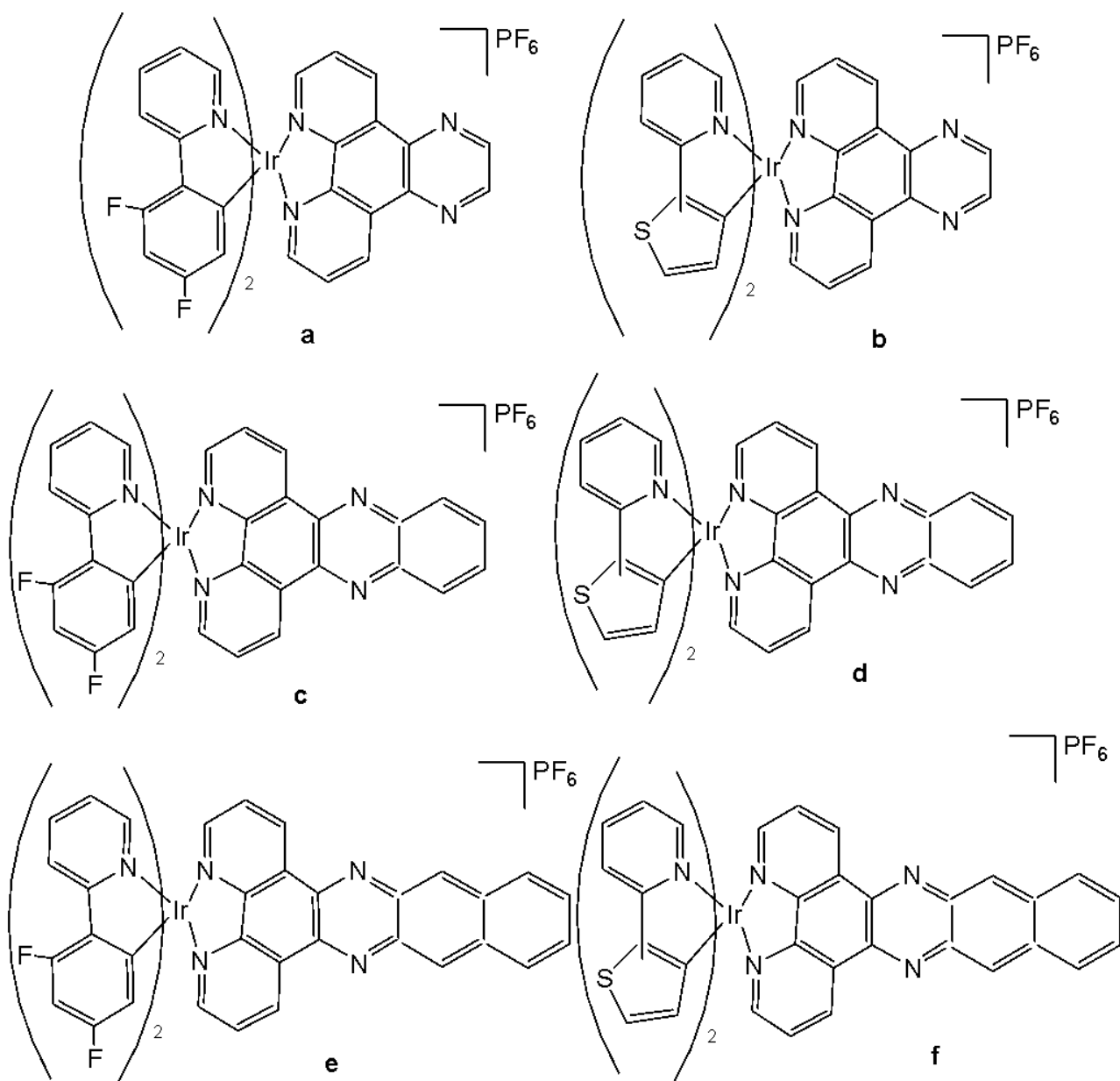


Fig. (21): Structures of cyclometalated Ir (III) complexes with extended planar ligands.

Wang and co-workers have reported the synthesis of a series of phosphorescent cyclometalated Ir (III) complexes containing 2,2'-bipyridine-4,4'-dicarboxylic acid and its diester derivatives as ligands (Fig. 22 a-j), along with studies on their chemotherapeutic properties, focusing on their antineoplastic potency [68]. The authors have prepared structurally diverse ester-appending moieties with different alkyl chain lengths (CH₃, C₂H₅, n-C₄H₉, CH₂CH(CH₃)₂) on the 2,2'-bipyridine N⁺N ligand, and compared these complexes with the analogues featuring dicarboxylic acid-functionalized 2,2'-bipyridine N⁺N ligand. Esterification is an efficient and convenient optimisation method for carboxylic acid-containing compounds, which can markedly improve their cellular uptake efficacy. In this study, the effects of ester modifications on the photophysical properties, lipophilicity, cellular uptake, and anticancer activity of cyclometalated iridium(III) complexes were investigated in detail. A

clear correlation between the alkyl chain length of the esters and cytotoxicity was observed. Notably, the complexes shown in Fig. 22e and Fig. 22i exhibited the highest antiproliferative activity across a panel of cancer cell lines, including HeLa, A549, A549R, MCF-7, and HepG2, as well as cisplatin-resistant tumor cells.

On the other hand, the ester-functionalized complexes in Fig. 22e and Fig. 22i would be expected to be hydrolyzed by esterase, and their intracellular staining experiment has shown that these luminescent complexes would be localised in the mitochondria in A549 cells with the validation of red MitroTracker (MTDR). In this regard, the cell-death mechanism has been investigated in several key aspects, including the cell cycle arrest, ROS level, autophagy and apoptosis. It has been found that both complexes in Fig. 22e and Fig. 22i would lead to mitochondrial dysfunctions, related to the intracellular ROS level, and would induce concentration-dependent cell cycle arrest, pro-death autophagy and caspase-dependent apoptosis simultaneously in A549 cells. The study has demonstrated that ester modification was a practical, feasible and straightforward strategy for structural optimisation of antineoplastic cyclometalated Ir(III) complexes [68].

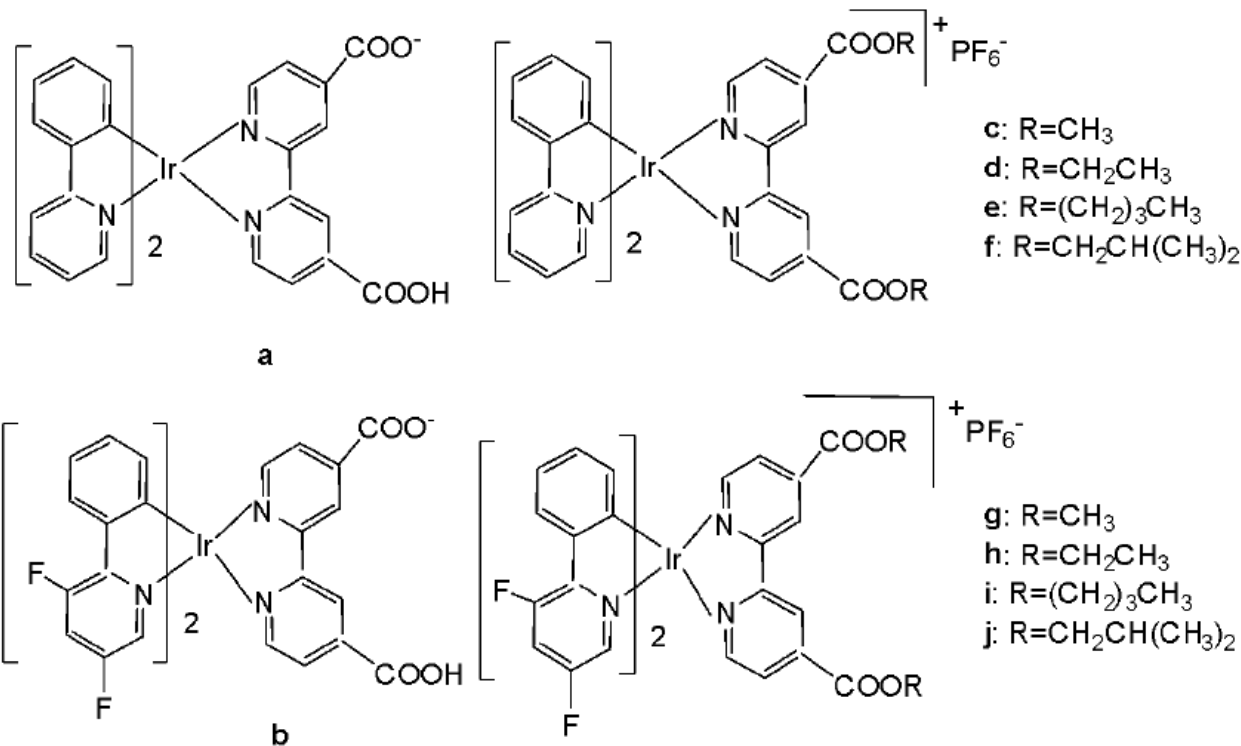


Fig. (22): Ir (III) complexes, containing 2,2'-bipyridine-4,4'-dicarboxylic acid and its diesters.

New series of anticancer and photophysical neutral Ir (III) biscyclometalated complexes with auxiliary N⁺O ligands of the type [Ir(III)(C⁺N)₂(N⁺O)], Fig. 23, where N⁺O = 2-(benzimidazolyl) phenolate-N,O and 2-(benzothiazolyl) phenolate-N,O, and C⁺N = 2- (phenyl)pyridinate or its derivatives, have been described as PDT agents [69]. Complexes of the two series have exhibited dissimilar photophysical and biological properties. The proliferation effects of Ir(III) complexes against the colon adenocarcinoma SW-840 cell line have been studied by MTT in the dark and with UV irradiation. In the dark, the complexes with benzimidazole derivatives (X = NH) were not cytotoxic, whereas the benzothiazole-substituted compounds (X = S) were more cytotoxic than cisplatin. Consequently, the ancillary N⁺O ligand is the key factor in terms of cytotoxic activity both in the dark and upon irradiation. However, the C⁺N ligands play a central role concerning the metal accumulation in cells. The benzothiazole complexes preferred to be located in the nucleus, while the benzimidazole

complexes remained outside the cell nucleus. Notably, the complex of 2-(4,6-difluorophenyl) pyridinate has been identified as both an efficient photosensitizer for ${}^1\text{O}_2$ generation and a potential agent for photodynamic therapy. Both categories of complexes have exhibited notable catalytic activity in the photooxidation of thioanisole and S-containing amino acids with full selectivity.

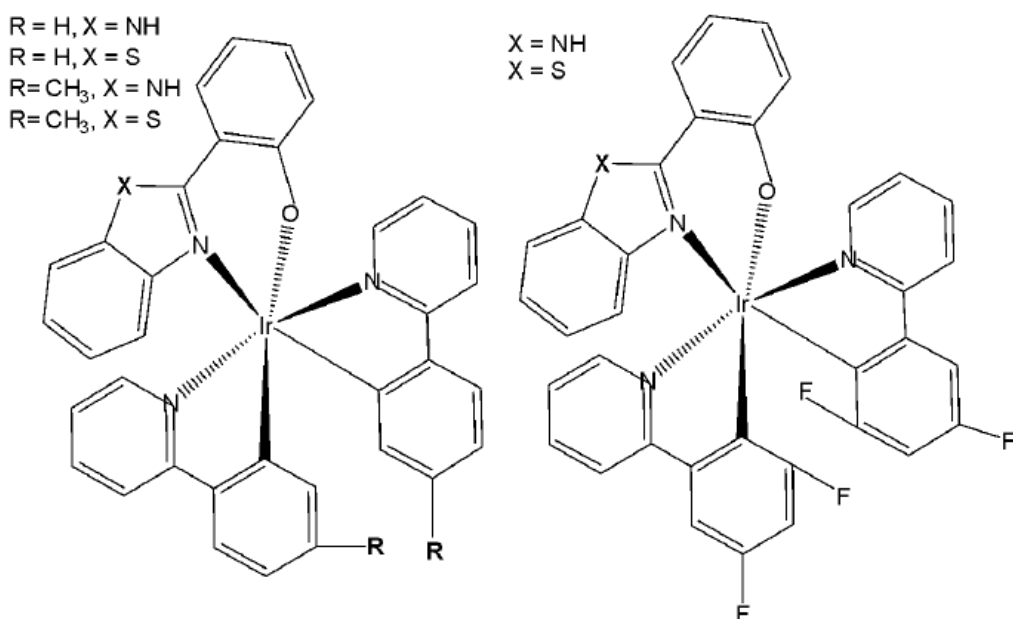


Fig. (23): Ir (III) complexes with different bidentate benzimidazole ligands and N^{^C} co-ligands.

III. CYCLOMETALATED Ir(III) COMPLEXES WITH MODIFIED AROMATIC C^{^N} LIGANDS

Many researchers have tried to replace the C^{^N} ligand of widely studied 2-phenylpyridine iridium complexes by different bidentate C^{^N} ligands to improve their biological activity [70].

Wu *et al.* have synthesised iridium(III) complexes, shown in Fig. 24(a-l), and evaluated them for potency against malignant melanoma metastasis [71]. The authors first obtained three Ir(III) complexes (Fig. 24a-c) with a general structure $[\text{Ir}(\text{C}^{\text{^N}})_2(\text{N}^{\text{^N}})]^+$ bearing either methyl, t-butyl, and/or nonyl aliphatic groups attached to their C^{^N} and N^{^N} ligands (Fig. 24). To investigate the effects of the aliphatic groups in these Ir(III) complexes on S100B inhibitory activity, the authors further designed Ir(III) complexes (Fig. 24d-f), each containing two fewer aliphatic groups (Fig. 24) than their corresponding congeners (Fig. 24a-c), which were replaced with either bromine or hydrogen. For the most active compound (Fig. 24a), replacing the two t-butyl groups on the N^{^N} ligands with bromine groups (Fig. 24d) led to a significant decrease in inhibition activity, suggesting the importance of the aliphatic group in S100B inhibitor. It should be noted that the higher activities of the complexes (Fig. 24 - a, c, and f) compared to the complexes (Fig. 24 - b and e) suggested that the t-butyl group was superior to the nonyl group in conferring S100B/p53 inhibitory activity. Based on these results, a subsequent series of Ir(III) complexes (Fig. 24g-i) has been synthesised, which contained the 4,4'-ditert-butyl-2,2'-bipyridyl (NN3) ligand identified as being the best N^{^N} ligand in the first round of screening but varied in their C^{^N} ligands (Fig. 24). Among these complexes, the complex in Fig. 24-g bearing the 1-phenylisoquinoline (CN4) C^{^N} ligand emerged as the most potent complex, with 96% inhibitory potency against S100B/p53 at 10 μM . To test whether the potency of the compounds could be further improved by pairing the CN4 C^{^N} ligand with different N^{^N} ligands, Ir(III) complexes (Fig. 24j-l) have been designed and synthesised (Fig. 24). However, none of the final rounds of complexes

showed higher activity than the complex (Fig. 24g), indicating the superiority of the NN3 moiety in conferring S100B/p53 inhibitory activity.

The complex in Fig. 24-g has shown desirable photophysical properties including long lifetime, large Stokes shift, and high quantum yield with high photostability *in vitro*. This complex demonstrated a strong co-localization with S100B protein in melanoma cells along with the suppressing tumor growth. It blocked S100B dependent signal transduction and inhibited the migration of melanoma cells. The complex in Fig. 24-g has exhibited strong antiproliferative activity against cancerous A375 cells ($IC_{50} = 0.14$) and showed comparatively lower cytotoxicity against normal LO2 cells ($IC_{50} = 1.07$) [71]. In two separate melanoma mouse models, the complex (Fig. 24-g) suppressed tumor growth and restrained lung metastases with only slight toxicity to mice. Preliminary SAR analysis revealed that the nature of both the $N^{\wedge}N$ and $C^{\wedge}N$ ligands as well as the identity of the Ir(III) centre are important determinants for biological activity. The complex in Fig. 24-g was identified as a potent first reported theranostic agent with nanomolar potency and selectivity for simultaneously monitoring S100B and suppressing malignant melanoma metastasis *in vitro* and *in vivo* via targeting S100B protein.

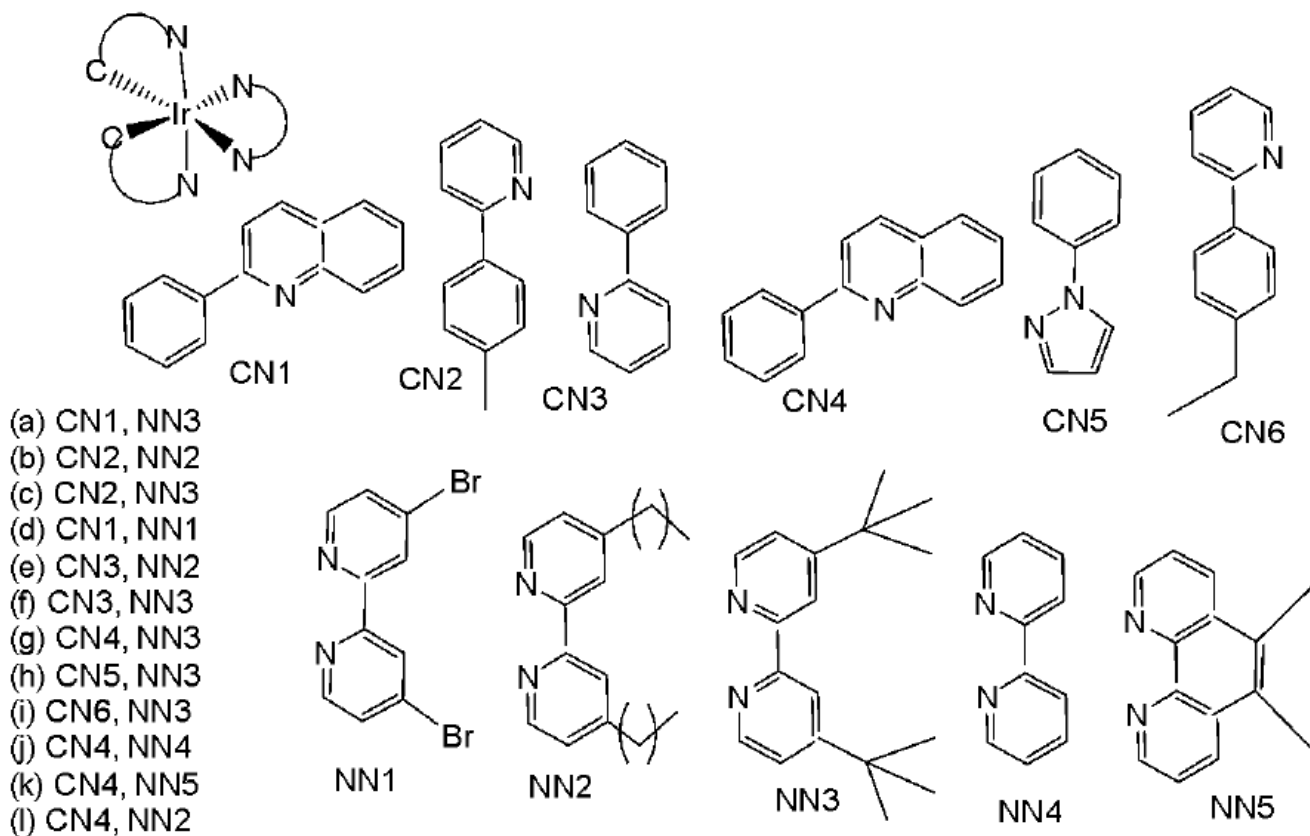


Fig. (24): Structures of iridium (III) complexes used for screening against S100B.

Xiang *et al.* have reported cyclometalated iridium(III) complexes for glutathione (GSH) activated targeted chemotherapy and photodynamic therapy (PDT) [27]. The complexes of the types $Ir(ppy)_2(bpy\text{-CPT})^+$, $Ir(ppy)_2(bpy)^+$, $Ir(pq)_2(bpy\text{-CPT})^+$, $Ir(pq)_2(bpy)^+$, where CPT = camptothecin, Fig. 25(a-d), have been synthesised and characterized [27]. The cyclometalated Ir(III) complexes were prepared by conjugating phosphorescent iridium(III) compounds with the chemotherapeutic drug CPT via GSH-responsive disulfide bond linkages. Cytotoxicity was evaluated using the MTT assay on HeLa cells under both dark and visible light conditions. The results indicated that the complexes exhibited negligible cytotoxicity toward HeLa cells. These complexes exhibited remarkable imaging capabilities, which were attributed to their inherent fluorescence. It was observed that the disulfide

bond could be cleaved by the high glutathione concentrations present in tumour cells, thereby releasing the free chemotherapeutic drug camptothecin for targeted chemotherapy [27].

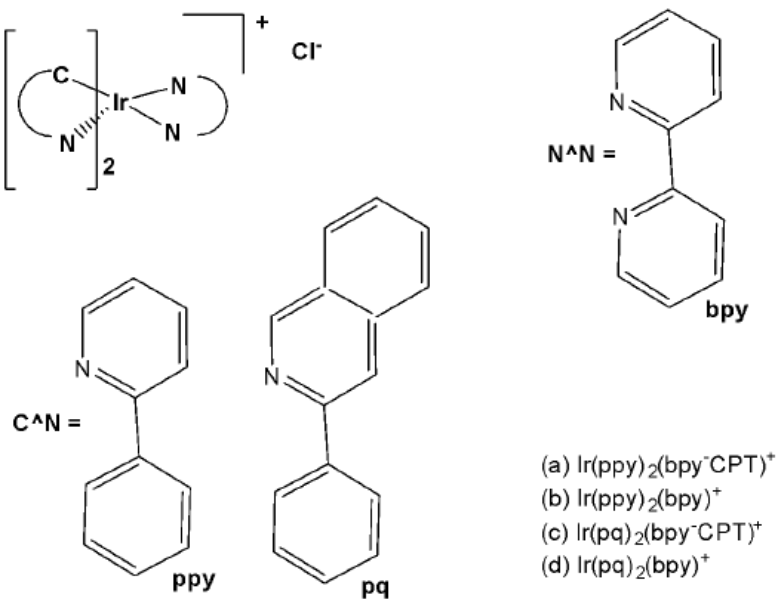


Fig. (25): Structures of complexes $\text{Ir}(\text{ppy})_2(\text{bpy-CPT})^+$, $\text{Ir}(\text{ppy})_2(\text{bpy})^+$, $\text{Ir}(\text{pq})_2(\text{bpy-CPT})^+$, $\text{Ir}(\text{pq})_2(\text{bpy})^+$.

Sun *et al.* have developed four iridium(III) anthraquinone complexes (Fig. 26) that can be excited *via* two-photon absorption, as hypoxia-sensitive imaging probes [72]. The four mitochondria-specific and two-photon phosphorescence iridium(III) complexes have been prepared by coordinating bridge splitting reactions of the binuclear precursor $[\text{Ir}(\text{C}^{\wedge}\text{N})_2\text{Cl}]_2$, where the $\text{C}^{\wedge}\text{N}$ ligand was 2-(benzo[d]thiazol-2-yl)anthracene-9,10-dione (AqSN) and the $\text{N}^{\wedge}\text{N}$ ligands (2,2'-bipyridine (Fig. 26a), 1,10-phenanthroline (Fig. 26b), 1,10-phenanthroline-thiazole (Fig. 26c), 1,10-phenanthroline-selenazole (Fig. 26d).

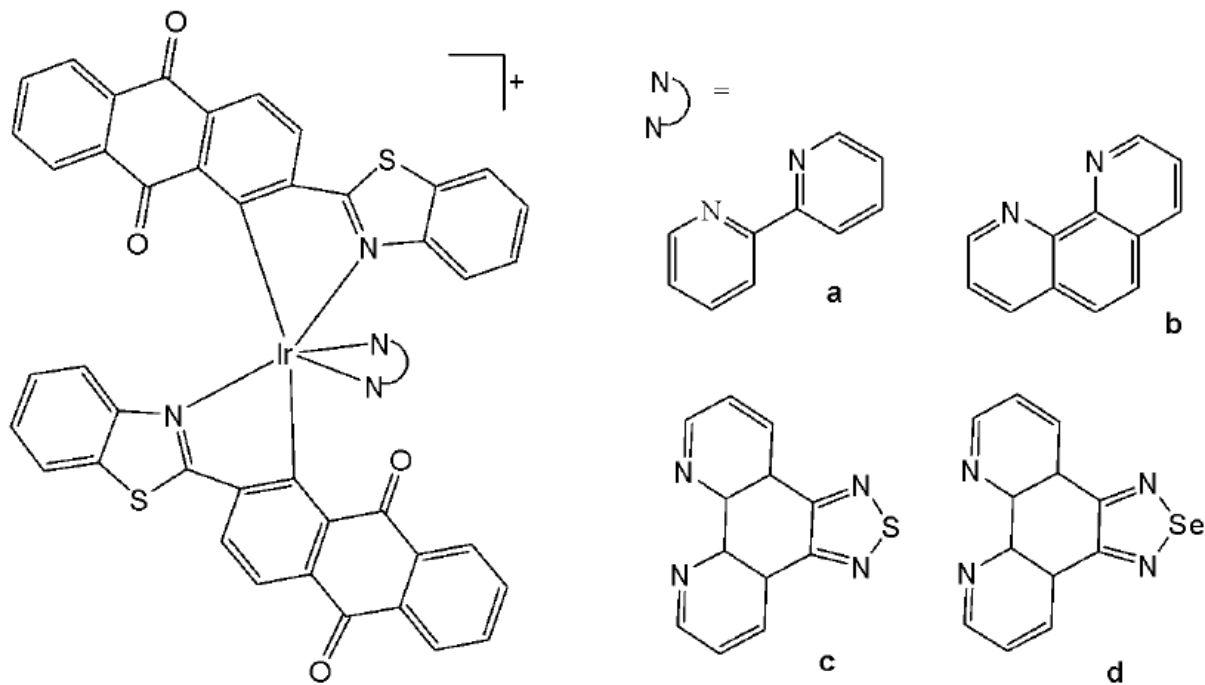


Fig. (26): Iridium(III) anthraquinone complexes.

The iridium(III) complexes (Fig. 26) have two anthraquinone groups as ancillary ligands that are hypoxia-sensitive moieties [72]. The anthraquinone units, as good electron acceptors, are efficient quenchers of the iridium luminescence. However, in hypoxic conditions, it can be converted into the hydroquinone form, thus restoring the emission of the probe [73]. In cells, the ligand could be reduced by the coenzyme nicotinamide adenine reductase phosphate (NAD(P)H) in the presence of cellular reductase [74]. It has been shown that the emission intensity of the complexes (Fig. 26) internalized within A549 cells, rapidly increased following enzymatic reactions with NAD(P)H under hypoxic conditions, without interference from other biological reductants. Moreover, the probes display different sensitivity toward oxygen. All the probes possessed excellent specificity for mitochondria of A549 cells, which allowed imaging and tracking of the mitochondrial morphological changes in a hypoxic environment over a long period of time. They have shown relatively low cytotoxicity with viability values greater than 80 % under both normoxic and hypoxic conditions, after 12 h incubation at a concentration of 10 μ M. Complexes, shown in Fig. 26, have potential applications for real-time tracking of mitochondrial changes, which offers a new method to recognise mitochondria-related physiological and pathological changes, and possibly offers novel medical strategies for diagnosis.

Du *et al.* have synthesised and reported three Ir(III) complexes $[\text{Ir}(\text{ppy})_2(\text{adppz})](\text{PF}_6)$ ($\text{adppz} = 7\text{-aminodipyrdo}[3,2\text{-a}:2',3'\text{-c}]phenazine$ and $\text{ppy} = 2\text{-phenylpyridine}$) Fig. 27(a), $[\text{Ir}(\text{bzq})_2(\text{adppz})](\text{PF}_6)$ ($\text{bzq} = \text{benzo}[h]\text{quinolone}$) Fig. 27(b), $[\text{Ir}(\text{piq})_2(\text{adppz})](\text{PF}_6)$ ($\text{piq} = 1\text{-phenylisoquinoline}$) Fig. 27(c) [75]. The complexes have shown effective inhibition of the cell colonies. The cytotoxicity *in vitro* of the complexes against A549, HepG2, SGC-7901, BEL-7402 and normal NIH3T3 cells was evaluated by MTT method. The intracellular reactive oxygen species (ROS) levels, mitochondrial membrane potential, intracellular Ca^{2+} levels, the release of cytochrome c, the expression of B-cell lymphoma/leukemia-2 (Bcl-2) family protein and apoptosis induced by the complexes have been investigated under fluorescence microscopy. All complexes showed strong inhibitory effect towards selected cancer cells. Their IC_{50} values ranged from 1.2 μM – 17.3 μM . The data revealed that these complexes, Fig. 27(a–c) have high ability to inhibit cell growth in A549 cells with very low IC_{50} value of

3.2 μ M, 4.8 μ M and 1.2 μ M, respectively. The antitumor *in vivo* trial showed that the complex in Fig. 27(c) can inhibit tumour growth with an inhibitory rate of 76.34 %. The studies on the mechanism of action have indicated that these complexes caused apoptosis in A549 cell via a ROS-mediated lysosomal-mitochondrial dysfunction pathway. In addition, the interaction of the complexes with BSA, was explored. The complexes could also cause DNA damage and inhibit cell growth at G₀/G₁ phase [75].

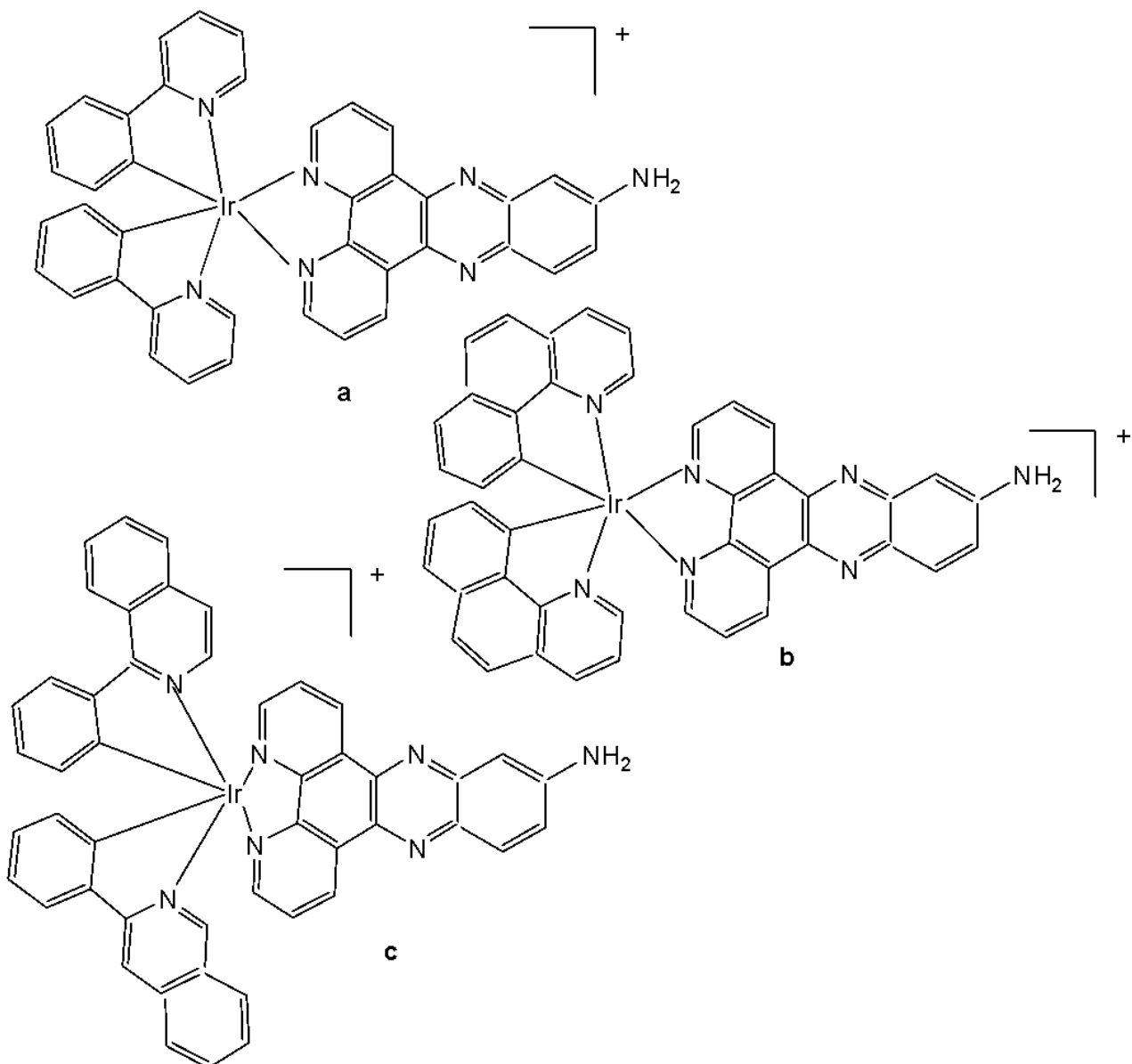


Fig. (27): Ir(III) complexes $[\text{Ir}(\text{ppy})_2(\text{adppz})](\text{PF}_6)$, $[\text{Ir}(\text{bzq})_2(\text{adppz})](\text{PF}_6)$ and $[\text{Ir}(\text{piq})_2(\text{adppz})](\text{PF}_6)$.

Other examples of substitutionally inert Ir(III) anticancer compounds have been reported by Lo and co-workers [76-78]. The authors have prepared a series of biological probes containing inert cyclometalated Ir(III) centers such as those depicted for a biotinyl reagent [76-78]. Luminescent tris(chelate) Ir(III) fragments were connected to substrates (indole, biotin) for biological target molecules via long alkyl chains attached to a polypyridyl ligand (bpy-dppz). Cytotoxicity similar to that of cisplatin was established towards the human cervix epithelioid carcinoma HeLa cells and found to correlate with the compounds' lipophilicity. A series of organoiridium(III) polypyridine complexes $[\text{Ir}(\text{N}^{\text{C}}\text{N})_2](\text{PF}_6)$ of $\text{HN}^{\text{C}} = 2\text{-phenylpyridine}$, 1-phenylpyrazole and 2-phenylquinoline with

$N^{\wedge}N$ ligands bearing an alkyl pendant: 4-*n*-octadecylaminocarbonyl-4'-methyl-2,2'-bipyridine, 4-*n*-decylaminocarbonyl-4'-methyl-2,2'-bipyridine and 4-ethylaminocarbonyl-4'-methyl-2,2'-bipyridine, shown in Fig. 28, have been synthesised and characterized [76]. The lipophilicity of the polypyridine complexes $[\text{Ir}(\text{N}^{\wedge}\text{C})_2(\text{bpy}-\text{C}_n\text{H}_{2n+1})]^+$ ($n = 18, 10, 2$) (Fig. 28) bearing an aliphatic alkyl chain ranged from -0.34 to 9.89 [76]. Although efficient internalization of the complexes was supposed to be assisted by high lipophilicity, the most lipophilic complex of this family $[\text{Ir}(\text{pq})_2(\text{bpy}-\text{C}_{18}\text{H}_{37})]^+$ was taken up the least efficiently by cells. This could be a consequence of it having the largest molecular size and/or undergoing a higher degree of self-aggregation in aqueous solution [76].

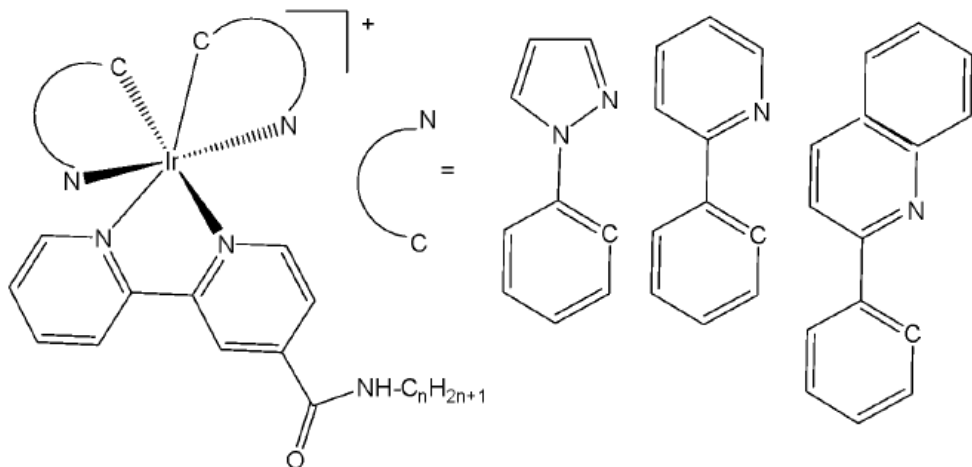


Fig. (28): Structure of the complexes $[\text{Ir}(\text{N}^{\wedge}\text{C})_2(\text{bpy}-\text{C}_n\text{H}_{2n+1})]^+$.

A series of luminescent cyclometalated Ir(III) polypyridine indole complexes with the general formula $[\text{Ir}(\text{N}^{\wedge}\text{C})_2(\text{N}^{\wedge}\text{N})](\text{PF}_6)$, where $\text{HN}^{\wedge}\text{C} = 2\text{-phenylpyridine, 7,8-benzoquinoline, 2-phenylquinoline}$ (Fig. 29) and $\text{N}^{\wedge}\text{N} =$ derivatives of 4-((2-(indol-3-yl)ethyl)aminocarbonyl)-4'-methyl-2,2'-bipyridine have been synthesised, characterized, and their photophysical and electrochemical properties and lipophilicity investigated [77]. Indole is known to bind to bovine serum albumin (BSA). The interactions of the Ir(III) complexes with BSA, have been studied. In addition, the cytotoxic activity of Ir(III) complexes against human cervix epithelioid carcinoma HeLa cell line has been tested. The IC_{50} values of Ir(III) complexes, ranging from 1.1 to $6.3 \mu\text{M}$, were significantly lower than that of cisplatin against HeLa cells [77]. Furthermore, the cellular uptake of the complexes has been investigated by flow cytometry and laser-scanning confocal microscopy [78].

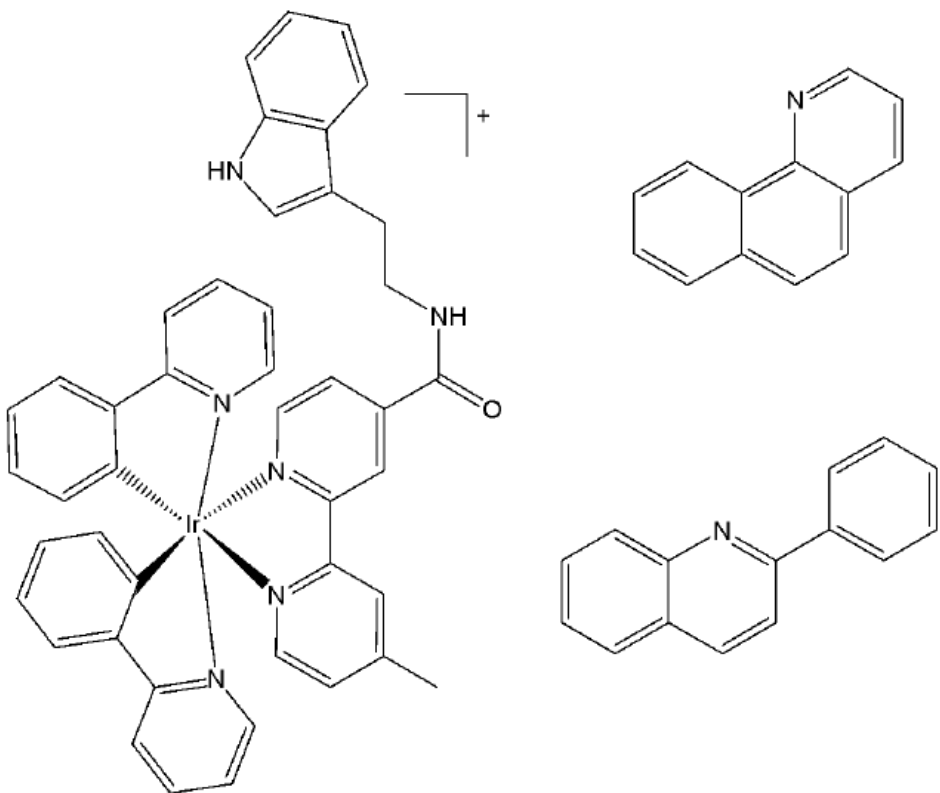


Fig. (29): Structure of $[\text{Ir}(\text{N}^{\wedge}\text{C})_2(\text{N}^{\wedge}\text{N})](\text{PF}_6)$ with $\text{N}^{\wedge}\text{C}$ = 2-phenylpyridine, 7,8-benzoquinoline, 2-phenylquinoline ligands.

Chen *et al.* have synthesised and reported Ir(III) complexes, shown in Fig. 30(a-d), for tracking mitochondrial dysfunction. These complexes were designed to function by controlling the protonation of the benzimidazole and carboxyl groups. The complexes were tested for cytotoxicity on A549, A549R and Hep-G2 cells and all complexes were found to be non-cytotoxic in the dark, but highly toxic to cells after light radiation [79]. It has been found that the complexes in Fig. 30(b), Fig. 30(c) and Fig. 30(d) could be used in efficient cancer photodynamic therapy. The phototoxicity followed the order: Fig. 30(d) > 30(c) > 30(b) > 30(a). These pH-responsive probes can be used to monitor changes in mitochondrial pH and detect mitochondrial damage during photodynamic therapy (PDT), providing a convenient method for *in situ* assessment of therapeutic effects and treatment outcomes. The studied complexes also generated abundant intracellular ROS, such as ${}^1\text{O}_2$ and exhibited high phototoxicity against cancer cells (Fig. 30) [79].

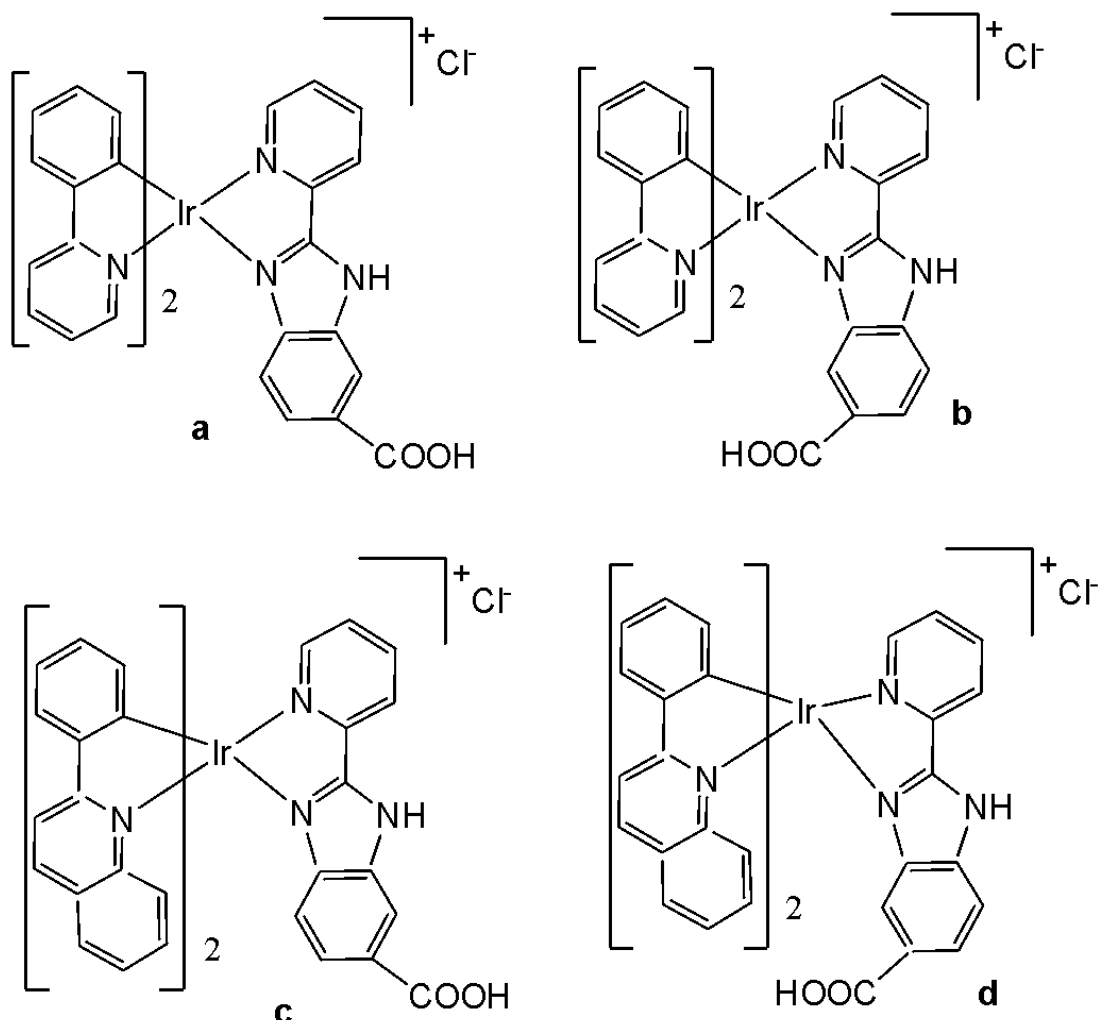


Fig. (30): Isomeric phosphorescent Ir(III) complexes.

Apart from benzimidazole, other ligands of the benzoxazole and benzothiazole type have been studied in the synthesis of new iridium(III) complexes. Novel bicyclometalated octahedral Ir(III) compounds $[(cf_3piq)_2Ir(N^+N)][PF_6]$, based on two different heterocyclic ligands, have recently been designed [80]. The used C⁺N ligand is 1-(4-(trifluoromethyl)phenyl)isoquinoline ((cf₃piq)), and the variable auxiliary N⁺N ligands are 2-(pyridine-2-yl)-1H-benzo[d]imidazole, 2-(pyridine-2-yl) benzo[d]oxazole and 2-(pyridine-2-yl)benzo[d]thiazole (Fig. 31). The structure-property relationships of these complexes have been discussed by spectroscopic, computational, and electrochemical studies. The cytotoxicity of the complexes against A-431, HeLa and SGC-7901 tumour cell lines has been evaluated using the MTT method. The complexes with 2-(pyridine-2-yl) benzo[d]oxazole and 2-(pyridine-2-yl)benzo[d]thiazole have shown better inhibition with respect to 2-(pyridine-2-yl)-1H-benzo[d]imidazole derivative and cisplatin. The introduction of O and S atoms into the secondary ligands has induced increased antineoplastic activity. Microscopic study has shown that 2-(pyridine-2-yl) benzo[d]oxazole and 2-(pyridine-2-yl)benzo[d]thiazole derivatives could enter cells, causing changes in cell morphology, which indicated biocompatibility for bioimaging applications [80].

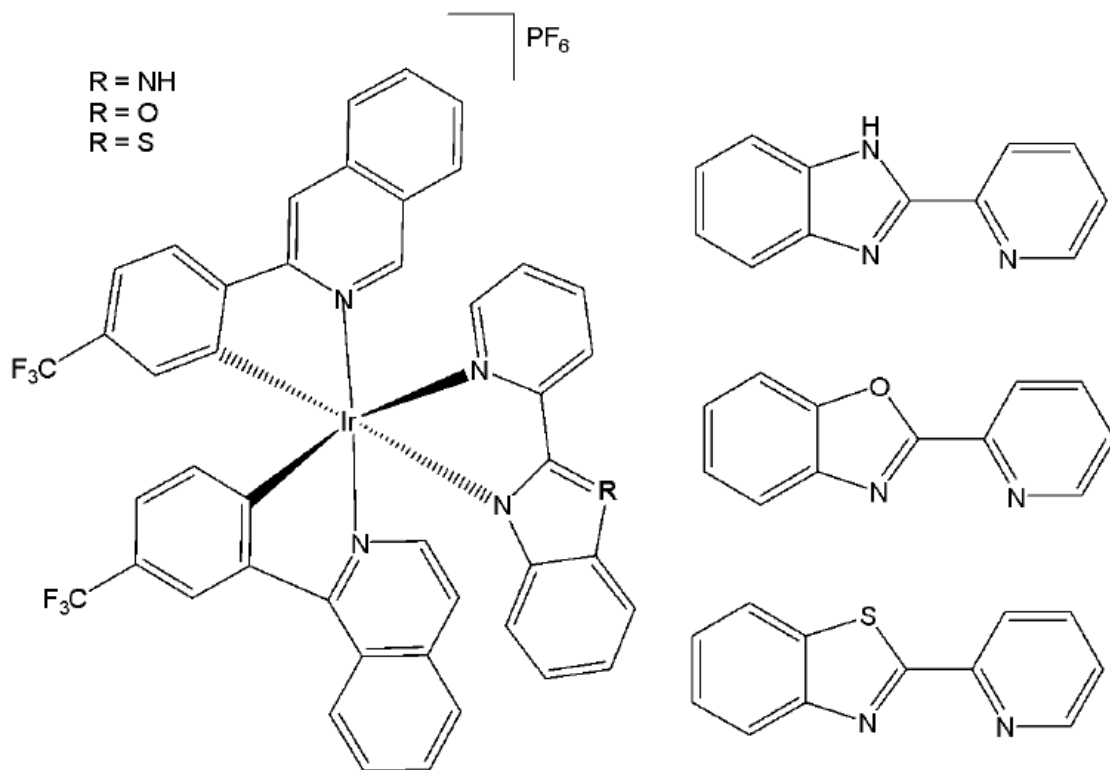


Fig. (31): Ir(III) compounds with 1-(4-(trifluoromethyl)phenyl)isoquinoline ligand and N⁺N co-ligands.

Zhang *et al.* have synthesised three Ir(III) complexes with formulas [Ir(ppy)₂(ipbc)](PF₆) Fig. 32(a), [Ir(bzq)₂(ipbc)](PF₆) Fig. 32(b), [Ir(piq)₂(ipbc)](PF₆) Fig. 32(c), containing aldehyde groups, where ppy = 2-phenylpyridine, bzq = benzo [h]quinolone, piq = 1-phenylisoquinoline, ipbc = 4'-(1H-imidazo [4,5-f][1,10]phenanthrolin-2-yl)-(1,10 -biphenyl)-4-carbaldehyde. The antineoplastic activity was investigated by cytotoxicity, apoptosis, cellular uptake, reactive oxygen species, mitochondrial membrane potential, autophagy, cell invasion, cell cycle arrest, intracellular Ca²⁺ levels, release of cytochrome c, tubules and western blot analysis [81]. The cytotoxicity studies were carried out by MTT assay with Bel 7402, A549, HeLa and Hep G2 cells in both the dark and light. These complexes have shown no cytotoxicity in dark. However, upon irradiation with white light they showed cytotoxicity towards Bel 7402 and HeLa cells. The complex in Fig. 32(c) showed inhibitory effects on cell growth against all the tested cells. The order of cytotoxicity towards Bel 7402 cells was Fig. 32(a) > 32(b) > 32(c), and was observed that the complex in Fig. 32(b) showed higher cytotoxicity than cisplatin. The IC₅₀ values of the complexes in Fig. 32(a) and Fig. 32(b) were 5.5 and 7.3 μM. The effect of complexes on mitochondrial membrane potential (MMP) followed the order Fig. 32(c) > 32(b) > 32(a). These complexes increased intracellular ROS and Ca²⁺ levels and entered into mitochondria causing decrease in MMP, thus inducing the release of cytochrome c. They inhibited cell invasion and cell growth at S phase, causing apoptosis (Fig. 32).

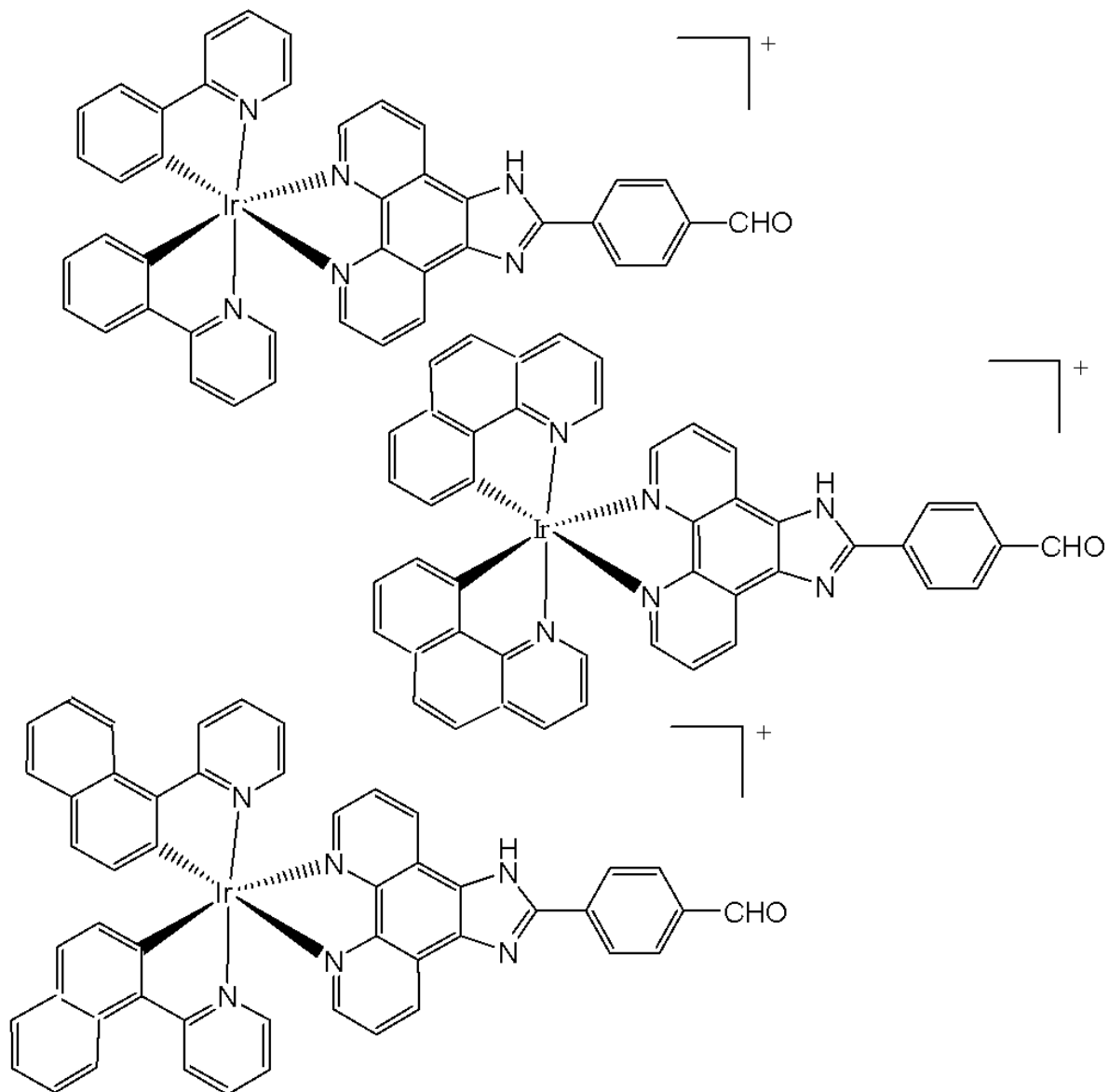


Fig. (32): Structures of $[\text{Ir}(\text{ppy})_2(\text{ipbc})](\text{PF}_6)$, $[\text{Ir}(\text{bzq})_2(\text{ipbc})](\text{PF}_6)$ and $[\text{Ir}(\text{piq})_2(\text{ipbc})](\text{PF}_6)$ complexes.

Qin *et al.* have obtained two iridium(III) complexes, Fig. 33(a and b), with β -carboline alkaloid ligands. These complexes showed high potency towards cell lines tested with IC_{50} ranging between $0.52 \mu\text{M}$ and $1.3 \mu\text{M}$ [25]. The complex in Fig. 33(a) was 97 times more active than cisplatin in lung cancer A549 cells. The complexes were 10 times less cytotoxic towards HLF cells, suggesting selectivity of these complexes towards cancer cells. Both these complexes were effective singlet oxygen photosensitizers (PSs). Studies have shown that they exhibit excellent anticancer activity in the dark, with their antineoplastic effects further enhanced in the presence of light. The complex in Fig. 33(a) could induce intercellular reactive oxygen species levels to overproduce and ATP to fall under dark conditions. In the presence of light, it could specifically be enriched in the mitochondria to damage mitochondrial DNA, increase lipid peroxidation levels and inhibit proteasome activity in cells. The complex in Fig. 33(a) is self-medicated PDT. The photophysical properties of complexes were studied at room temperature in CH_2Cl_2 , CH_3CN , and phosphate-buffered saline. The complexes exhibited two leading absorption bands at $250\text{--}360 \text{ nm}$ and $370\text{--}450 \text{ nm}$, corresponding to inter-ligand transitions and singlet and triplet metal-to-ligand charge transfer transitions, respectively [25]. Overall, it has been demonstrated that these iridium complexes have dual activities of chemotherapy and

photodynamic therapy, which may help to design new metal-based anticancer agents for combined chemo-photodynamic therapy.

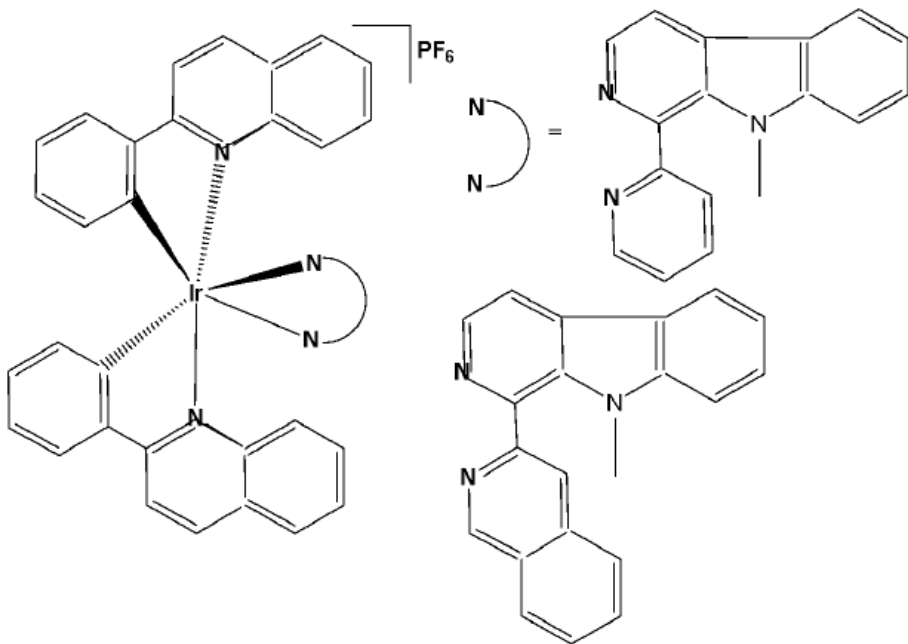


Fig. (33): Iridium(III) complexes with β -carboline alkaloid ligands.

He *et al.* developed iridium(III)- β -carboline complexes that not only caused an increase in ROS in the cell but also triggered the destruction of the cell by an autophagy mechanism. The authors reported the synthesis and anticancer investigations of two red-emitting Ir(III) complexes, shown in Fig. 34a and Fig. 34b, with an N⁺N ligand based on β -carboline [82]. The antineoplastic properties of the two complexes and their ligands were tested against A549, A549cisR, HepG2, HeLa, and Lo2 cell lines by MTT assay. As a result, the complexes outperformed cisplatin in terms of antiproliferative activity against the tested malignant cell lines, and the complex in Fig. 34b was more active than cisplatin in A549cisR cells. A similar study on HepG2 and Lo2 cells revealed that both complexes were more potent in malignant cells. TEM images of A549 cells treated with the complexes in Fig. 34a and Fig. 34b demonstrated the initiation of the autophagic process with the production of autophagic vacuoles and autolysosomes. The interactions between autophagy and the complex in Fig. 34b were investigated using 3-methyladenine, an autophagy inhibitor, to examine the autophagy-inducing mechanism of the complex in Fig. 34b. These findings showed that the complex in Fig. 34b functioned as an autophagy promoter in cancer cells. The complex in Fig. 34b increased ROS levels in A549 cells, and it has been proposed that intracellular ROS play a crucial role in triggering autophagy. Additionally, apoptosis assays showed that the complex in Fig. 34b only induced caspase-independent autophagic cell death, whereas cisplatin-induced cell death was through both apoptotic and caspase-dependent pathways.

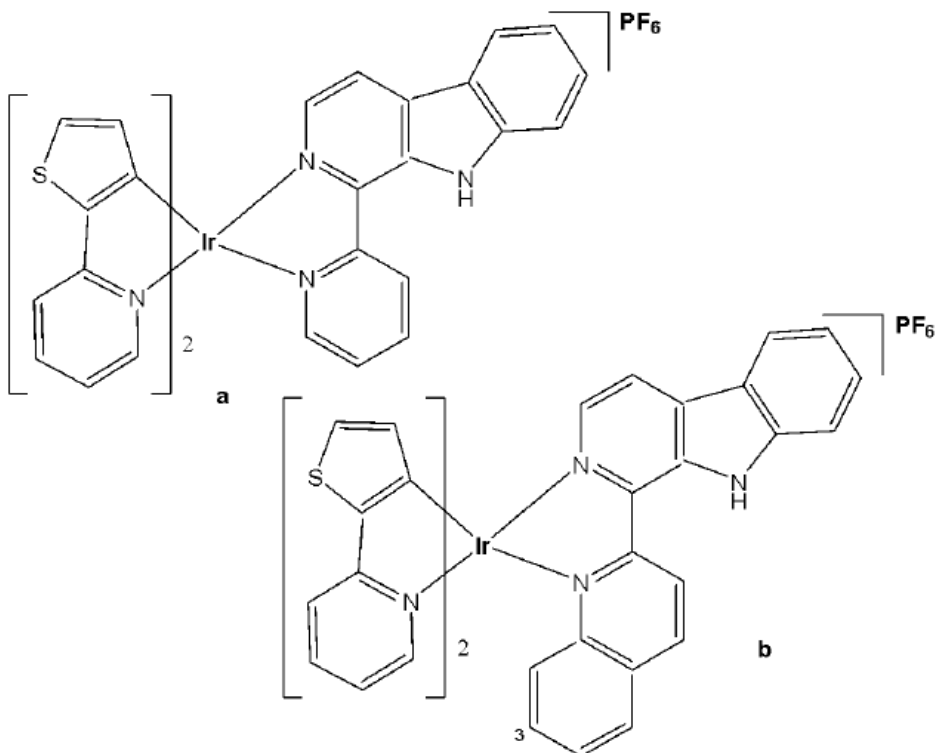


Fig. (34): Iridium(III)– β -carboline complexes.

Based on the previous work [42], He *et al.* have reported iridium(III) complexes with β -carboline ligands as pH-responsive tumor/lysosome-targeted PDT agents. Lysosomes (pH 4.5–5.5) contain a variety of hydrolytic enzymes that are capable of degrading almost all kinds of biomolecules. Imidazole and benzimidazole groups, which are known to be important pharmacophores and pH-responsive groups, were introduced to the β -carboline ligands to enhance their selectivity toward cancer cells and sensitivity to acidic environments. Since tumour microenvironments and lysosomes are typically acidic (pH \approx 5–6), this can lead to protonation-driven activation or localization of the studied complexes. Additionally, the dual role of the β -carboline moiety, as both a biological targeting unit and an extended π -conjugated chromophore for light absorption, could be elaborated to emphasize its multifunctional contribution. Ir(III) complexes with the general formula $[\text{Ir}(\text{N}^{\wedge}\text{C})_2(\text{N}^{\wedge}\text{N})](\text{PF}_6)$ (the complexes in Fig. 35(a-d), where $\text{N}^{\wedge}\text{C}$ = ppy (2-phenylpyridine) or dfppy (2-(2,4-difluorophenyl)pyridine); $\text{N}^{\wedge}\text{N}$ = (1-(2-imidazolyl)- β -carboline or (1-(2-benzimidazolyl)- β -carboline), have been synthesised [43]. The pH-response could be achieved with the introduction of the protonation sites on the imidazole and benzimidazole groups. On the other hand, the selectivity toward acidic environment could be enhanced by the presence of the β -carboline ligand.

The cytotoxicity in the dark and PDT activity of the complexes, Fig. 35(a-d), β -carboline $\text{N}^{\wedge}\text{N}$ ligands, the dimeric iridium(III) precursors and cisplatin were assessed against human lung carcinoma A549 cells, cisplatin-resistant A549cisR cells, breast cancer MCF-7 cells and human normal liver LO2 cells. The complexes bearing (1-(2-imidazolyl)- β -carboline as $\text{N}^{\wedge}\text{N}$ ligand displayed moderate cytotoxicity in the dark in A549 cells, whereas the IC_{50} values determined for the complexes in Fig. 35(a) and Fig. 35(c) were 19.5 and 29.9 μM , respectively. Negligible cytotoxicity in the dark in A549 cells was observed for complexes Fig. 35(b) ($\text{IC}_{50} \geq 100 \mu\text{M}$) and Fig. 35(d) ($\text{IC}_{50} = 55.6 \mu\text{M}$) that incorporated (1-(2-benzimidazolyl)- β -carboline ligand. Similar results were also observed in A549cisR, MCF-7 and LO2 cells. The complexes showed similar lipophilicity values (1.97–2.12), with a greater cell penetration for the smaller imidazole-derivatives. In terms of the mechanism of action, it should be noted that the

imidazole-containing complexes (Figs. 35a and 35c) displayed higher cytotoxicity than their benzimidazole analogues (Figs. 35b and 35d), which may correlate with their smaller steric bulk effect and better cellular uptake.

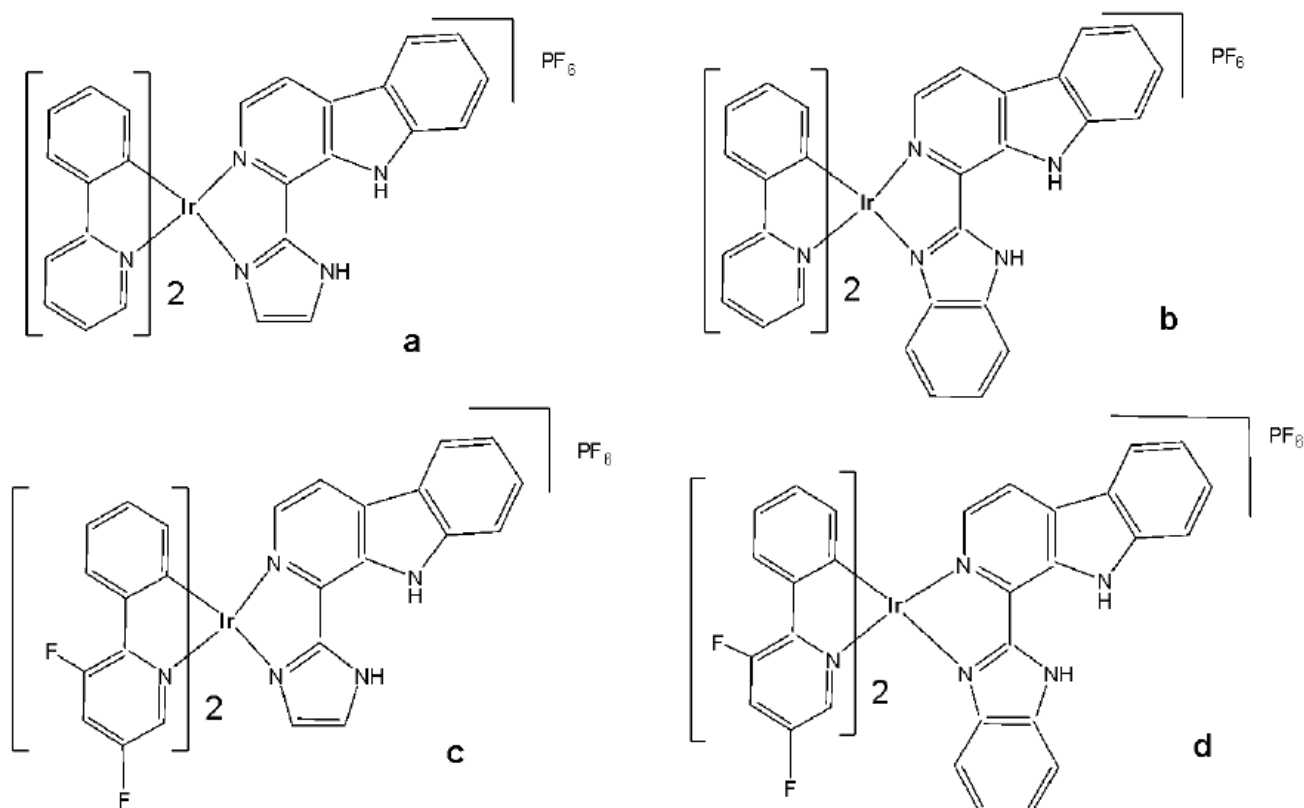


Fig. (35): Iridium(III) complexes with 1-(2-imidazolyl)- β -carboline or (1-(2-benzimidazolyl)- β -carboline ligands.

These complexes showed enhanced phosphorescent emission and ROS generation (${}^1\text{O}_2$) in tumour/lysosome-related acidic environments ($\text{pH} \leq 6.5$). Complex in Fig. 35(b) displayed remarkable phototoxicity against cancer cells and high selectivity for cancer cells over normal cells. Mechanism studies have shown that complex-mediated PDT in Fig. 35(b) mainly induced caspase- and ROS-dependent apoptotic cell death through lysosomal damage and cathepsin B release. Even if all the complexes localised within the lysosomes, the complex shown in Fig. 35(b) appeared more promising for tracking lysosomal integrity during PDT, providing a reliable and convenient method for *in situ* monitoring of treatment outcomes and therapeutic effects. Stimuli-responsive iridium complexes with longer absorption/emission wavelengths or larger multi-photon absorption cross-sections were likely to be more valuable for the image-guided therapy of deep-seated tumours. Overall, this work provided new insight into the design of multifunctional theranostic phosphorescent metal complexes as intelligent targeted PDT agents that can enhance tumour selectivity and monitor the therapeutic outcome simultaneously [43,44]. Later, the same research group designed new cyclometalated Ir(III) complexes incorporating benzimidazole derivatives as ancillary ligands, which demonstrated dual anticancer activities as both effective photosensitizers (PSs) and metastasis inhibitors [44]. The studied Ir(III) complexes could effectively inhibit several cancerous processes, including cell migration, invasion, colony formation, and angiogenesis.

Guan *et al.* have reported a series of mitochondria-targeting cyclometalated oncosis-inducing cationic Ir(III) complexes with benzothiazole substituted ligands (Fig. 36) and their antitumor cellular

investigation [66]. Oncosis, or “ischemic cell death”, could be referred to a distinct cell-death mechanism, which is a non-apoptotic form of programmed cell death (PCD). It differs from apoptosis in both morphological characteristics and intracellular pathways, and may hold the key to overcoming a significant challenge in cancer therapy – drug-resistance, which often arises from tumours’ intrinsic resistance to apoptosis. All the metal complexes $[\text{Ir}(\text{ppy})_2(\text{bbtb})]^+$, $[\text{Ir}(\text{DFppy})_2(\text{bbtb})]^+$, $[\text{Ir}(2\text{pq})_2(\text{bbtb})]^+$, and $[\text{Ir}(\text{pbt})_2(\text{bbtb})]^+$ possessed two substituted benzothiazole units in the bpy-based N^N ligand (4,4'-bis(benzothiazole-2-yl)-2,2'-bipyridine (bbtb)) and different common cyclometalating ligands (e.g. ppy, dfppy, pq and pbt). The chemical derivatives were tested against more than 10 cancer cell lines from various body parts including lungs, colon, kidneys, and liver, 10 drug-resistant cancer cell lines as well as two noncancerous cell lines (normal liver cells HL-7702 and normal kidney cells HEK 293). They showed IC_{50} values indicating considerable cytotoxicity against various cancer cells and drug-resistant cell lines, with selectivity towards normal cell lines. On the other hand, these Ir(III) complexes were all localised in the mitochondria of A549cisR cells. In contrast to the other typical Ir(III) antitumor agents, the enhanced ROS level was determined not to express the caspase 3/7 activity for the complexes, thus not inducing caspase-dependent apoptosis. In order to probe the origin of oncosis induced by these complexes, the membrane permeability and porin expression were studied in detail. The results confirmed that the Ir(III) complexes activated the oncosis-specific protein porin and calpain in cisplatin-resistant cell line A549R [66].

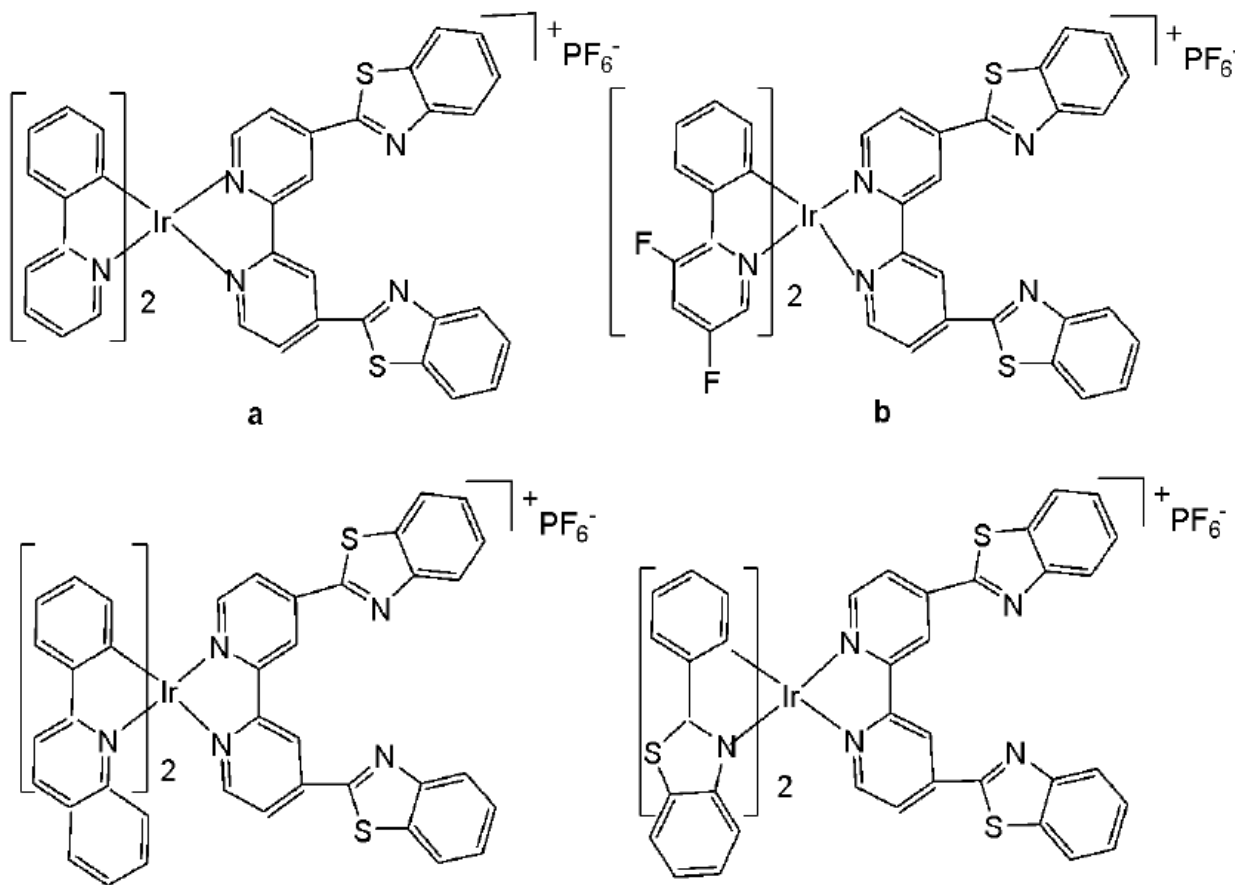


Fig. (36): Ir(III) complexes with benzothiazole substituted ligands.

Ye *et al.* synthesised and reported valproic acid (VPA)-functionalized cyclometalated Ir(III) complexes, Fig. 37(a-f), which exhibited excellent two-photon properties and were highly efficient for live cell imaging [32]. Valproic acid (short-chain, fatty acid) is a histone deacetylase inhibitor (HDACi), which enables cell cycle arrest [83]. By conjugation of valproic acid to Ir(III) complexes

through an ester bond, VPA-functionalized cyclometalated iridium(III) complexes, shown in Fig. 37(a-c) and their analogous complexes Fig. 37(d-f), were designed and synthesised. These complexes displayed excellent two-photon properties, which were favourable for live-cell imaging. The ester bonds in them could be hydrolysed quickly by esterase and display similar inhibition of HDAC activity to VPA. Four groups of entities were used to probe their antiproliferative activity: Ir(III) complexes, hydrolyzed Ir(III) complexes, mixtures of VPA with hydrolyzed Ir(III) complexes, and cisplatin. The order of their antiproliferative efficacy was Fig. 37(a), 37(b), 37(c) > 37(d), 37(e), 37(f). The cytotoxicity studies were determined by MTT assay against human hepatocellular liver carcinoma HepG2, human normal liver cell lines LO2, human cervical carcinoma HeLa and human primary carcinoma A549, with the values for Fig. 37(a) ($IC_{50} = 1.0 \mu\text{M}$), for Fig. 37(b) ($IC_{50} = 0.79 \mu\text{M}$) and for Fig. 37(c) ($IC_{50} = 1.3 \mu\text{M}$), being approximately 70, 89 and 54.5 times more potent than cisplatin against A549R cancer cells. Notably, the VPA-conjugated complexes can overcome cisplatin resistance effectively and are about 54.5–89.7 times more cytotoxic than cisplatin against cisplatin-resistant human lung carcinoma A549R cells. The complexes exhibited 6.6-, 4.4-, and 4.1-fold lower cytotoxicity against LO2 cells, indicating that they possess a certain selectivity toward human tumour cells. Hence, the VPA-conjugation effectively enhanced the anticancer potency of Ir(III) complexes. Mechanistic studies have indicated that iridium(III) complexes, shown in Fig. 37(a-c), penetrated human cervical carcinoma (HeLa) cells quickly and efficiently, accumulated in mitochondria, and induced a series of cell-death-related events mediated by mitochondria. Mechanistic studies of cell death, including ROS level elevation, cell cycle arrest, and caspase-activated apoptosis, indicated that Ir(III) complexes effectively inhibit tumour cell growth [32].

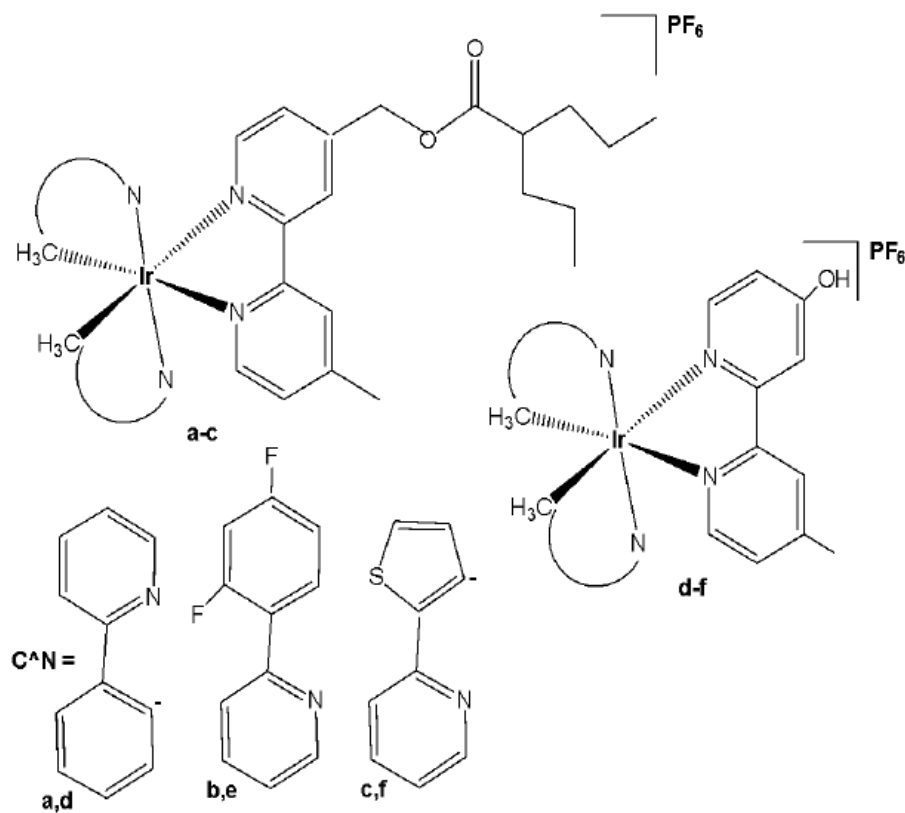


Fig. (37): Structures of valproic acid functionalized cyclometalated iridium(III) complexes.

Yuan *et al.* have described iridium complexes (Fig. 38a-c) that target the endoplasmic reticulum, a crucial organelle responsible for protein synthesis, folding, transport, and the maintenance of Ca^{2+} homeostasis [84]. The synthesis of a series of ER-targeted Ir(III) complexes (Fig. 38a-c) as photodynamic therapy (PDT) photosensitizers, featuring a gradually extended conjugation in the

primary ligand, and the investigation of the relationship between conjugation extent and PDT performance have been conducted. The results have shown that all of the presented complexes could accumulate in the ER and effectively induce cell apoptosis after PDT therapeutics by an ER stress mechanism, and both their singlet oxygen quantum yields and cytotoxicity increased as the conjugation area extended. All complexes showed PDT potency towards different cancer cell lines. Among them, the complex in Fig. 38(b) showed an impressive PI value (94.3) compared to cisplatin against A549 cells with an IC_{50} down to 0.65 μ M, acting as an efficient PDT photosensitizer. Studies have shown that post PDT-ER, stress-induced apoptosis accompanied by Ca^{2+} efflux from the ER occurs, indicating that this complex could be a potential photosensitizer, with apoptosis resulting from severe and prolonged ER stress [84].

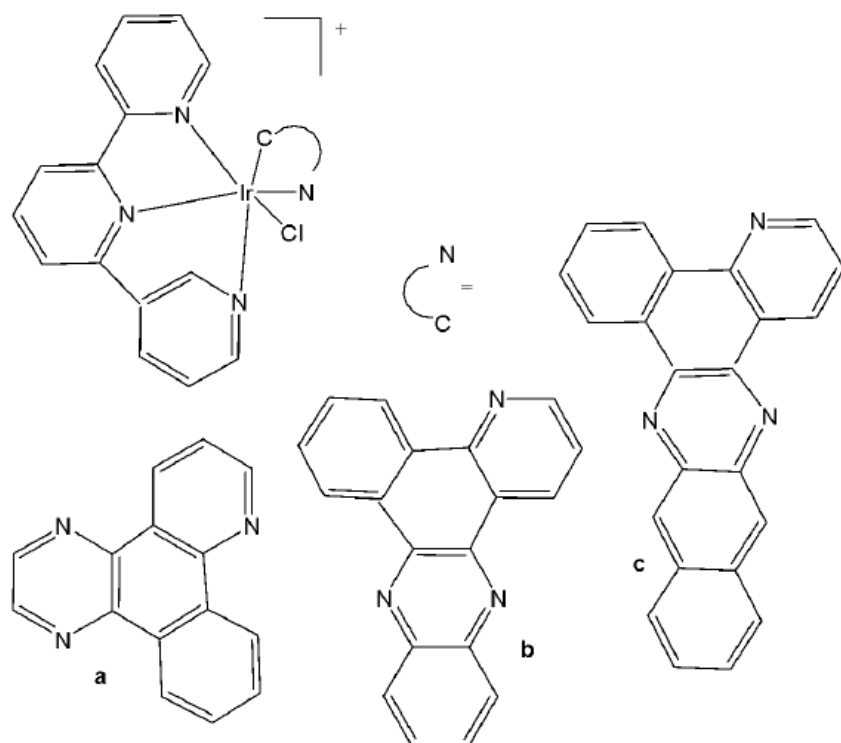


Fig. (38): Structures of terpyridyl ER-targeted Ir(III) complexes.

Zhang *et al.* have obtained novel nanoparticles (NPs) comprising Zr-MOF, a biscyclometalated Ir(III) complex (Fig. 39) and a dual responsive BP-PDM-PG as an antitumor delivery platform [85]. The nanoparticles entered the tumour cells via endocytosis and caused enhanced lysosome escape due to ROS production of the iridium(III) complex. This complex demonstrated efficient PDT, exhibiting red-shifted absorption and emission bands with NIR luminescence, making it highly suitable for real-time cell imaging with an improved signal-to-noise ratio. It also showed good biocompatibility in the dark [85].

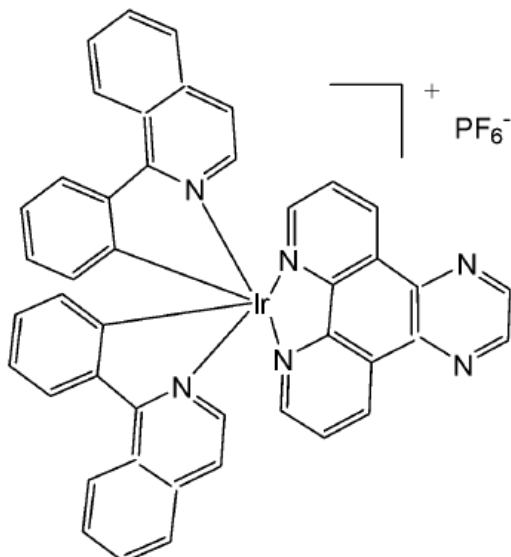


Fig. (39): Structure of biscyclometalated Ir(III) complex.

The best complementary rational approach to designing Ir(III) complexes with increased activity involves the coordination of ligands that themselves are cytotoxic and that can potentially participate in specific interactions with the biological targets. This approach may also improve the pharmacokinetic properties and bioavailability of the coordinated ligands through factors such as charge modification, enhanced solubility and cellular uptake. The use of the pharmacophore benzimidazole as a ligand has given rise to a wide variety of metal-based compounds that act either as antiangiogenic and/or antitumor agents. The integration of anticancer activity of benzimidazoles into cyclometalated Ir(III) complexes could provide, therefore, an opportunity for the construction of novel theranostic platforms.

It has been reported that biscyclometalated iridium(III) compounds bearing C^N ligands based on the benzimidazole core were able to photo-potentiate their activity in tumour cells due to a significant enhancement of intracellular ROS [86]. Within the group of Ir(III) organometallic and coordination complexes, the development of small heterocyclic chelating ligands has been carried out successfully to obtain promising metallodrugs with anticancer potency. A series of Ir(III)-based compounds with cyclometalated benzimidazole ligands (Fig. 40) and their cytotoxicity evaluation against epithelial ovarian carcinoma A-2780, A-2780cisR, colon cancer HT-29, breast cancer T-47D cell lines has been reported [87]. Their apoptosis, accumulation, cell cycle arrest, protein binding and DNA binding effects were also discussed. The complexes were synthesised by employing the heterocyclic C^N ligand 1-butyl-2-phenyl-1H-benzo[d]imidazole-5-carboxylate of methyl. The effects of different substitution (methyl, butyl, benzyl groups) on the benzimidazole nitrogen which modulated the lipophilicity, hydrophilicity and ultimately the cytotoxicity of the metal complexes have been studied. It was found that the phenyl substitution at the C4 position was a determining factor for the SAR analysis. All iridium(III) derivatives of the first series (Fig. 40) were more active than cisplatin towards the A-2780cisR, HT-29 and T-47D lines in the following order Me > Bnz > nBu > cisplatin. The complexes showed high apoptosis, good accumulation and S-phase cell arrest and strongly bonded to HSA at sites I and II and also weakly bonded to DNA at the minor groove.

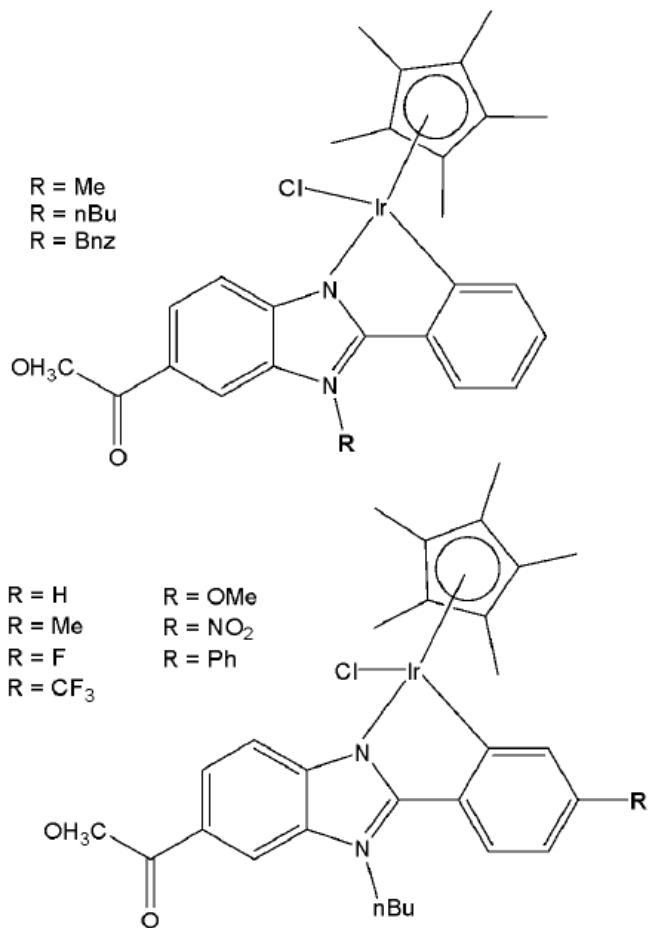


Fig. (40): Iridium(III) compounds with cyclometalated benzimidazole ligands.

Another class of various biscyclometalated Ir(III) complexes with imidazole-based ligands of varying alkyl chain length have attracted attention for their stability, biocompatibility, selectivity, and antitumor activity. The attendance of alkyl chains in the ligands of variable size is identified to play a key role in solubility, emission behavior and cell uptake. Some of these derivatives have been alkylated at N1 of the benzimidazole to observe their influence on biological activity. The C^N ligands 1-nonyl-2-phenyl-1H-benzo[d]imidazole and 1-isopentyl-2-phenyl-1Hbenzo[d]imidazole have been used in the synthesis of octahedral Ir(III) complexes, Fig. 41, [88]. The complexes were found to be luminescent with a moderate emission quantum yield and lifetime in CH₃CN. The compounds were tested against MCF-7 cancer and MCF-10 normal cell lines. The *in vitro* growth inhibition assay of the complexes with a shorter alkyl chain (complexes of 1-isopentyl-2-phenyl-1Hbenzo[d]imidazole) displayed higher antineoplastic activity (IC₅₀ < 0.5 μ M) compared to the complexes with a longer alkyl chain (complexes of 1-nonyl-2-phenyl-1H-benzo[d]imidazole) with IC₅₀ < 30 μ M against human breast cancer MCF-7 cells. The flow cytometry assay and fluorescence microscopy analysis suggested that cellular accumulation was primarily responsible for the variation in anticancer activity. Therefore, tuning the anticancer activity and cellular imaging property mediated by the alkyl chain would be of great importance and would be useful in anticancer research. Additionally, some N^N donating aromatic bidentate ancillary ligands based on 2,2'-bipyridine and 1,10-phenanthroline have also been studied [88]. It has been indicated that there was an obvious relationship between the cellular accumulation and antitumor activity with the size of the alkyl chain existing in the compounds. The alkyl chain variation has allowed not only modulation of antitumor activity, but also of luminescent potential properties.

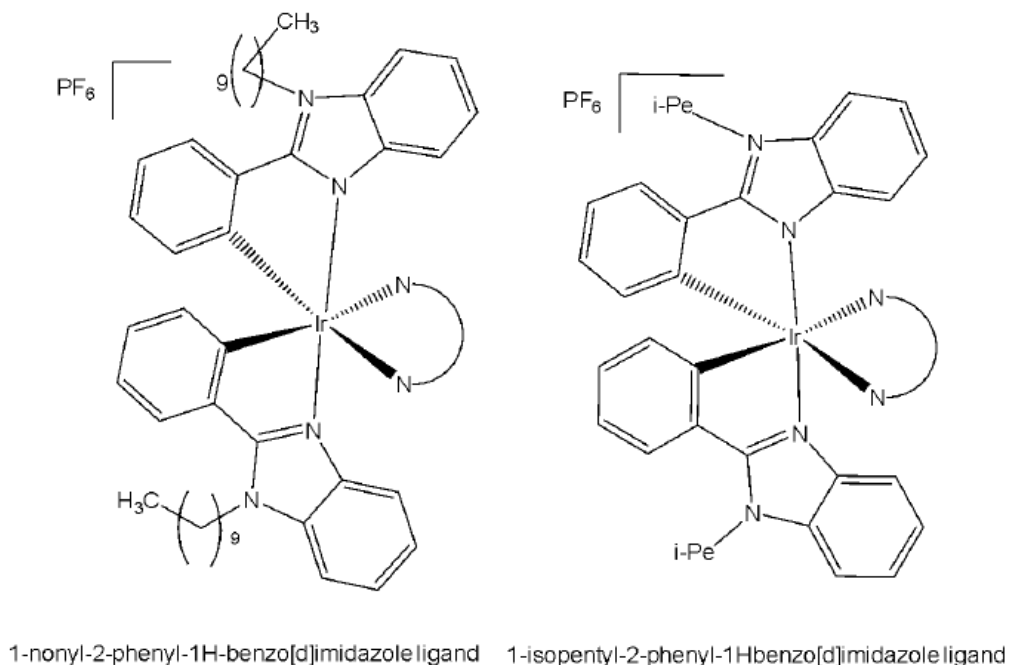


Fig. (41): Iridium compounds with two cyclometalated benzimidazole ligands.

Similar to platinum-based drugs, iridium(III) complexes can form adducts with DNA very easily, triggering apoptotic cell death. A series of luminescent biscyclometalated antitumor derivatives of the type $[\text{Ir}(\text{III})(\text{C}^{\text{N}})^2(\text{N}^{\text{N}})]\text{PF}_6$ of benzimidazole-based N^{N} bidentate ligands with ester and n-butyl groups for their functionalization in C5 and N1 positions have been reported [89]. The complexes had distorted octahedral structures. Two of the N^{N} ligands were attached with a methyl ester as a handle for further chemical functionalization in the future. Different substituents in the ligands have allowed to improve the lipophilic properties of iridium(III) complexes. Iridium(III) complexes with functionalized ligands 2-(pyridine-2-yl)-1H-benzo[d]imidazole, 1-butyl-2-(pyridine-2-yl)-1H-benzo[d]imidazole-5-carboxylate of methyl and 1-butyl-2-(quinoline-2-yl)-1H-benzo[d]imidazole-5-carboxylate of methyl have been synthesised, Fig. 42, [89]. The cytotoxicity tests have been performed with the malignant A-2780, A-2780cisR, MCF-7(ER+) and MDAMB-231 cell lines, as well as the benign BGM cell line. These complexes have exhibited low IC_{50} values in the nanomolar order against the ovarian and breast cancer cell lines, some of them being 100 times more active than cisplatin in MDAMB-231. The least active were the iridium(III) complexes with 2-(pyridine-2-yl)-1H-benzo[d]imidazole ligand, because of the lesser lipophilicity of the ligand. Almost all of the compounds have shown low cytotoxicity against normal BGM cells. The bioimaging experiment was performed based on red-emitting complexes and A2780 cells, and it was found that the complexes were predominantly localized in actin cortex, which was a protein-based modulator for cell membrane and cell surface behaviors, as shown by confocal luminescence microscopy. This discovery could open the door to a new large family of drug bioconjugates with diverse and simultaneous functions. In addition, the authors proposed that the higher hydrophobicity probably accounted for their higher anticancer potency against the cancer cells. On the other hand, the ICP-MS analysis of metal contents in nuclear DNA and total cellular RNA in MCF-7 cells revealed the high antineoplastic potency was not associated with the nucleic acids binding, according to the investigation of the metal levels in nuclear DNA and total cellular RNA in MCF-7 cells.

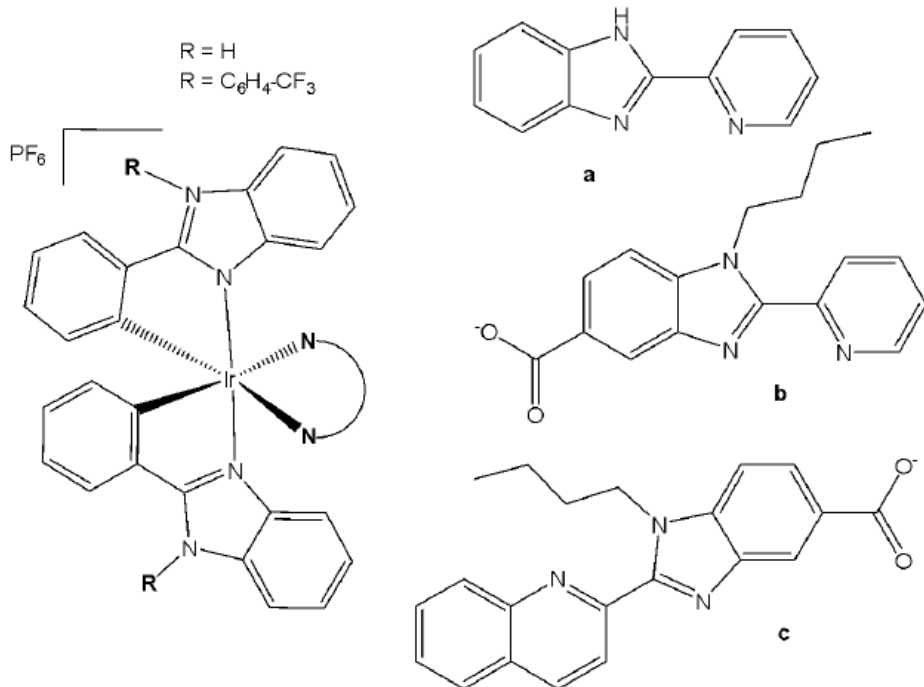


Fig. (42): Iridium compounds with one functionalized 2-(pyridine-2-yl)-1H-benzo[d]heteroazole ligand and N⁺C bidentate co-ligands.

Bicycometalated iridium(III) compounds have displayed good potential as PDT candidates in the treatment of different types of cancer, as shown above. A series of kinetically inert bis-cyclometalated octahedral [Ir(III)(C⁺N)₂(N⁺N)]PF₆ compounds of 2-phenyl-1-(4-(trifluoromethyl) benzyl)-1H-benzo[d]imidazole (C⁺N) and a second highly aromatic N⁺N donor ligands based on 1,10-phenanthroline, dipyrdo[3,2-d:2',3'-f]quinoxaline, dipyrdo[3,2-a:2',3'-c]phenazine, benzo[i]dipyrdo[3,2-a:2',3'-c]phenazine, and dipyrdo[3,2-a:2',3'-c]phenazine-10,11-imidazolone. The effect of the degree of π conjugation of the polypyridyl ligand on the toxicity in cancer cells has been investigated. The cytotoxic activity of the compounds was evaluated against A-2780, A-2780cisR, HeLa, and MCF-7 tumour cell lines, as well as against the healthy MCF-10A cell line. The less lipophilic compounds with 1,10-phenanthroline and dipyrdo[3,2-d:2',3'-f]quinoxaline have exhibited an activity greater than that of cisplatin in the tested A2780, HeLa, and MCF-7 tumour cells and showed the lowest level of cellular accumulation. The complexes displayed the capability to overcome acquired and inherent resistance to conventional cisplatin (in A2780cisR and MCF-7 cells, respectively). The results have suggested that a greater cytotoxic potency and less lipophilicity were promoted by decreasing the size of the auxiliary N⁺N ligand. The authors have demonstrated that the Ir(III) complexes, unlike clinically used platinum antitumour drugs, do not kill cells through the DNA damage response. Instead, they killed cells by inhibiting protein translation by targeting preferentially the endoplasmic reticulum. The obtained findings have also revealed that the toxic effect of the Ir(III) complexes could be significantly potentiated by irradiation with visible light (by more than two orders of magnitude). The photo-potentiation of the studied Ir(III) complexes could be attributed to a marked increase (\approx 10–30-fold) in intracellular reactive oxygen species. Together, these data highlighted the functional diversity of anticancer metal-based drugs and the usefulness of a mechanism-based rationale for selecting candidate agents that are effective against chemo-resistant tumours for further preclinical testing. All compounds have overcome the resistance to cisplatin and have exhibited greater selectivity than cisplatin towards malignant cells with regard to benign ones [90].

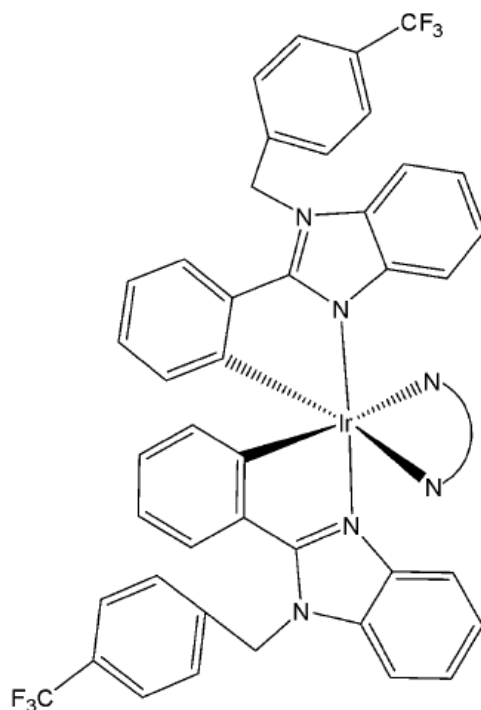


Fig. (43): Iridium compound with two cyclometalated 2-phenyl-1-(4-(trifluoromethyl)benzyl)-1H-benzo[d]imidazole ligands.

Somatostatin receptor-targeted luminescent iridium(III) biscyclometalated complexes and their hypothetical application as targeted theranostics have been reported [91]. A new series of antitumor complexes $[\text{Ir}(\text{III})(\text{C}^{\wedge}\text{N})_2(-\text{N}^{\wedge}\text{N})]\text{PF}_6$ (Fig. 44), featuring highly distorted octahedral geometries, have been employed as octreotide peptide-based tumor-targeting vectors to investigate their potential as theranostic agents [91]. In the studied highly cytotoxic and luminescent Ir(III) complexes, the $\text{C}^{\wedge}\text{N}$ ligand 1-phenylpyrazole was conjugated with $\text{N}^{\wedge}\text{N}$ ligands, 1-butyl-2-pyridyl- benzimidazole-5-carboxylate derivatives. Their cytotoxic effects against HeLa and MDA-MB-231 cells have been investigated. Methyl-substituted derivative has displayed higher antiproliferative activity, and it has been found that visible light irradiation led to a slight enhancement in IC_{50} values. The attachment of the Ir(III) complex to octreotide (OCT) was designed through the formation of an amide bond between a carboxylic function in the benzimidazole diimine ligand and the N-terminal end of the peptide sequence. Besides octreotide, the authors have also selected a dicarba analogue, since the replacement of the disulfide bond by a CH_2-CH_2 linkage increased stability in the reductive cellular environment without significantly altering the binding affinity for somatostatin receptors. Conjugation of Ir(III) derivative ($\text{R} = \text{H}$) with the peptide moieties octreotide (OCT-S or OCT- CH_2) correlated with its accumulation since peptide vehicles were non-cytotoxic and the cytotoxicity was increased in all cases upon visible light irradiation and ROS production was confirmed [91].

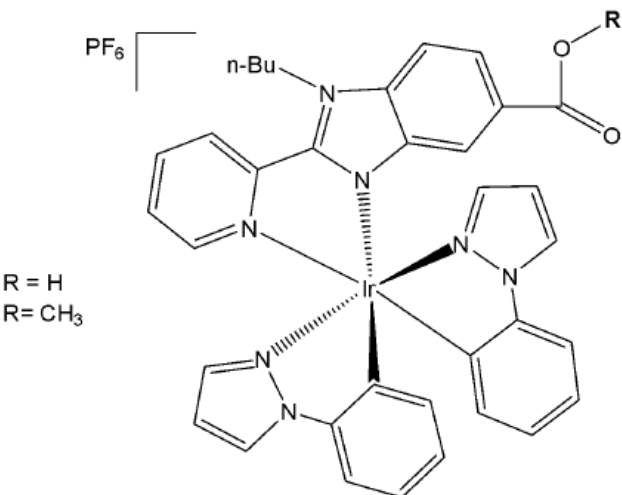


Fig. (44): Iridium compounds conjugated with octreotide peptides.

IV. OTHER IRIDIUM(III) COMPLEXES

4.1. Cyclopentadienyl Iridium Complexes

The half-sandwiched organo-iridium cyclopentadienyl anticancer complexes with cyclometalating agents and a chloride as a monodentate ligand are the most popular. Only some specific representatives of them are presented in this review. Hartinger *et al.* have reported that unstable dithio- and diselenobenzoquinones could be trapped by coordination to an $[(\eta^5\text{-C}_5\text{Me}_5)\text{Ir}]$ moiety thus resulting iridium complexes with anticancer activity, comparable to cisplatin [92]. The $\{\text{Cp}^*\text{Ir}\}$ fragment ($\text{Cp}^* =$ pentamethylcyclopentadienyl) is a stabilizing entity for isolation of reactive intermediates, often used for the synthesis of successful organometallic linkers to construct functional coordination assemblies. Quinones play an important role in scavenging of reactive oxygen species, in electron transport in the respiratory chain and photosynthesis. Their potential uses as anticancer drugs and central components of antibiotics have been investigated [93,94]. In contrast to benzoquinone, only a few quinones with heavier chalcogen elements have been reported, due to their inherent instability. The biological action of quinones is often linked to their electron-transfer rates and redox behavior. The replacement of the oxygen atoms in quinone by the heavier chalcogen atoms, sulfur or selenium, leads to highly reactive intermediates with functional groups $\text{C}=\text{E}$ ($\text{E} = \text{S, Se}$) [95]. It is noteworthy, that selenium is an essential dietary component for many living systems, and there is increasing evidence for the efficacy of certain forms of selenium as cancer-chemopreventive compounds.

In order to increase the stability of chalcogen-benzoquinone species, the $[(\eta^5\text{-C}_5\text{Me}_5)\text{Ir}]$ fragment has been introduced to the reactive dithio- and diseleno-benzoquinone species, leading to the isolation of the iridium complexes $[\text{Ir}(\eta^4\text{-C}_6\text{H}_4\text{E}_2)(\eta^5\text{-C}_5\text{Me}_5)]$, Fig. 45(a–c), [92,95]. The first stable η^4 -diseleno-p-benzoquinone complex, $[\text{Cp}^*\text{Ir}(\eta^4\text{-C}_6\text{H}_4\text{Se}_2)]$, has been isolated by Amouri *et al.* [95]. The X-ray structure confirmed the coordination of the elusive diselenobenzoquinone intermediate. The structure of diseleno-iridium complex (Fig. 45c) clearly showed that the Cp^*Ir moiety coordinated to only four diene carbons of the π -selenoquinone ligand. Inspection of the crystal packing in the complex (Fig. 45c) showed that the individual diselenoquinone molecules exhibited π – π interactions between the $\eta^5\text{-}\{\text{Cp}^*\text{Ir}\}$ moiety and the $\text{Se}=\text{C}$ unsaturated bonds in the $\eta^4\text{-}(\text{SeC}_6\text{H}_4\text{Se})$ unit of another selenoquinone complex, thus providing a one-dimensional supramolecular chain along a axis. Spectroscopic and structural data supported stabilization of the complex by metal-to-ligand π -backbonding.

The anticancer activity of this complex was compared to the related O and S analogues. The dithiobenzoquinone complexes, Fig. 45(a–c), have shown moderate cytotoxic activity toward A2780 cells, whereas the diselenobenzoquinone complex in Fig. 45(c), which contained the trapped unstable p-diselenobenzoquinone moiety, with $IC_{50} = 5 \mu\text{M}$, was as active as cisplatin ($IC_{50} = 3 \mu\text{M}$), although its mode of action is probably quite distinct. Indeed, the high cytotoxicity of the diselenobenzoquinone complex in Fig. 45(c) illustrates the role of selenium as an important element to combat cancer, and paves the way for the preparation of other functionalized selenoquinone metal complexes with medicinal properties. Modest cytotoxicity ($IC_{50} = 49 \mu\text{M}$ and $154 \mu\text{M}$) was established for the $\text{Cp}^*\text{Ir}(\text{III})$ complexes of o- and p-dithiobenzoquinone. Nevertheless, these sandwich complexes, Fig. 45(a–c), [92,95], were found to be highly potent towards A2780 cells, in striking contrast to its inactive p-benzoquinone Ir(III) analogue. Contrary to other iridium anticancer drugs described above, which were hypothesized to act by DNA targeting, the benzoquinone complexes acted in a mechanism similar to that of menadione. Although the mode of action of the benzoquinone complexes was not investigated, it seems probable that rapid release of Se or Se-containing metabolites will be responsible for the potency of the p-diselenobenzoquinone complex.

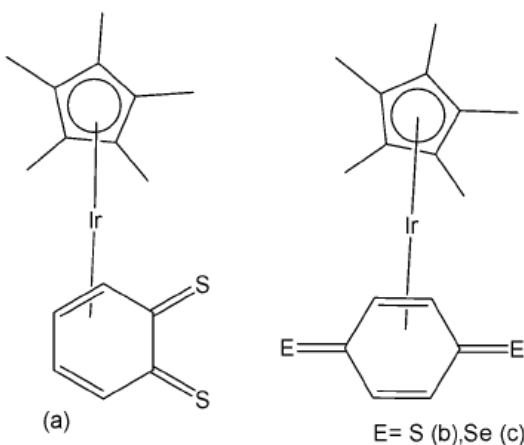


Fig. (45): Iridium compounds of dithio- and diselenobenzoquinones.

The low-spin $5d^6$ organo-iridium complexes with N,N-chelating agents and a chloride anion have been found to be highly unstable toward aquation but inactive as antineoplastic agents [96,97]. The cyclometalated complexes $[\text{Ir}(\text{N}^{\text{A}}\text{C})(\eta^5\text{-C}_5\text{Me}_5)\text{Cl}]$ with $\text{C}^{\text{A}}\text{N}$ ligands, such as 2-phenylpyridine, 2-(p-tolyl)pyridine, 2-phenylquinoline, 2-(2,4-difluorophenyl)pyridine, Fig. 46(d–g), have shown high activity toward A2780 human ovarian cancer cells with IC_{50} values ranging from 2.5 to $10.8 \mu\text{M}$, which are comparable to that of cisplatin ($1.2 \mu\text{M}$) [96]. The $\text{N}^{\text{A}}\text{O}$ complex $[\text{Ir}(\text{N}^{\text{A}}\text{O})(\eta^5\text{-C}_5\text{Me}_5)\text{Cl}]$ with 1,2-naphthoquinone-1-oximato ligand (Fig. 46h) exhibited much higher cytotoxicity toward HUVEC, HeLa, and HL60 cancer cell lines compared to cisplatin [98]. The remarkable cytotoxicity of this complex has been attributed to necrotic cell death. The $\text{N}^{\text{A}}\text{O}$ complex $[\text{Ir}(\text{N}^{\text{A}}\text{O})(\eta^5\text{-C}_5\text{Me}_5)\text{Cl}]$ with quinolin-8-ol (Fig. 46i) was not only cytotoxic toward SK-Mel, SNB-19, and C-32 cancer cells, but also active against Gram-positive bacteria including *M. luteus*, *S. aureus*, *E. faecalis*, and *S. epidermidis* [99]. The use of extended planar diimine ligands allowed the synthesis of organometallic complexes with the formula $[\text{Ir}(\text{N}^{\text{A}}\text{N})(\eta^5\text{-C}_5\text{Me}_5)\text{Cl}]^+$, Fig. 46(j–l), to initially intercalate into the base pairs of double-stranded DNA, which was followed by substitution of the labile chloride ligands by the N7 atom of purine bases [100,101]. Complexes were potent cytotoxic agents towards the human cancer cell lines MCF-7 and HT-29 and the *in vitro* cytotoxicity of the chlorido complexes was dependent on the size of the polypyridyl ligands. The dipyridophenazine (dppz) complex in Fig. 46k exhibited high cytotoxicity toward MCF-7 and HT-29 cells with IC_{50} values 2.3 and $7.4 \mu\text{M}$, respectively, similar to those of cisplatin (2.3 and $7.0 \mu\text{M}$, respectively).

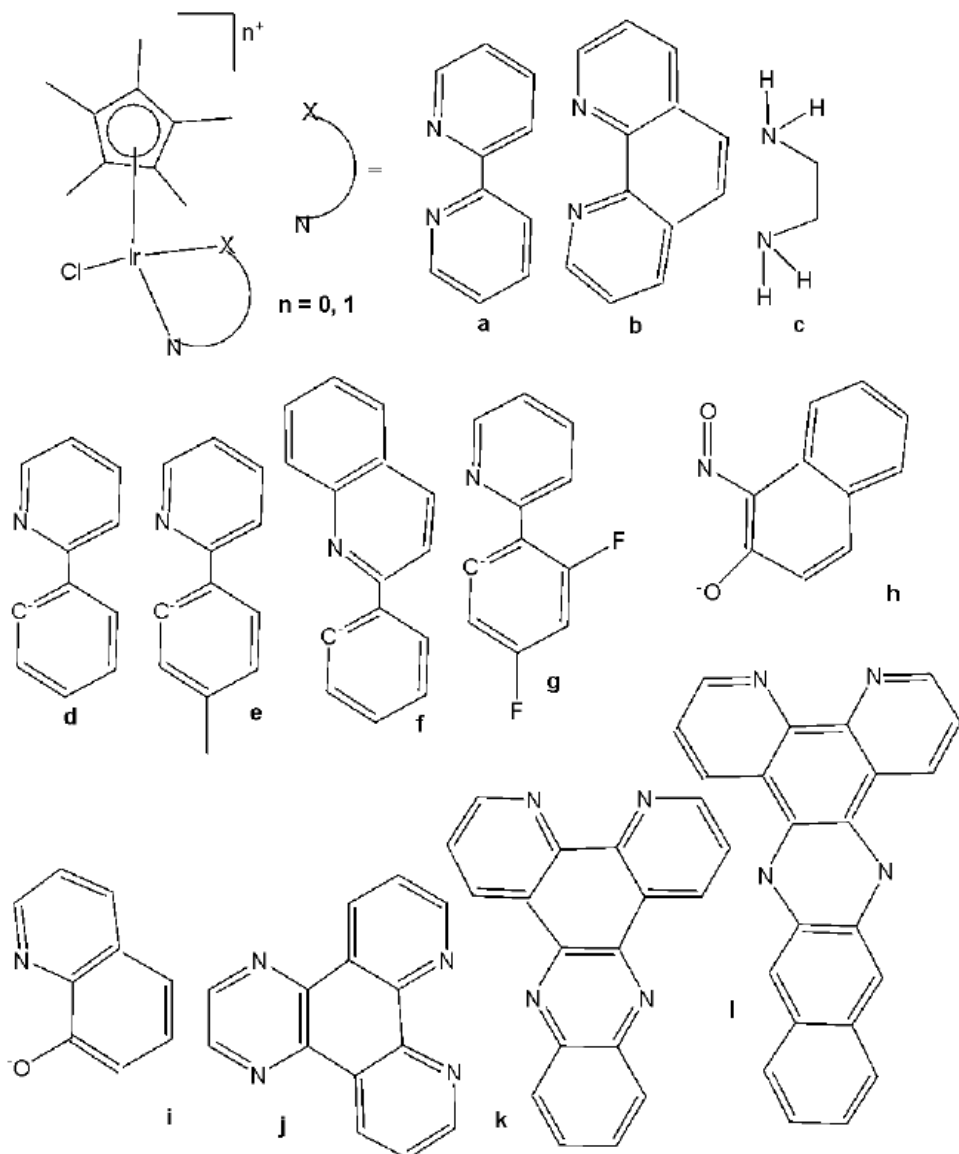


Fig. (46): Cyclopentadienyl iridium complexes with N^N , N^C and N^O cyclometalating ligands.

The obtained results of the activity of cyclopentadienyl iridium complexes with pyridine derivatives encouraged many scientific groups to explore the activity of complexes containing different N^N , N^C and N^O cyclometalating ligands. These half-sandwiched cyclopentadienyl iridium(III) complexes contained Cp^{xph} ($Cp^{xph} = C_5Me_4C_6H_5$ or tetramethyl-(phenyl)cyclopentadienyl) and C^N -bound 2-phenylpyridine (phpy) as the cyclopentadienyl and chelating ligands, and various pyridine derivatives as monodentate ligands Z (Fig. 47) [102]. The half-sandwich Ir(III) coordination compounds of the type $[(\eta^5-Cp^{xph})Ir(phpy)Z]PF_6$, where Z = pyridine or its derivatives, have been synthesised and characterized. Their antiproliferative activity toward A2780 human ovarian, A549 lung, and MCF-7 breast cancer cells has been investigated. All the complexes displayed high potency toward the tested human cancer cells, comparable and higher than that of cisplatin, thus being potent anticancer agents according to their *in vitro* studies. The antineoplastic activity could be adjusted by varying the pyridine-based ligands. The IC_{50} values of the complexes were less than that of cisplatin suggesting that all these complexes were highly active. The complex containing a 4-dimethylamine substituent on pyridine with IC_{50} value $0.20\ \mu M$ towards MCF-7 cell line was the most active (4–5 times more potent than cisplatin) with sub-micromolar activity in a wide range of cancer cell lines, particularly against leukemia, CNS cancer, colon cancer, and breast cancer [102]. In general,

complexes containing electron withdrawing groups on pyridine ring have shown less anticancer activity compared to complexes with electron donating groups. The antiproliferative investigations have shown that N,N-dimethylpyridin-4-amine (electron-donating) demonstrated an increased activity in the cell growth inhibition. Meanwhile, the high cytotoxicity of the complexes was attributed to the promotion of generation of intracellular ROS and the resultant collapse of mitochondrial membrane potential.

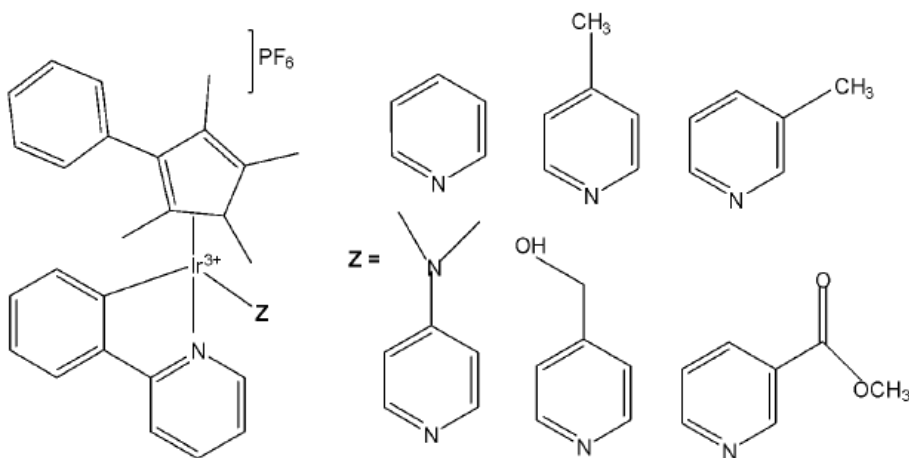


Fig. (47): Ir(III) tetramethyl-(phenyl)cyclopentadienyl complexes with 2-phenylpyridine

4.2. Other Iridium(III) Complexes

Four cyclometalated iridium(III) complexes, shown in Fig. 48(a-d), with 2,4-diamino1,3,5-triazine derivatives with the general formula $[\text{Ir}(\text{dfppy})_2(\text{py})_2(\text{L})]^+$, where dfppy = 2-(2,4-difluorophenyl)pyridine and L = 6-(pyridin-2-yl)-1,3,5-triazine-2,4-diamine, Fig. 48(a); 6-(isoquinolin-1-yl)-1,3,5-triazine-2,4-diamine, Fig. 48(b); 6-(quinolin-2-yl)-1,3,5-triazine-2,4-diamine, Fig. 48(c); 6-(isoquinolin-3-yl)-1,3,5-triazine-2,4-diamine, Fig. 48(d), have been described by Xiong *et al.* [103]. The mitochondria-specific target, cellular uptake and antitumor activity, as well as cell-cycle arrest and apoptosis signaling pathways of the compounds were investigated. The studies were carried out using MTS kit on various cancer cell lines which included MCF-7, NCI-H460, HePG2, Bel-7402, HCT-116, HeLa, A549 and cisplatin resistant cell line A5649R. The cytotoxicity results revealed that the complex 17(a) had activity comparable with cisplatin whereas the complexes in Fig. 48(b) and Fig. 48(c) showed higher cytotoxicity. Interestingly, the complex in Fig. 48(d) which is the isomer of Fig. 48(b) and Fig. 48(c) showed excellent activity towards many of the tested cell lines. Further studies have shown that the complexes had higher selectivity towards tumour cell lines than normal cell lines which was attributed to the mechanism of entering the cell which was different for both cancer and normal cell lines. The complexes in Fig. 48(a) and Fig. 48(b) showed higher selectivity whereas these in Fig. 48(c) and Fig. 48(d) showed selectivity almost similar to cisplatin. All these complexes could generate reactive oxygen species, and induce apoptosis by mitochondrial dysfunction [103]. As evidenced by ICP-MS, energy-independent pathway was the cellular uptake mechanism for LO2 cells while all the complexes were taken up by A549R cells via energy-dependent pathway. Moreover, the intracellular iridium amounts as well as the distribution of localisation of the complexes in A549R were similar.

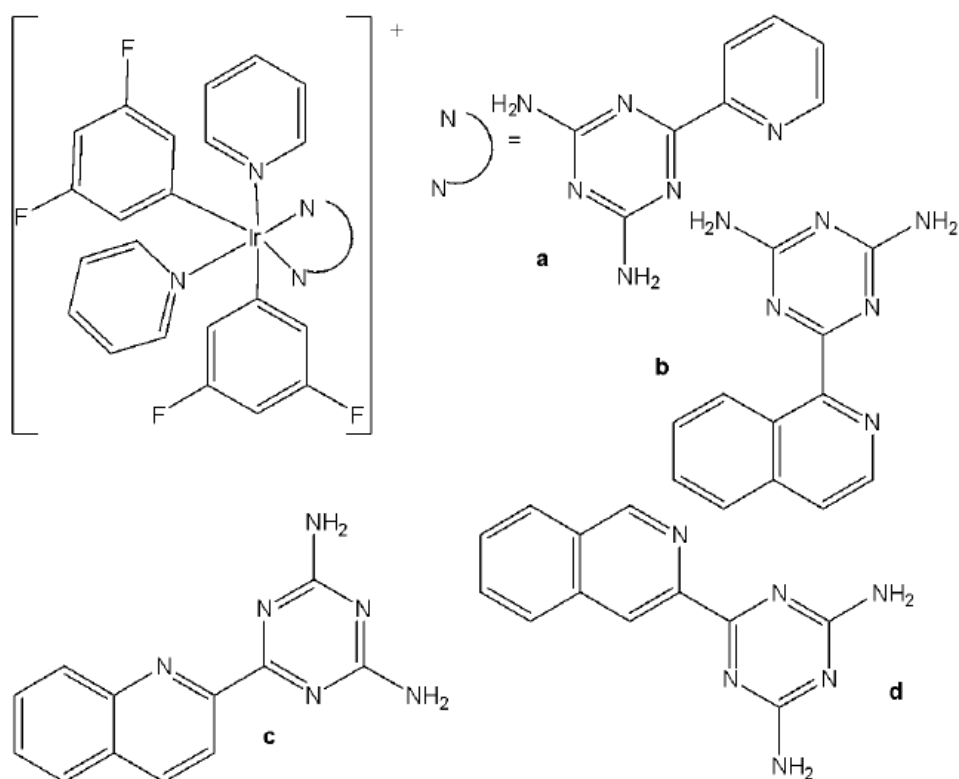


Fig. (48): Structures of Ir(III) complexes $[\text{Ir}(\text{dfppy})_2(\text{py})_2(\text{L})]^+$.

A range of substitutionally inert metal complexes, bearing unprotected maleimide moieties, have been specifically designed as structural analogues of known organic anticancer drugs or as topographically suitable substrates for enzyme active sites [104,105]. In the absence of redox activity, their mechanism of action must be based on non-covalent interactions such as p-stacking (intercalation) or hydrogen bonding to target molecules. Chemically inert noncytotoxic metal complexes are promising scaffolds for targeting enzyme active sites, which may allow them to serve as enzyme inhibitors. Meggers and co-workers have reported phototoxic activity for (diene)Ir(III) complexes, which contain a trans sited chelating pyridocarbazole ligand, originally designed as protein and lipid kinase inhibitors [104]. The studied pyridocarbazole complexes $[\text{Ir}(\text{pcz})(\text{cod})(\text{X})(\text{Y})]$, Fig. 49(a–e), bearing different substituents R at the maleimide nitrogen atom, were noncytotoxic and have been shown to inhibit the receptor tyrosine kinase FLT4, which plays an essential role in the maintenance of lymphatic vessels as well as in the development of the embryonic cardiovascular system [104]. The FLT4 inhibition properties were strongly dependent on the ligands X and Y. The dichloro complex in Fig. 49(a) showed the highest activity ($\text{IC}_{50} = 123 \text{ nM}$), and was much more potent than the dimethyl complex in Fig. 49(d) ($\text{IC}_{50} = 1007 \text{ nM}$). Also, the complex in Fig. 49(a) displayed high selectivity for FLT4 among 229 protein kinases. This complex was found to inhibit both angiogenesis in developing zebrafish embryos and cancer cell-induced angiogenesis. It strongly inhibited vessel formation of the zebrafish embryos being affected 3 days postfertilization at a concentration of $5 \mu\text{M}$. This bioactivity has been ascribed to FLT4 inhibition, because the complex in Fig. 49(f), having an identical coordination sphere around the iridium(III) center but lacking the protein inhibition ability, did not show any effect on the zebrafish assays because of a methylated maleimide moiety. It has been found that the free maleimide nitrogen atom was essential for being capable of forming two canonical hydrogen bonds with the hinge region of the ATP-binding site of protein kinases.

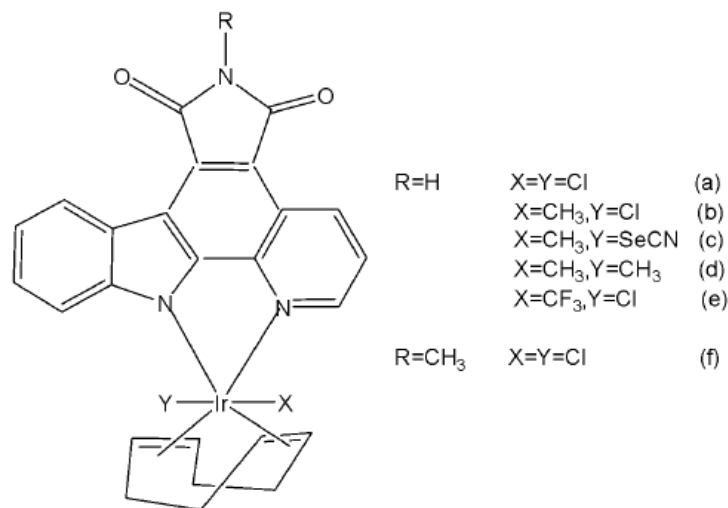


Fig. (49): Photocytotoxic (diene)Ir(III) protein kinase inhibitors.

Further studies of the same team have shown that the antiangiogenicity of the complex, shown in Fig. 50, was independent of light [105]. Interestingly, exposure to visible light for 1 h increased its cytotoxicity toward HeLa cells by *ca.* 34-fold and led to significant apoptosis. The investigation of photoreactivity revealed that, in the presence of chloride, visible light induced the substitution of the selenocyanate ligand with a chloride ligand. However, the reason why such ligand substitution led to efficient cellular apoptosis was unknown. This appeared to be the first time that phototoxicity has been observed for iridium complexes. The presence of the strongly labilizing methyl group was particularly beneficial for phototoxic activity and led in the case of the selenocyanate complex to rapid $\text{SeCN}^-/\text{Cl}^-$ substitution followed by cell apoptosis. Light-dependent antiangiogenic properties were also established for this compound using endothelial cell spheroids embedded in a collagen matrix [105,106].

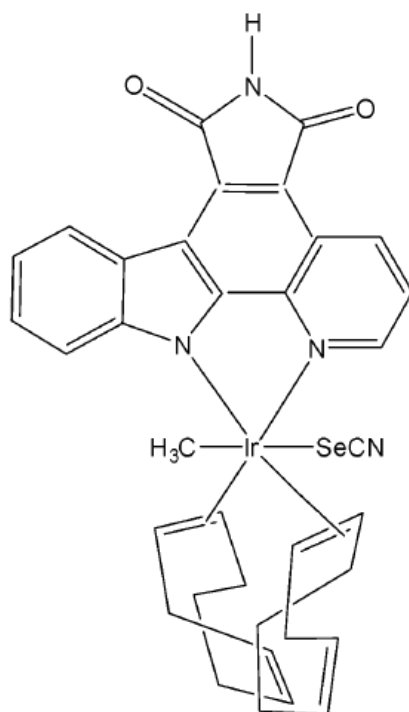


Fig. (50): Photocytotoxic (diene)Ir(III) complex with selenocyanate ligand.

Neutral metal complexes with 8-quinolinethiolate ligands displayed variable anticancer activity [107]. Most of them were very cytotoxic toward human fibrosarcoma HT-1080 and mouse hepatoma MG-22A cells. Among the 8-quinolinethiolate complexes $[M(N^S)_n]$ with different transition metals, the iridium(III) complex $[Ir(N^S)_3]$, Fig. 51(a), displayed the highest activity against human fibrosarcoma HT-1080, mouse hepatoma MG-22A, and mouse melanoma B-16 cells [107]. However, this complex was also highly cytotoxic toward NIH 3T3 normal mouse embryo fibroblasts, limiting its potential as an antineoplastic drug. It has been found that the nature of the substituent, its position in the quinoline ring, and the nature of the metal significantly affected the antitumor activity and toxicity of metal complexes of 8-quinolinethiolates. Interestingly, the introduction of a methyl group to the 4-position of the quinoline ring of these complexes significantly increased the selectivity of their cytotoxic activity. The iridium(III) 4-methyl-8-quinolinethiolate complex $[Ir(N^S)_3]$ in Fig. 51(b) was about 40 times more cytotoxic toward HT-1080 and MG-22A cancer cells than to 3T3 normal cells [108,109]. Systematic studies of the complexes with methyl- and methoxy-substituted 8-quinolinethiolate ligands revealed that complexes with high cytotoxicity substantially induced nitric oxide formation in the cells. The most cytotoxic towards human fibrosarcoma HT-1080 and mouse hepatoma MG-22A tumour cells was the iridium(III) 6-methoxy-8-quinolinethiolate complex, however it was highly toxic towards normal mouse embryonic NIH 3T3 fibroblasts. The iridium(III) 5-methyl-8-quinolinethiolate complex was somewhat less active to MG-22A cells but showed quite good selectivity because of its markedly lower toxicity. The iridium(III) 8-quinolineselenolate complexes $[Ir(N^Se)_3]$, Fig. 51(c–f), have shown analogous substituent-dependent cytotoxicity and selectivity [110,111]. The greatest selectivity in cytotoxic activity was noted for iridium(III) 4-methyl-8-quinolineselenolate complex. The cytotoxicity of the complexes was also found to be closely related to their ability to generate nitric oxide.

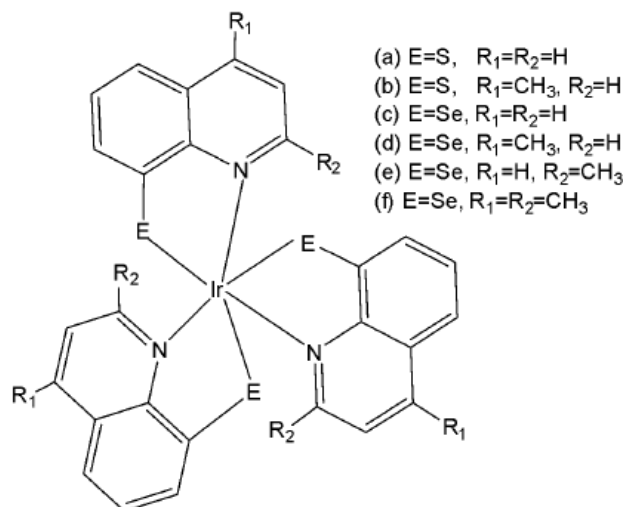


Fig. (51): Iridium(III) 8-quinolinethiolate and 8-quinolineselenolate complexes.

Recently, Conesa *et al.* have synthesised the iridium(III) half-sandwich complex with the formula $[Ir(\eta^5k^1-C_5Me_4CH_2py)(2\text{-phenylpyridine})]PF_6$, Fig. 52, where $C_4Me_4CH_2py = 2\text{-}((2,3,4,5\text{-tetramethylcyclopenta-1,3-dien-1-yl)methyl)pyridine}$, which was extraordinarily potent in a number of cancer cell lines [112]. The extraordinary feature of the structure of the complex resided on bearing a metal center sheltered by two chelate rings, one of which stabilized the metals' coordination sphere which helped to control the iridium reactivity. Thus, the metal was less eager to react with nucleophiles, it was preserved from detoxification, reaching with the biological targets more efficiently. The complex has been tested against A2780, HCT 116, MCF-7 cells and the results indicated that the complex, Fig. 52, had high sub-micromolar potency towards all human cancer cell lines with IC_{50} values between 0.11–0.82 μM , which means 85, 77, 25 and 15 times more potent than clinically used cisplatin in the tested MCF7, MDAMB231, HCT116 and A2780 cells, respectively. The complex

$[\text{Ir}(\eta^5\text{C}_5\text{Me}_4\text{CH}_2\text{py})(2\text{-phenylpyridine})]\text{PF}_6^-$ exclusively and effectively accumulated in the mitochondria of the human breast cancer MCF7 cell line, proven by cryo-3D correlative imaging method, which can be applied to a number of biochemical processes for specific elemental localisation within the native cellular landscape [112]. Furthermore, unique information is obtained toward the intracellular events at the essential metal level triggered by metallodrug exposure of cancer cells.

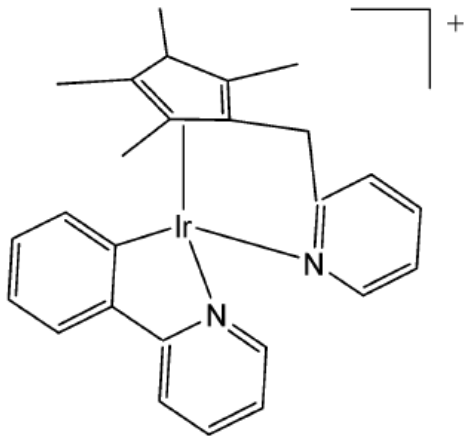


Fig. (52): Structure of Iridium(III) complex $[\text{Ir}(\eta^5\text{C}_5\text{Me}_4\text{CH}_2\text{py})(2\text{-phenylpyridine})]\text{PF}_6^-$.

Wang *et al.* have synthesised and reported a clickable iridium hydride complex, presented in Fig. 53, [113]. The cytotoxicity and production of reactive oxygen species study in A2780 and MCF-7 cancer cells indicated a potent anticancer activity of the iridium hydride complex towards A2780 cells with $\text{IC}_{50} = 0.98 \mu\text{M}$ and towards MCF-7 cells with $\text{IC}_{50} = 4.46 \mu\text{M}$, which was three times better value compared to cisplatin. The ICP-MS analysis and the cellular imaging suggested the accumulation of the iridium hydride complex in the nucleus and cytoplasm. Further label-free quantitative proteomic analysis indicated that the ECM–receptor interaction pathway was activated by the complex. The analysis of down-regulated proteins suggested that the complex affected cellular DNA transcription, post-translational glycosyl modification, and redox homeostasis. Besides, the complex also damaged several crucial proteins and enzymes in the mitochondria and nucleus, associated to cellular metabolism and DNA replication, leading to the disorder of the cellular processes. These results provided a new approach to mechanism studies of metallodrugs combining click chemistry and proteomic analysis [113].

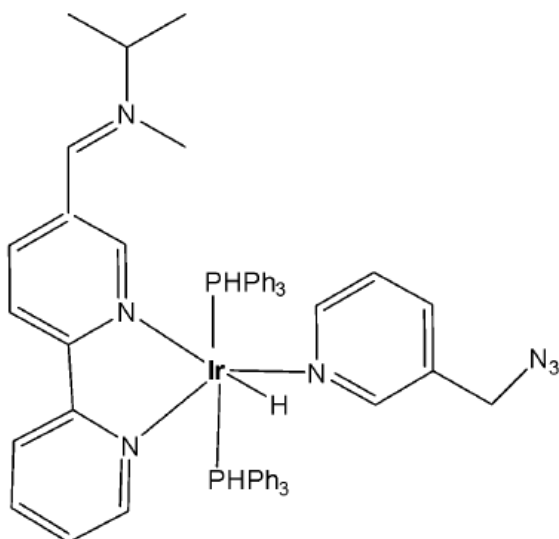


Fig. (53): Structure of iridium hydride complex.

V. CONCLUSION

The application of cyclometalated iridium(III) complexes as potential antitumor agents and cellular imaging probes has been extensively explored and reported. Although many known iridium(III) complexes are chemically inert, their cytotoxic activity can be enhanced by increasing the lability of the iridium–ligand bonds or by improving lipophilicity, which promotes cellular uptake. Numerous studies have demonstrated that the cytotoxic activity of these complexes depends on efficient cellular internalization, reactive oxygen species (ROS) generation, and cell cycle arrest—mechanisms that often differ from those induced by clinically used metal-based drugs. However, establishing a complete structure–activity relationship remains challenging.

It is noteworthy that most reported iridium(III) complexes exhibit IC_{50} values below 100 μM and show good selectivity and tolerance toward healthy cells. Their anticancer mechanisms are distinct from those of platinum-based drugs, offering cytotoxicity even against cisplatin-resistant cancer cell lines.

A significant strategy to enhance the biological activity of iridium(III) organometallic complexes involves incorporating organic ligands with known biological properties to design new complexes with improved therapeutic potential. The introduction of specific substituents into ligands can yield better activity and selectivity, novel mechanisms of action, and modified pharmacokinetic profiles. Furthermore, ligand functionalization enables organelle-targeted delivery—such as to lysosomes, mitochondria, nuclei, or subnuclear structures—broadening their biological applicability.

Unique structural and emissive characteristics, including structural complexity, tunable reactivity, diverse ligand substitution kinetics, redox versatility, high cellular uptake, and distinct spectroscopic features, make cyclometalated iridium(III) complexes promising scaffolds for modulation, sensing, and imaging of biological processes. These attributes contribute to the development of multifunctional reagents with broad biological and therapeutic applications.

Overall, the reviewed findings emphasize that this field of anticancer drug discovery warrants continued and systematic investigation to establish alternative classes of effective chemotherapeutic and theranostic agents. Nonetheless, challenges such as low aqueous solubility, off-target phototoxicity, limited *in vivo* stability, and difficulties in large-scale synthesis still impede clinical translation. It is expected that this review will serve as valuable guidance for the further development and rational design of these promising iridium-based anticancer candidates.

Authors' Contributions

The author confirms sole responsibility for the following: study conception and design, data collection, analysis and interpretation of results, and manuscript preparation.

Consent For Publication

Not applicable.

Conflict Of Interest

The author declares no conflict of interest, financial or otherwise.

Funding

None.

ACKNOWLEDGEMENTS

The financial support received by the European Union-Next Generation EU, through the National Recovery and Resilience Plan of the Republic of Bulgaria, project No. BGRRP-2.004-0004-Co1 is greatly acknowledged.

REFERENCES

1. Todorov, L.; Kostova, I. Recent Trends in the Development of Novel Metal-Based Antineoplastic Drugs. *Molecules*, **2023**, *28*(4), 1959.
2. Kostova, I. Rational Design and Synthesis of Bioactive Molecules. *Int. J. Mol. Sci.*, **2024**, *25*(18), 9927.
3. Kostova, I. Survey of Main Group Metals and Metalloids in Cancer Treatment. *Inorganics*, **2024**, *12*, 29.
4. Kostova, I. Rational Design of Metal-Based Pharmacologically Active Compounds. *Inorganics*, **2024**, *12*, 335.
5. Kostova I. Ruthenium Complexes as Anticancer Agents. *Curr. Med. Chem.*, **2006**, *13*(9), 1085-1107.
6. Jahromi, E.Z.; Divsalar, A.; Saboury, A.A.; Khaleghizadeh, S.; Mansouri-Torshizi, H.; Kostova I. Palladium complexes: new candidates for anti-cancer drugs. *J. Iran. Chem. Soc.*, **2016**, *13*(5), 967-989.
7. Kostova I. Platinum Complexes as Anticancer Agents, *Recent Pat. Rev. Anti -Canc. Drug Disc.*, **2006**, *1*(1), 1-22.
8. Shahlaei, M.; Asl, S. M.; Derakhshani, A.; Kurek, L.; Karges, J.; Macgregor, R.; Kostova, I.; Saboury A.A. Platinum-Based Drugs in Cancer Treatment: Expanding Horizons and Overcoming Resistance. *J. Mol. Struct.*, **2024**, *1301*, 137366.
9. Kostova, I. *Biological and Medical Significance of Chemical Elements*, Bentham Science Publishers, **2023**.
10. Ma, D. L.; Wu, C.; Wu, K. J.; Leung, C. H. Iridium (III) complexes targeting apoptotic cell death in cancer cells. *Molecules*, **2019**, *24*(15), 2739.
11. Cao, J. J.; Zheng, Y.; Wu, X. W.; Tan, C. P.; Chen, M. H.; Wu, N.; Mao, Z. W. Anticancer cyclometalated iridium(III) complexes with planar ligands: mitochondrial DNA damage and metabolism disturbance. *J. Med. Chem.*, **2019**, *62*, 3311–3322.
12. Kostova, I. Cytotoxic Organometallic Iridium(III) Complexes. *Molecules*, **2025**, *30*, 801.
13. Tan, C. P.; Zhong, Y. M.; Ji, L. N.; Mao, Z. W. Phosphorescent metal complexes as theranostic anticancer agents: combining imaging and therapy in a single molecule. *Chem. Sci.*, **2021**, *12*(7), 2357-2367.
14. Szymaszek, P.; Tyszka-Czochara, M.; Ortyl, J. Iridium (III) complexes as novel theranostic small molecules for medical diagnostics, precise imaging at a single cell level and targeted anticancer therapy. *Eur. J. Med. Chem.*, **2024**, 116648.
15. Liu, Z.; Salassa, L.; Habtemariam, A.; Pizarro, A. M.; Clarkson, G. J.; Sadler, P. J. Contrasting reactivity and cancer cell cytotoxicity of isoelectronic organometallic iridium(III) complexes. *Inorg. Chem.*, **2011**, *50*, 5777-5783.
16. Dörr, M.; Meggers, E. Metal complexes as structural templates for targeting proteins. *Curr. Opin. Chem. Biol.*, **2014**, *19*, 76-81.
17. Lo, K.K.W. Luminescent rhenium(I) and iridium(III) polypyridine complexes as biological probes, imaging reagents, and photocytotoxic agents. *ACC Chem. Res.*, **2015**, *48*, 2985-2995.
18. Ruiz, J.; Rodríguez, V.; Cutillas, N.; Samper, K. G.; Capdevila, M.; Palacios, O.; Espinosa, A. Novel C,N-chelate rhodium(III) and iridium(III) antitumor complexes incorporating a lipophilic steroid conjugate and their interaction with DNA. *Dalton Trans.*, **2012**, *41*, 12847-12856.
19. Li, T.Y.; Wu, J.; Wu, Z.G.; Zheng, Y.X.; Zuo, J.L.; Pan, Y. Rational Design of Phosphorescent Iridium(III) Complexes for Emission Color Tunability and Their Applications in OLEDs. *Coord. Chem. Rev.*, **2018**, *374*, 55–92.
20. Liu, Z.; Li, J.J.; Ge, X.X.; Zhang, S.; Xu, Z.; Gao, W. Design, Synthesis, and Evaluation of Phosphorescent Ir(III)Complexes with Anticancer Activity. *J. Inorg. Biochem.*, **2019**, *197*, 110703.

21. Anjong, T. F.; Kim, G.; Jang, H. Y.; Yoon, J.; Kim, J. Diiridium (iii) complexes: luminescent probes and sensors for G-quadruplex DNA and endoplasmic reticulum imaging. *New J. Chem.*, **2017**, *41*(1), 377–386.

22. Tso, K.K.S.; Lo, K.K.W. Strategic applications of luminescent iridium (III) complexes as biomolecular probes, cellular imaging reagents, and photodynamic therapeutics. *Iridium (III) in optoelectronic and photonics applications*, **2017**, 415–477.

23. Baschieri, A.; Muzzioli, S.; Fiorini, V.; Matteucci, E.; Massi, M.; Sambri, L.; Stagni, S. Introducing a new family of biotinylated Ir (III)-pyridyltriazole lumophores: Synthesis, photophysics, and preliminary study of avidin-binding properties. *Organometallics*, **2014**, *33*(21), 6154–6164.

24. Zamora, A.; Vigueras, G.; Rodríguez, V.; Santana, M. D.; Ruiz, J. Cyclometalated iridium (III) luminescent complexes in therapy and phototherapy. *Coord. Chem. Rev.*, **2018**, *360*, 34–76.

25. Qin, W. W.; Pan, Z. Y.; Cai, D. H.; Li, Y.; He, L. Cyclometalated iridium(III) complexes for mitochondria-targeted combined chemo-photodynamic therapy. *Dalton Trans.*, **49**, *2020*, 3562–3569.

26. Liu, X.; Hao, H.; Ge, X.; He, X.; Liu, Y.; Wang, Y.; Liu, Z. Triphenylamine-appended cyclometalated iridium(III) complexes: preparation, photophysical properties and application in biology/luminescence imaging. *J. Inorg. Biochem.*, **2019**, *199*, 110757.

27. Xiang, H.; Chen, H.; Tham, H. P.; Phua, S. Z. F.; Liu, J. G.; Zhao, Y. Cyclometalated iridium(III)-complex-based micelles for glutathione-responsive targeted chemotherapy and photodynamic therapy. *ACS Appl. Mater. Interfaces*, **2017**, *9*, 27553–27562.

28. Meksawangwong, S.; Gohil, B.; Punyain, W.; Pal, R.; Kielar, F. Synthesis and investigation of a tris-cyclometalated iridium complex bearing a single quaternary ammonium group. *Inorg. Chim. Acta*, **2019**, *497*, 119066.

29. Song, X. D.; Chen, B. B.; He, S. F.; Pan, N. L.; Liao, J. X.; Chen, J. X.; Sun, J. Guanidine-modified cyclometalated iridium(III) complexes for mitochondria-targeted imaging and photodynamic therapy. *Eur. J. Med. Chem.*, **2019**, *179*, 26–37.

30. Ye, R. R.; Tan, C. P.; Ji, L. N.; Mao, Z. W. Coumarin-appended phosphorescent cyclometalated iridium(III) complexes as mitochondria-targeted theranostic anticancer agents. *Dalton Trans.*, **2016**, *45*, 13042–13051.

31. Hisamatsu, Y.; Suzuki, N.; Masum, A. A.; Shibuya, A.; Abe, R.; Sato, A.; Aoki, S. Cationic amphiphilic tris-cyclometalated iridium(III) complexes induce cancer cell death via interaction with Ca^{2+} -calmodulin complex. *Bioconjug. Chem.*, **2016**, *28*, 507–523.

32. Ye, R. R.; Cao, J. J.; Tan, C. P.; Ji, L. N.; Mao, Z. W. Valproic acid-functionalized cyclometalated iridium(III) complexes as mitochondria-targeting anticancer agents. *Chemistry*, **2017**, *23*, 15166–15176.

33. Steunenberg, P.; Ruggi, A.; van den Berg, N. S.; Buckle, T.; Kuil, J.; van Leeuwen, F. W.; Velders, A. H. Phosphorescence imaging of living cells with amino acid-functionalized tris (2-phenylpyridine) iridium (III) complexes. *Inorg. Chem.*, **2012**, *51*, 2105.

34. Berkers, C. R.; van Leeuwen, F. W.; Groothuis, T. A.; Peperzak, V.; van Tilburg, E. W.; Borst, J.; Ovaa, H. Profiling proteasome activity in tissue with fluorescent probes. *Mol. Pharmac.*, **2007**, *4*(5), 739–748.

35. Moromizato, S.; Hisamatsu, Y.; Suzuki, T.; Matsuo, Y.; Abe, R.; Aoki, S. Design and synthesis of a luminescent cyclometalated iridium (III) complex having N, N-diethylamino group that stains acidic intracellular organelles and induces cell death by photoirradiation. *Inorg. Chem.*, **2012**, *51*(23), 12697–12706.

36. Nakagawa, A.; Hisamatsu, Y.; Moromizato, S.; Kohno, M.; Aoki, S. Synthesis and photochemical properties of pH responsive tris-cyclometalated iridium (III) complexes that contain a pyridine ring on the 2-phenylpyridine ligand. *Inorg. Chem.*, **2014**, *53*(1), 409–422.

37. Qiu, K.; Huang, H.; Liu, B.; Liu, Y.; Huang, Z.; Chen, Y.; Chao, H. Long-term lysosomes tracking with a water-soluble two-photon phosphorescent iridium (III) complex. *ACS Appl. Mater. Interfaces*, **2016**, 8(20), 12702-12710.

38. Lv, W.; Zhang, Z.; Zhang, K. Y.; Yang, H.; Liu, S.; Xu, A.; Huang, W. A mitochondria-targeted photosensitizer showing improved photodynamic therapy effects under hypoxia. *Angew. Chem. Int. Ed.*, **2016**, 55, 9947-9951.

39. Chen, M. H.; Wang, F. X.; Cao, J. J.; Tan, C. P.; Ji, L. N.; Mao, Z. W. Light-Up mitophagy in live cells with dual-functional theranostic phosphorescent iridium(III) complexes. *ACS Appl. Mater. Interfaces*, **2017**, 9, 13304-13314.

40. Liu, J.; Jin, C.; Yuan, B.; Liu, X.; Chen, Y.; Ji, L.; Chao, H. Selectively lighting up two photon photodynamic activity in mitochondria with AIE-active iridium(III) complexes. *Chem. Commun.*, **2017**, 53, 2052-2055.

41. Jin, C.; Liu, J.; Chen, Y.; Guan, R.; Ouyang, C.; Zhu, Y.; Chao, H. Cyclometalated iridium(III) complexes as AIE phosphorescent probes for real-time monitoring of mitophagy in living cells. *Sci. Rep.*, **2016**, 6, 22039.

42. He, L.; Tan, C. P.; Ye, R. R.; Zhao, Y. Z.; Liu, Y. H.; Zhao, Q.; Mao, Z. W. Theranostic iridium(III) complexes as one- and two-photon phosphorescent trackers to monitor autophagic lysosomes. *Angew. Chem. Int. Ed.*, **2014**, 53, 12137-12141.

43. He, L.; Li, Y.; Tan, C. P.; Ye, R. R.; Chen, M. H.; Cao, J. J.; Mao, Z. W. Cyclometalated iridium(III) complexes as lysosome-targeted photodynamic anticancer and real-time tracking agents. *Chem. Sci.*, **2015**, 6, 5409-5418.

44. Wang, F. X.; Chen, M. H.; Lin, Y. N.; Zhang, H.; Tan, C. P.; Ji, L. N.; Mao, Z. W. Dual functions of cyclometalated iridium(III) complexes: anti-metastasis and lysosome-damaged photodynamic therapy. *ACS Appl. Mater. Interfaces*, **2017**, 9, 42471-42481.

45. Cao, R.; Jia, J.; Ma, X.; Zhou, M.; Fei, H. Membrane localized iridium(III) complex induces endoplasmic reticulum stress and mitochondria-mediated apoptosis in human cancer cells. *J. Med. Chem.*, **2013**, 56, 3636-3644.

46. Mandal, S.; Poria, D. K.; Ghosh, R.; Ray, P. S.; Gupta, P. Development of a cyclometalated iridium complex with specific intramolecular hydrogen-bonding that acts as a fluorescent marker for the endoplasmic reticulum and causes photoinduced cell death. *Dalton Trans.*, **2014**, 43, 17463-17474.

47. Tian, X.; Zhu, Y.; Zhang, M.; Luo, L.; Wu, J.; Zhou, H.; Tian, Y. Localization matters: a nuclear targeting two-photon absorption iridium complex in photodynamic therapy. *Chem. Commun.*, **2017**, 53, 3303-3306.

48. Li, C.; Yu, M.; Sun, Y.; Wu, Y.; Huang, C.; Li, F. A nonemissive iridium(III) complex that specifically lights-up the nuclei of living cells. *J. Am. Chem. Soc.*, **2011**, 133, 11231-11239.

49. Wu, N.; Cao, J. J.; Wu, X. W.; Tan, C. P.; Ji, L. N.; Mao, Z. W. Iridium(III) complexes with five-membered heterocyclic ligands for combined photodynamic therapy and photoactivated chemotherapy. *Dalton Trans.*, **2017**, 46, 13482-13491.

50. Cao, J. J.; Tan, C. P.; Chen, M. H.; Wu, N.; Yao, D. Y.; Liu, X. G.; Mao, Z. W. Targeting cancer cell metabolism with mitochondria-immobilized phosphorescent cyclometalated iridium(III) complexes. *Chem. Sci.*, **2017**, 8, 631-640.

51. Zhang, W. Y.; Du, F.; He, M.; Bai, L.; Gu, Y. Y.; Yang, L. L.; Liu, Y. J. Studies of anticancer activity *in vitro* and *in vivo* of iridium(III) polypyridyl complexes-loaded liposomes as drug delivery system. *Eur. J. Med. Chem.*, **2019**, 178, 390-400.

52. Venkatesh, V.; Berrocal-Martin, R.; Wedge, C. J.; Romero-Canelón, I.; Sanchez-Cano, C.; Song, J. I.; Sadler, P. J. Mitochondria-targeted spin-labelled luminescent iridium anticancer complexes. *Chem. Sci.*, **2017**, 8, 8271-8278.

53. He, L.; Zhang, M. F.; Pan, Z. Y.; Wang, K. N.; Zhao, Z. J.; Li, Y.; Mao, Z. W. A mitochondria-targeted iridium(III)-based photoacid generator induces dualmode photodynamic damage within cancer cells. *Commun. Chem.*, **2019**, *55*(70), 10472–10475.

54. McKenzie, L. K.; Sazanovich, I. V.; Baggaley, E.; Bonneau, M.; Guerchais, V.; Williams, J. G.; Bryant, H. E. Metal complexes for two-photon photodynamic therapy: A cyclometalated iridium complex induces twophoton photosensitization of cancer cells under near-IR light. *Chem. Eur. J.*, **2017**, *23*(2), 234–238.

55. Murphy, L.; Congreve, A.; Pålsson, L. O.; Williams, J. G. The time domain in co-stained cell imaging: time-resolved emission imaging microscopy using a protonatable luminescent iridium complex. *Chem. Commun. (Camb.)*, **2010**, *46*, 8743–8745.

56. Wang, M. M.; Xue, X. L.; Sheng, X. X.; Su, Y.; Kong, Y. Q.; Qian, Y.; Liu, H. K. Unveiling the anti-cancer mechanism for half-sandwich and cyclometalated Ir(III)-based complexes with functionalized α -lipoic acid. *RSC Adv.*, **2020**, *10*, 5392–5398.

57. Pérez-Arnaiz, C.; Acuña, M. I.; Bustos, N.; Echevarría, I.; Martínez-Alonso, M.; Espino, G.; Domínguez, F. Thiabendazole-based Rh(III) and Ir(III) biscyclometalated complexes with mitochondria-targeted anticancer activity and metal-sensitive photodynamic activity. *Eur. J. Med. Chem.*, **2018**, *157*, 279–293.

58. Thomas, S. J.; Balónová, B.; Cinatl Jr, J.; Wass, M. N.; Serpell, C. J.; Blight, B. A.; Michaelis, M. Thiourea and guanidine compounds and their iridium complexes in drug-resistant cancer cell lines: Structure-activity relationships and direct luminescent. *ChemMedChem*, **2020**, *15*(4), 349–353.

59. Zhao, J.; Sun, S.; Li, X.; Zhang, W.; Gou, S. Enhancing photodynamic therapy efficacy of upconversion-based nanoparticles conjugated with a long-lived triplet excited state iridium(III)-naphthalimide complex: toward highly enhanced hypoxia-inducible factor-1. *ACS Appl. Bio Mater.*, **2019**, *3*, 252–262.

60. Xue, F.; Lu, Y.; Zhou, Z.; Shi, M.; Yan, Y.; Yang, H.; Yang, S. Two in one: luminescence imaging and 730 nm continuous wave laser driven photodynamic therapy of iridium complexes. *Organometallics*, **2015**, *34*(1), 73–77.

61. Hong, X. L.; Zhou, Y. H.; Zeng, C. C.; Wu, X. C.; Liu, Y. J. Apoptosis *in vitro* in PC-12 cells induced by an organometallic Ir(III) complex through a ROS-mediated mitochondrial pathway. *J. Organomet. Chem.*, **2017**, *846*, 312–320.

62. Liang, Z. H.; Wan, D.; Yi, Q. Y.; Zhang, W. Y.; Liu, Y. J. A cyclometalated iridium(III) complex induces apoptosis and autophagy through inhibition of the PI3K/AKT/mTOR pathway. *Trans. Met. Chem.*, **2018**, *43*, 243–257.

63. Wang, B.; Liang, Y.; Dong, H.; Tan, T.; Zhan, B.; Cheng, J.; Cheng, S. H. A luminescent cyclometalated iridium (III) complex accumulates in mitochondria and induces mitochondrial shortening by conjugation to specific protein targets. *ChemBioChem*, **2012**, *13*(18), 2729–2737.

64. Lo, K. K. W.; Leung, S. K.; Pan, C. Y. Luminescent iridium (III) arylbenzothiazole complexes: Photophysics, electrochemistry, bioconjugation, and cellular uptake. *Inorg. Chim. Acta*, **2012**, *380*, 343–349.

65. Kuang, S.; Liao, X.; Zhang, X.; Rees, T. W.; Guan, R.; Xiong, K.; Chao, H. FerriIridium: A Lysosome-targeting iron(III)-activated iridium(III) prodrug for chemotherapy in gastric cancer cells. *Angew. Chem. Int. Ed.*, **2020**, *59*, 3315–3321.

66. Guan, R.; Chen, Y.; Zeng, L.; Rees, T. W.; Jin, C.; Huang, J.; Chao, H. Oncosis-inducing cyclometalated iridium(III) complexes. *Chem. Sci.*, **2018**, *9*, 5183–5190.

67. Yi, S.; Lu, Z.; Zhang, J.; Wang, J.; Xie, Z.; Hou, L. Amphiphilic gemini iridium(III) complex as a mitochondria-targeted theranostic agent for tumor imaging and photodynamic therapy. *ACS Appl. Mater. Interfaces*, **2019**, *11*, 15276–15289.

68. Wang, F. X.; Chen, M. H.; Hu, X. Y.; Ye, R. R.; Tan, C. P.; Ji, L. N.; Mao, Z. W. Ester-modified cyclometalated iridium (III) complexes as mitochondria-targeting anticancer agents. *Sci. Rep.*, **2016**, *6*, 38954.

69. Martínez-Alonso, M.; Busto, N.; Aguirre, L. D.; Berlanga, L.; Carrión, M. C.; Cuevas, J. V.; Espino, G. Strong influence of the ancillary ligand over the photodynamic anticancer properties of neutral biscyclometalated Ir(III) complexes bearing 2-benzoazole-phenolates. *Chem. Eur. J.*, **2018**, *24*(66), 17523–17537.

70. Ho, P. Y.; Ho, C. L.; Wong, W. Y. Recent advances of iridium (III) metallophosphors for health-related applications. *Coord. Chem. Rev.*, **2020**, *413*, 213267.

71. Wu, K. J.; Ho, S. H.; Dong, J. Y.; Fu, L.; Wang, S. P.; Liu, H.; Ma, D. L. Aliphatic group-tethered iridium complex as a theranostic agent against malignant melanoma metastasis. *ACS Appl. Bio Mater.*, **2020**, *3*, 2017–2027.

72. Sun, L.; Chen, Y.; Kuang, S.; Li, G.; Guan, R.; Liu, J.; Chao, H. Iridium (III) anthraquinone complexes as two-photon phosphorescence probes for mitochondria imaging and tracking under hypoxia. *Chem. - A Eur. J.*, **2016**, *22*, 8955–8965.

73. Wendlandt, A. E.; Stahl, S. S. Quinone-catalyzed selective oxidation of organic molecules. *Angew. Chem. Int. Ed.*, **2015**, *54*(49), 14638–14658.

74. Liu, Z.; Deeth, R. J.; Butler, J. S.; Habtemariam, A.; Newton, M. E.; Sadler, P. J. Reduction of quinones by NADH catalyzed by organoiridium complexes. *Angew. Chem. Int. Ed.*, **2013**, *52*(15), 4194.

75. Du, F.; Bai, L.; He, M.; Zhang, W. Y.; Gu, Y. Y.; Yin, H.; Liu, Y. J. Design, synthesis and biological evaluation of iridium(III) complexes as potential antitumor agents. *J. Inorg. Biochem.*, **2019**, *201*, 110822.

76. Lo, K. K. W.; Lee, P. K.; Lau, J. S. Y. Synthesis, characterization, and properties of luminescent organoiridium (III) polypyridine complexes appended with an alkyl chain and their interactions with lipid bilayers, surfactants, and living cells. *Organometallics*, **2008**, *27*(13), 2998–3006.

77. Lau, J. S.-Y.; Lee, P.-K.; Tsang, K. H.-K.; Ng, C. H.-C.; Lam, Y.-W.; Cheng, S.-H.; Lo, K. K.-W. Luminescent cyclometalated iridium(III) polypyridine indole complexes—synthesis, photophysics, electrochemistry, protein-binding properties, cytotoxicity, and cellular uptake. *Inorg. Chem.*, **2009**, *48*, 708–718.

78. Leung, S. K.; Kwok, K. Y.; Zhang, K. Y.; Lo, K. K. W. Design of luminescent biotinylation reagents derived from cyclometalated iridium (III) and rhodium (III) bis (pyridylbenzaldehyde) complexes. *Inorg. Chem.*, **2010**, *49*(11), 4984–4995.

79. Chen, H.; Ge, C.; Cao, H.; Zhang, X.; Zhang, L.; Jiang, L.; Zhang, Q. Isomeric Ir(III) complexes for tracking mitochondrial pH fluctuations and inducing mitochondrial dysfunction during photodynamic therapy. *Dalton Trans.*, **2019**, *48*, 17200–17209.

80. Yang, X. H.; Zhang, Q.; Dou, S. B.; Xiao, L.; Jia, X. L.; Yang, R. L.; Niu, Z. G. Synthesis, properties, DFT calculations, and cytotoxic activity of phosphorescent iridium(III) complexes with heteroatom ancillary ligands. *J. Coord. Chem.*, **2020**, *73*(14), 2004–2014.

81. Zhang, W. Y.; Yi, Q. Y.; Wang, Y. J.; Du, F.; He, M.; Tang, B.; Huang, H. L. Photoinduced anticancer activity studies of iridium(III) complexes targeting mitochondria and tubules. *Eur. J. Med. Chem.*, **2018**, *151*, 568–584.

82. He, L.; Liao, S. Y.; Tan, C. P.; Lu, Y. Y.; Xu, C. X.; Ji, L. N.; Mao, Z. W. Cyclometalated iridium (III)- β -carboline complexes as potent autophagy-inducing agents. *Chem. Commun.*, **2014**, *50*(42), 5611–5614.

83. Kaiser, M.; Zavrski, I.; Sterz, J.; Jakob, C.; Fleissner, C.; Kloetzel, P. M.; Heider, U. The effects of the histone deacetylase inhibitor valproic acid on cell cycle, growth suppression and apoptosis in multiple myeloma. *Haematologica*, **2006**, *91*(2), 248–251.

84. Yuan, B.; Liu, J.; Guan, R.; Jin, C.; Ji, L.; Chao, H. Endoplasmic reticulum targeted cyclometalated iridium(iii) complexes as efficient photodynamic therapy photosensitizers. *Dalton Trans.*, **2019**, *48*, 6408–6415.

85. Zhang, Y.; Fu, H.; Chen, S.; Liu, B.; Sun, W.; Gao, H. Construction of an iridium(iii)-complex-loaded MOF nanoplatform mediated with a dual-responsive polycationic polymer for photodynamic therapy and cell imaging. *Chem. Commun.*, **2020**, *56*, 762–765.

86. Novohradsky, V.; Vigueras, G.; Pracharova, J.; Cutillas, N.; Janiak, C.; Kostrhunova, H.; Kasparkova, J. Molecular superoxide radical photogeneration in cancer cells by dipyridophenazine iridium(III) complexes. *Inorg. Chem. Front.*, **2019**, *6*(9), 2500–2513.

87. Yello, G. S.; Donaire, A.; Yello, J. G.; Vasylyeva, V.; Janiak, C.; Ruiz, J. On the antitumor properties of novel cyclometalated benzimidazole Ru(II), Ir(III) and Rh(III) complexes. *Chem. Commun.*, **2013**, *49*(98), 11533–11535.

88. Laha, P.; De, U.; Chandra, F.; Dehury, N.; Khullar, S.; Kim, H. S.; Patra, S. Alkyl chainmodified cyclometalated iridium complexes as tunable anticancer and imaging agents. *Dalton Trans.*, **2018**, *47*(44), 15873–15881.

89. Yello, J.; Pérez, S. A.; Yello, G.; Zajac, J.; Donaire, A.; Vigueras, G.; Ruiz, J. Highly potent extranuclear-targeted luminescent iridium(III) antitumor agents containing benzimidazole based ligands with a handle for functionalization. *Chem. Commun.*, **2016**, *52*(98), 14165–14168.

90. Pracharova, J.; Vigueras, G.; Novohradsky, V.; Cutillas, N.; Janiak, C.; Kostrhunova, H.; Brabec, V. Exploring the effect of polypyridyl ligands on the anticancer activity of phosphorescent iridium (III) complexes: From proteosynthesis inhibitors to photodynamic therapy agents. *Chem. Eur. J.*, **2018**, *24*(18), 4607–4619.

91. Novohradsky, V.; Zamora, A.; Gandioso, A.; Brabec, V.; Ruiz, J.; Marchán, V. Somatostatin receptor-targeted organometallic iridium(III) complexes as novel theranostic agents. *Chem. Commun.*, **2017**, *53*(40), 5523–5526.

92. Hartinger, C. G. Trapping Unstable Benzoquinone Analogues by Coordination to a [(η₅-C₅Me₅)Ir] Fragment and the Anticancer Activity of the Resulting Complexes. *Angew. Chem. Int. Ed.*, **2010**, *45*(49), 8304–8305.

93. Steinberg-Yfrach, G.; Liddell, P. A.; Hung, S. C.; Moore, A. L.; Gust, D.; Moore, T. A. Conversion of light energy to proton potential in liposomes by artificial photosynthetic reaction centres. *Nature*, **1997**, *385*(6613), 239–241.

94. Larsen, P. L.; Clarke, C. F. Extension of life-span in *Caenorhabditis elegans* by a diet lacking coenzyme Q. *Science*, **2002**, *295*(5552), 120–123.

95. Amouri, H.; Moussa, J.; Renfrew, A. K.; Dyson, P. J.; Rager, M. N.; Chamoreau, L. M. Discovery, structure, and anticancer activity of an iridium complex of diselenobenzoquinone. *Angew. Chem. Int. Ed.*, **2010**, *49*(41), 7530–7533.

96. Liu, Z.; Habtemariam, A.; Pizarro, A. M.; Clarkson, G. J.; Sadler, P. J. Organometallic iridium (III) cyclopentadienyl anticancer complexes containing C, N-chelating ligands. *Organometallics*, **2011**, *30*(17), 4702–4710.

97. Millett, A. J.; Habtemariam, A.; Romero-Canelón, I.; Clarkson, G. J.; Sadler, P. J. Contrasting anticancer activity of half-sandwich iridium (III) complexes bearing functionally diverse 2-phenylpyridine ligands. *Organometallics*, **2015**, *34*(11), 2683–2694.

98. Wirth, S.; Rohbogner, C. J.; Cieslak, M.; Kazmierczak-Baranska, J.; Donevski, S.; Nawrot, B.; Lorenz, I. P. Rhodium (III) and iridium (III) complexes with 1, 2-naphthoquinone-1-oximate as a bidentate ligand: synthesis, structure, and biological activity. *JBIC J. Biol. Inorg. Chem.*, **2010**, *15*, 429–440.

99. Śliwińska, U.; Pruchnik, F. P.; Ułaszewski, S.; Latocha, M.; Nawrocka-Musiał, D. Properties of η₅-pentamethylcyclopentadienyl rhodium (III) and iridium (III) complexes with quinolin-8-ol and their cytostatic activity. *Polyhedron*, **2010**, *29*(6), 1653–1659.

100. Schäfer, S.; Ott, I.; Gust, R.; Sheldrick, W. S. Influence of the Polypyridyl (pp) Ligand Size on the DNA Binding Properties, Cytotoxicity and Cellular Uptake of Organoruthenium (II) Complexes of the Type $[(\eta_6\text{-C}_6\text{Me}_6)\text{ Ru (L)(pp)}]^{n+}$ [L= Cl, n= 1; L=(NH₂)₂CS, n= 2]. *Eur. J. Inorg. Chem.*, **2007**, 3034-3046.

101. Schäfer, S.; Sheldrick, W. S. Coligand tuning of the DNA binding properties of half-sandwich organometallic intercalators: Influence of polypyridyl (pp) and monodentate ligands (L= Cl, (NH₂)₂CS, (NMe₂)₂CS) on the intercalation of (η_5 -pentamethylcyclopentadienyl)-iridium (III)-dipyridoquinoxaline and-dipyridophenazine complexes. *J. Organomet. Chem.*, **2007**, 692(6), 1300-1309.

102. Liu, Z.; Romero-Canelón, I.; Habtemariam, A.; Clarkson, G. J.; Sadler, P. J. Potent half-sandwich iridium (III) anticancer complexes containing C⁴N-chelated and pyridine ligands. *Organometallics*, **2014**, 33(19), 5324-5333.

103. Xiong, K.; Chen, Y.; Ouyang, C.; Guan, R. L.; Ji, L. N.; Chao, H. Cyclometalated iridium(III) complexes as mitochondria-targeted anticancer agents. *Biochimie*, **2016**, 125, 186-194.

104. Wilbuer, A.; Vlecken, D. H.; Schmitz, D. J.; Kräling, K.; Harms, K.; Bagowski, C. P.; Meggers, E. Iridium complex with antiangiogenic properties. *Angew. Chem. Int. Ed.*, **2010**, 49(22), 3839-3842.

105. Kastl, A.; Wilbuer, A.; Merkel, A. L.; Feng, L.; Di Fazio, P.; Ocker, M.; Meggers, E. Dual anticancer activity in a single compound: visible-light-induced apoptosis by an antiangiogenic iridium complex. *Chem. Commun.*, **2012**, 48(13), 1863-1865.

106. Lo, K. K. W.; Zhang, K. Y. Iridium(III) complexes as therapeutic and bioimaging reagents for cellular applications. *RSC Adv.*, **2012**, 2, 12069-12083.

107. Lukevics, E.; Shestakova, I.; Domracheva, I.; Nesterova, A.; Zaruma, D.; Ashaks, J. Cytotoxicity of metal 8-quinolinethiolates. *Chem. Heteroc. Comp.*, **2006**, 42, 761-764.

108. Lukevics, E.; Shestakova, I.; Domracheva, I.; Yashchenko, E.; Zaruma, D.; Ashaks, J. Synthesis and cytotoxicity of metal 4-methyl-8-quinolinethiolates. *Chem. Heteroc. Comp.*, **2007**, 43, 634-636.

109. Lukevics, E.; Zaruma, D.; Ashaks, J.; Shestakova, I.; Domracheva, I.; Gulbe, A.; Bridane, V. Synthesis and cytotoxicity of methyl-and methoxy-substituted metal 8-quinolinethiolates. *Chem. Heteroc. Comp.*, **2008**, 44, 559-564.

110. Ashaks, J.; Bankovsky, Y.; Zaruma, D.; Shestakova, I.; Domracheva, I.; Nesterova, A.; Lukevics, E. Synthesis of quinoline-8-selenol, its complex compounds with metals and their cytotoxic activity. *Chem. Heteroc. Comp.*, **2004**, 40, 776-780.

111. Lukevics, E.; Zaruma, D.; Ashaks, J.; Shestakova, I.; Domracheva, I.; Bridane, V.; Yashchenko, E. Synthesis and cytotoxicity of methyl-substituted 8-quinolineselenolates of ruthenium, rhodium, osmium, and iridium. *Chem. Heteroc. Comp.*, **2009**, 45, 182-187.

112. Conesa, J. J.; Carrasco, A. C.; Rodríguez-Fanjul, V.; Yang, Y.; Carrascosa, J. L.; Cloetens, P.; Pizarro, A. M. Unambiguous intracellular localization and quantification of a potent iridium anticancer compound by correlative 3D cryo X-ray imaging. *Angew. Chem. Int. Ed.*, **2020**, 59, 1270-1278.

113. Wang, X.; Zhang, J.; Zhao, X.; Wei, W.; Zhao, J. Imaging and proteomic study of a clickable iridium complex. *Metallomics*, **2019**, 11, 1344-1352.

This page is intentionally left blank



Scan to know paper details and
author's profile

From Infinity (Wuji 无极) to Taiji (太极), Yin-Yang (阴阳) to Heaven-Earth (Qiankun 乾坤): A Yin-Yang (阴阳) Philosophical Exploration of Existence and Cosmic Origins

Samo Liu

ABSTRACT

The contradictions between quantum mechanics and relativity are not the result of physics itself; rather, they stem from the “gaps” in our knowledge as reflected in metaphysical theories. The knowledge derived from Eastern cosmological philosophies can help to fill these gaps. Previous articles have explored the relationship between Eastern cosmological philosophies and physics, and have identified the directions and methods that could be used to resolve the contradictions within modern physics.

By combining the concepts of metaphysical philosophy and materialist dialectical logic with the findings of modern physics, we can identify the gaps in the ancient Greek philosophers' understanding of the “origin” and “substance” of “space” and “time”. Subsequent articles will explore the relationship between the works “Physics” and “Metaphysics”, as well as the contradictions inherent within physics. This article serves as a link between the previous and subsequent studies, facilitating our understanding of the logical connections between concepts such as “the Absolute Nothing (wuji 无极)”, “the Primordial Unity (yuanyi 元一)”, “the substance (benti 本体)”, and “the Origin (benyuan 本原)”, as well as the relationship between unknown and known knowledge.

Keywords: cosmic origin philosophy, material philosophy, yin-yang cosmology, dialectical materialism, quantum mechanics, relativity theory, information and energy ontology, philosophy of science, human cognition, metaphysics.

Classification: LCC Code: QC6, BD511, BD631

Language: English



Great Britain
Journals Press

LJP Copyright ID: 925615

Print ISSN: 2631-8490

Online ISSN: 2631-8504

London Journal of Research in Science: Natural & Formal

Volume 25 | Issue 14 | Compilation 1.0



From Infinity (Wuji 无极) to Taiji (太极), Yin-Yang (阴阳) to Heaven-Earth (Qiankun 乾坤): A Yin-Yang (阴阳) Philosophical Exploration of Existence and Cosmic Origins

Samo Liu

ABSTRACT

The contradictions between quantum mechanics and relativity are not the result of physics itself; rather, they stem from the “gaps” in our knowledge as reflected in metaphysical theories. The knowledge derived from Eastern cosmological philosophies can help to fill these gaps. Previous articles have explored the relationship between Eastern cosmological philosophies and physics, and have identified the directions and methods that could be used to resolve the contradictions within modern physics.

By combining the concepts of metaphysical philosophy and materialist dialectical logic with the findings of modern physics, we can identify the gaps in the ancient Greek philosophers' understanding of the “origin” and “substance” of “space” and “time”. Subsequent articles will explore the relationship between the works “Physics” and “Metaphysics”, as well as the contradictions inherent within physics. This article serves as a link between the previous and subsequent studies, facilitating our understanding of the logical connections between concepts such as “the Absolute Nothing (wuji 无极)”, “the Primordial Unity (yuanyi 元一)”, “the substance (benti 本体)”, and “the Origin (benyuan 本原)”, as well as the relationship between unknown and known knowledge.

Material philosophy and material science have enabled humans to understand human society as well as the three-dimensional material world. Quantum mechanics and the theory of relativity, on the other hand, have prompted humans to contemplate the philosophies of energy and information, leading us towards a deeper understanding of the fundamental nature of the universe. These developments have not only expanded our knowledge and information but also broadened the paths through which we can explore the truths of the universe.

Humans have created languages, writing systems, numbers, mathematics, coordinate systems, science, as well as philosophy and religion, thus forming the system of knowledge and information that we possess today. The accuracy of the knowledge and information created by humans must be verified through the repeatability of scientific experiments. In other words, the correctness of such knowledge and information can only be established through scientific methods and the principles of probability. The purpose of creating this knowledge and information is to explore the truths of the universe in order to ensure our survival and development. However, the creations of humans can never be equated with ultimate truths; they merely represent attempts to get closer to those truths.

Keywords: cosmic origin philosophy, material philosophy, yin-yang cosmology, dialectical materialism, quantum mechanics, relativity theory, information and energy ontology, philosophy of science, human cognition, metaphysics.

I. LITERATURE REVIEW

1.1 The philosophical concept of the origin of the universe:

The new philosophical mode of thought refers to the human thinking pattern before Aristotle, based on Taoist philosophy, Buddhist philosophy, and ancient Greek philosophy, combined with modern physics information. It posits that the 'original existence' of matter comes from the information of 'non-being' and 'emptiness', both matter and existence possess a sense of 'spirituality', this 'spirituality of the mind' leads to the movement and change of all things in the universe, and returns to the original state of 'emptiness' and 'non-being'. Modern physics and science have revealed the basic principles of the ontological philosophy of the universe. (Samo Liu, 2025f)

To be precise, the philosophy of the cosmic origin gave birth to the material philosophy. The science influenced by the material philosophy conversely validates the philosophy of cosmic origins. The two are integrated.

Humans are material beings living in a material world. Contemplating a universe devoid of matter, space without matter, or a world without matter is a profoundly challenging question (Russell, 2017; Samo Liu, 2020a; 2020b; Liu Hongjun&Samo Liu, 2020)

Based on existing human knowledge and information: employing Daoist and Buddhist cosmic origin philosophy, ancient Greek primal existential thought, dialectical materialist logic analysis, and integrating contemporary physics knowledge, space is fundamentally empty—a universe initially devoid of anything. First, this state (懲tan) is Yin-Yang's living, zero dimension intangible existence (Infinity无极). Expressed through time, it is an infinite process with a minimum value of zero (absolute zero). Expressed spatially, it is boundlessly expansive outwardly and infinitesimally inward, infinite, with a minimum of zero. An intangible space and zero-dimensional universe created a finite, living, three-dimensional universe (太极Taiji), whose boundaries remain beyond human comprehension (Samo Liu, 2021a; 2021b; 2021c).

This intangible space and zero-dimensional universe are termed Infinity, existing as Yin-Yang, material existence, and non-material existence—informational and energetic “causes因” and “formal existence” (Laozi, 2019; Shakyamuni, 2019). Without matter, it exists purely in a Yin-Yang binary relationship (Samo Liu, 2024a).

Under certain causal conditions, information gives rise to energy—living Yin-Yang energy within the realm of quantum mechanics. Subsequently, energy, under strong and weak interactions, produces atoms (Liu Hongjun & Samo Liu, 2020; 2021b).

Thus emerged the material Yin-Yang Taiji: matter and non-matter, energy and matter, forming a ternary relationship of matter, information, and energy. Nonetheless, its fundamental binary relationship remains information and energy, as matter itself is a form of energy (Samo Liu, 2024i).

Atoms, as living Yin-Yang existence, gave rise to molecules. Molecules, also living Yin-Yang entities, created plant cells, animal cells, and human cells—all Yin-Yang living beings—subsequently producing humanity (Samo Liu, 2025d). Humans, capable of thought, sensation, and perception, invented languages, scripts, numbers, mathematics, science, and coordinate systems, forming knowledge and information systems (Liu Hongjun & Samo Liu, 2021a). Yet human existence involves birth and death, a lifespan from zero to a certain temporal unit symbolizing both individual existence and the existence of the entire universe and all things therein measured by time process.

Consequently, Yin-Yang relationships among heaven, earth, and humans, as well as humans and space, universe, and Heaven-Earth emerged.

Humans, through languages, scripts, numbers, mathematics, and scientific systems, further created philosophy, religion, and science. Without quantum mechanics and relativity, we cannot conceive a universe or world arising from nothingness; without dialectical materialism, we cannot grasp the unity of opposites and the dialectical transition from quantitative to qualitative changes. Nevertheless, contemporary physics confirms that humanity indeed exists within such a space, universe, and world (Samo Liu, 2017; 2019). The cosmic origin philosophies handed down by ancestors have consistently indicated this reality, though humans have doubted and debated it until modern scientific confirmation (Liu Hongjun & Samo Liu, 2020).

In times of insufficient information, Aristotle developed material philosophy and material science (Garrett Thomson & Marshall Missner, 2019). Humans have pursued these for over two thousand years, culminating in the apex of material philosophy and science, rediscovering and validating ancestral cosmic origin philosophy (Samo Liu, 2024a; 2024b; 2024c).

Guided by modern physics, humanity completed this grand project in material philosophy and science at considerable cost. Modern physics and ancestral cosmic origin philosophy align perfectly, leading humanity toward the cosmic origin of energy philosophy and information philosophy (Samo Liu, 2024d; 2024e; 2024f).

When modern scientific information revealed that dark matter and dark energy occupy 95.1% of the universe's finite space, leaving matter only 4.9% (Liu Hongjun & Samo Liu, 2021c), Daoist, Buddhist, and ancient Greek philosophies had already provided answers (Liu Hongjun & Samo Liu, 2021d; 2024).

Humans became ensnared in the trap of material philosophy and science (Samo Liu, 2024g; 2024h; 2024i), perpetually questioning and bearing this answer, using material philosophy to create modern physics and its inherent contradictions (Samo Liu, 2025a; 2025b; 2025c).

Without quantum mechanics and relativity providing scientific answers, humanity might have continued doubting and debating indefinitely. Modern scientific knowledge and information have allowed humans to confirm and verify principles of cosmic origins. Thus, humanity can reconsider fundamental philosophical questions about space and time (Samo Liu, 2025e; 2024i), inherit and develop ancestral philosophical insights, and establish new philosophical paradigms (Samo Liu, 2025f). The significant invention of computers and robots encourages humans to reexamine humanity's origin (Samo Liu, 2025d).

Express gratitude to space, the universe, the beautiful world, and of course, humanity itself. Please discuss this viewpoint in the academic community.

II. HUMANITY AND HUMAN-CREATED EXISTENCE

Interestingly, humans can discover and create knowledge and information using language, words, and numbers. This is undoubtedly a remarkable collaborative achievement between the universe and humanity (Samo Liu, 2025d).

Humans continue to develop information through mathematics, measure and verify directional information using coordinate systems, and validate the repeatability, probability, and reality of this information scientifically. There should be no doubt about this. The existence and metaphysics created

through human philosophy are knowledge and information discovered and constructed by humans—essentially artificial existences (Liu Hongjun & Samo Liu, 2021a).

The universe could be considered a Yin-Yang dualistic existence, embodying contradiction. Precisely because of this contradictory dualism, space can be judged as a living Yin-Yang "Wuji无极" and the universe as a living Yin-Yang "Taiji太极" (Liu Hongjun & Samo Liu, 2020). Both Wuji and Taiji are contradictory unities, processes that transition from quantitative to qualitative changes.

All universal existences created within space are living entities, integrated manifestations of Yin-Yang information and energy. Consequently, everything created by space and the universe, including humans, is a living existence. Each has its own natural structural form, expressible through temporal zero-base coordinate processes and spatial zero-base coordinate forms devised by humans (Samo Liu, 2024g; 2024h; 2024i).

These existences, named by humans through language, words, and numbers, possess self-perception and mutual awareness, becoming integrated through causes and conditions. Such natural perceptions have no subjective consciousness (Liu Hongjun & Samo Liu, 2021b). They identify and naturally resolve contradictions effortlessly ("doing by non-doing无为而为"), and accomplish motion, change, and cycles through thermodynamic creation and equilibrium (Samo Liu, 2024e; 2024i).

Force is the soul 灵魂 of all existential perception (Samo Liu, 2024g; 2024h); heat is the mind 心灵 of all existential perception (Samo Liu, 2024i).

However, humans possess thought and subjective consciousness, enabling creativity. Humans engage in both material and energetic creations, as well as informational creations—a synthesis of perception and sensation. When such creativity loses philosophical coherence, consistency, and standardization, it results in a series of contradictory information (Samo Liu, 2025a; 2025b; 2025c). When science becomes humanity's confrontational tool, the double-edged sword of science emerges.

Humans can create happiness, problems, and contradictions. The crucial question is whether humans can resolve contradictions. For instance, modern physics is characterized by human-created contradictions. Humans have even generated existential contradictions that threaten their own destruction (Samo Liu, 2024f).

Humans have learned to scientifically verify the probability and reality of all existence and confirm the directionality and positionality of scientific existence via coordinate systems. Yet, the accuracy remains unknown (Liu Hongjun & Samo Liu, 2020).

Philosophy has long informed humanity that, due to ignorance or misunderstanding of cosmic origin, Socrates and Aristotle brought philosophical thinking from the heavens back to the earthly realm (Aristotle, 2019; 2016). They clearly indicated that all human research and exploration concern on human society and the material world. The concepts of space, time, and the existence within them were long ago relegated to the realm of theology. Scientific development thus occurred within this historical context. Hence, philosophical reflection in science has been Zero-Dimensional Universe - The Absolute Space Test limited to human society and the material world. When unaware of universal existence and origins, humans regarded the universe and world as purely material, forming the logical foundation of all scientific philosophy (Liu Hongjun & Samo Liu, 2021a).

When scientific research reached modern physics, represented by quantum mechanics and relativity, Aristotle's material philosophy and material science left behind philosophical traps, a point overlooked by the scientific community (Aristotle, 2016; Liu Hongjun & Samo Liu, 2021b).

As quantum mechanics and relativity peaked within material sciences, they opened doors to cosmic origins of energy and information. Yet, space and time concepts continued to be individually designed using material philosophical and scientific frameworks. Arbitrary definitions of these unknown foundational concepts inevitably led to logical contradictions within scientific philosophy, producing the contradictory situation of modern physics (Liu Hongjun & Samo Liu, 2021c).

The rapid advancement of Western science allowed Western philosophy—material philosophy—to dominate philosophical discourse, profoundly influencing human thought. However, very few philosophers actively participated in scientific research, reflection, or practice. Newton, Leibniz, and Descartes contributed significantly, but most professional philosophers remained entrenched in their respective philosophical domains (Samo Liu, 2025a).

Thus, when science and modern physics reached their zenith, the philosophical community remained silent, offering neither opposition nor skepticism. This allowed modern physics' contradictions to persist for over a century.

Scientists are deeply influenced by theology and material philosophy. They have forgotten Aristotle's research on the 'cosmic origin' 宇宙本原 and 'substance' 本体, as well as 'infinity' 无限. They have also neglected that physics is 'theology'. (Aristotle, 2019; 2016; Samo Liu, 2025b)

Humanity once again stands at a juncture requiring comprehensive reflection upon its ideologies, knowledge and information, subjective consciousness, and artificially created existences.

III. KNOWLEDGE AND INFORMATION

Humans create knowledge and information, an ability and talent endowed by the universe, as well as a result of human endeavor. Yet, humanity must recognize clearly that the knowledge and information it creates are always developed during specific stages of human survival and existence. They inherently possess elements of known, unknown, exploratory, and imperfect nature, never constituting "absolute truths".

The universe created an intelligent form of matter called humanity. Humans, in turn, created intelligent machines—computers and robots.

Robots operate through software programs that humans create using their minds and intellect, subsequently powered by electrical energy (Samo Liu, 2020b).

The "mind" of humanity is software created by the universe. Initially, information inputs into this "software" originate from universal creation. Subsequently, this software self-operates via structured, standardized tools of language, text, and numerical information. Such informational tools enable self-reception, self-creation, and self-transmission of information. In this process, humans continually design their mental software programs, thereby creating, accepting, transforming, and perfecting knowledge and information. Human life's working energy is thermal energy, the foundational force of the universe (Samo Liu, 2024e; 2024f).

Without the informational tools of language, words, and numbers, and without the capacity for such creativity, human existence would be indistinguishable from that of other animals.

Language, words, and numbers represent humanity's indispensable hallmark as intelligent matter in the universe. These tools manifest the universe's information in visibility, standardized, and materialized forms.

The human form is intelligent matter, crafted by the universe using human cells. This humanoid form itself is profoundly significant. Whether describing personalized gods or demons and mythical creatures, humanity predominantly employs this human-like form, though other forms occasionally emerge.

Why do humans use anthropomorphic shapes and language-based numerical forms to portray personalized deities and anthropomorphic demons? This question is worthy of contemplation. Such depictions form specialized knowledge and information born from human hearts and minds, intertwined with artistic reflection and faith, and recognized as sacred knowledge and information—beyond the scope of current discussion.

For precise investigation of existence, humans have crafted mathematics through language, words, and numbers. Mathematics has become a scientific tool, evolving into a rigorous, systematic, and standardized discipline of knowledge and information. Independently, mathematics serves as a powerful assistant in human scientific research.

To explore the authenticity or real probability of existence, humans created science, scientific experiments, and scientific methods using language, words, and numbers. By repeatedly examining existential realities, science validates or disproves humanity's understanding of existence. Nevertheless, scientific correctness fundamentally relies on philosophical frameworks. The absence of unified philosophical consensus inevitably leads to confusion in scientific philosophy (Samo Liu, 2024g; 2024h; 2024i).

Contemporary human scientific knowledge and information are profoundly influenced by Aristotle's material philosophy, restricting understanding primarily to human society and material existence. Aristotle's great innovation was to set aside contradictions and focus on contemplating human society and material existence. This monumental innovation significantly impacted material science and societal development, profoundly transforming human society (Samo Liu, 2025a; 2025b).

Aristotle shelved the philosophical contradictions, avoided reflection on space and the existence of space, and no longer considered the origin of time and space. He directed human energy fully towards understanding societal and material existence, emphasizing tangible, material, and social realities. Exploration of concepts such as "emptiness" and "nothingness" was thus deferred (Samo Liu, 2025c).

Upon resolving philosophical contradictions and achieving unified understanding, humanity saw material philosophical thought and material sciences accelerate and diversify rapidly, as evidenced by over two thousand years of history (Samo Liu, 2024d).

Unexpectedly, philosophical thought and material sciences eventually entered the informational and energetic realms of quantum mechanics and relativity. Science validated Aristotle conceptions of cosmic origins 本原 and substance 本体, reopening doors to fundamental cosmic inquiries. Newly created knowledge and information uncovered cosmic origin principles, compelling humanity to reinvent philosophical thought and explore fresh knowledge and information.

IV. KNOWN KNOWLEDGE AND INFORMATION

Based on humanity's existing knowledge and information, it is inferred that the universe represents living Yin-Yang, creating naturally through non-action (wu wei 无为). Within space exists an objective Yin-Yang state of "nothingness" and "emptiness" (Yin-Yang Wuji 阴阳无极), which gave rise to the universe (Yin-Yang Taiji 阴阳太极), also known as "Qian Kun 乾坤" (Heaven and Earth), representing Yin-Yang existence.

It is deduced from existing knowledge and information that space (Yin-Yang Wuji 阴阳无极) created the universe (Yin-Yang Taiji 阴阳太极), which then produced atoms, molecules, plants, animals, and humans. Humans subsequently developed knowledge and information through language, words, and numbers, leading to the creation of mathematics, coordinate systems, philosophy, religion, and science (Samo Liu, 2020; 2020a; 2020b).

Existing knowledge and information also suggest that from the moment of their inception, humans possessed philosophical contemplation abilities. Driven by survival and existence, humans persistently contemplated the universe, employing dual capacities of perception and sensation to explore their cosmic environment and relationships among existences (Samo Liu, 2025d). Such insights were documented and passed down following the creation of language, words, and numbers.

Modern physics and scientific knowledge indicate that ancestors' perception-based understanding of the universe was clear, yet expressed vaguely through language, words, and numbers. Human language and numerical systems describe material existence precisely, yet remain ambiguous in expressing concepts of "emptiness and nothingness", leading to philosophical contradictions.

To resolve these philosophical contradictions, Socrates proposed respectfully setting aside metaphysical issues concerning unknown space and existential matters, concentrating efforts on exploring human society and material existence. Aristotle implemented this idea (Aristotle, 2019; Samo Liu, 2025a).

Philosophical inquiries into cosmic origins were entrusted to religion for contemplation and preservation, while humans progressed along material philosophical and scientific paths. Eventually reaching modern physics, quantum mechanics, and relativity, science revealed that matter and non-material energy are mutually convertible under mechanical informational conditions, and are fundamentally equivalent. Quantum mechanics scientifically confirmed that matter emerges from non-material energy through mechanical interactions, subsequently balancing under mechanical conditions, reverting back into energy and information (Samo Liu, 2025b).

Logically, energy and matter represent a factor (Yang 阳), mechanics an impetus (Yin 阴), and the speed of light an extreme informational existence. Thus, matter, energy, and information form a triadic Yin-Yang dualistic relationship.

Under material philosophy's guidance, material science reached its pinnacle, transitioning into energy philosophy, energy science, information philosophy, and information science. Humanity thus discovered glimpses of the great universal origin—the natural divinity of the cosmos (Samo Liu, 2025c).

V. UNKNOWN KNOWLEDGE AND INFORMATION

5.1 Unknown Knowledge and Information about Material Existence

Under the guidance of material philosophy, humanity has achieved significant advancements in the field of material sciences. However, we still face numerous unknowns regarding material science. It can be said that the exploration of material science and philosophical reflections on matter remain extensive and filled with many unknown knowledge areas.

Humans, as material beings, confront material space, the material universe, and the material-based human society and world. For scientific purposes, it remains practical to treat space as three-dimensional, making material philosophy and science continually relevant.

According to existing knowledge, our scientific and philosophical reasoning categorizes matter, energy, and information, and even space and time, as material entities. This forms the basis of our current scientific understanding but simultaneously generates considerable unknowns and contradictions.

Modern scientific and technological knowledge is highly specialized and compartmentalized; experts in one field might be novices in another. Consequently, the pursuit and exploration of knowledge and information appear endless, requiring humans to embrace lifelong learning (Samo Liu, 2025a; 2025b). Quantum mechanics, relativity, modern physics, modern science, and three industrial revolutions have brought humanity into the realms of energy and information, both now critical to human survival and existence.

We know that the form of matter can be represented mathematically in three dimensions. This scientific method, employing coordinate systems and mathematics, is an extraordinary human achievement, despite matter existing in a multidirectional ("six-sided 六合") external form (Samo Liu, 2021a; 2021b; 2021c).

This scenario gave rise to contradictions within modern physics, persisting for over a century. Analyzed from a conceptual and foundational logical perspective, this problem cannot be resolved by physics or mathematics alone. Aristotle's material philosophy has led us into a labyrinthine trap (Aristotle, 2019; Samo Liu, 2025e).

Philosophical reasoning in science developed after Aristotle's reflections on space, the existence within it, and the relationship between space and time were set aside for theology. humanity lacks unified, standardized philosophical thinking about time and space.

The contradictions in modern physics concern genuine space and time, compelling us to reconsider these concepts. Ancestors contemplated these issues within cosmic-origin philosophy 2,500 years ago but were abandoned as contradictory by later generations. Precisely speaking, humans at that time lacked rational, scientific knowledge about space and existence, relying instead on perception—something most people neither comprehended nor trusted.

Quantum mechanics and relativity have validated our ancestors' intuitive knowledge, allowing cosmic-origin philosophy to serve as a philosophical framework for modern physics (Samo Liu, 2024g; 2024h; 2024i).

Perhaps adopting cosmic-origin philosophy to study energy and information can more effectively enhance our understanding of the material universe and material world, enriching our grasp of material knowledge and information.

Since the industrial revolution—especially following the third, information-based industrial revolution—the rise of computers and robotics has exponentially accelerated human-generated information. As modern physics and science reopened the door to cosmic-origin studies, humanity now confronts non-material philosophical inquiries into cosmic origins. Undoubtedly, the information humanity must now handle is infinite and immense, and its impacts are unpredictable.

cosmic-origin philosophy tells us that the universe's existence and information are infinite. At its core, cosmic-origin philosophy challenges humans to grasp, process, and understand information and knowledge, using these tools to solve existential contradictions in survival and existence.

5.2 Unknown Knowledge and Information about Non-material Existence

Physics introduced the concept of antimatter, yet it remains uncertain whether antimatter was genuinely discovered or if the concept merely represents certain experimental outcomes (Samo Liu, 2024h; 2024i). This result is like a philosophical contemplation of gravitational lenses. (Samo Liu, 2025e)

Analyzed logically from cosmic-origin philosophy, antimatter fundamentally does not exist; conceptually, it conflicts with thermodynamics. Matter exists realistically, involving motion and transformation, wherein physics identifies mechanics, energy, and information. What then is antimatter's nature?

Whether approached through material philosophy or cosmic-origin logic, the universe consists solely of matter, energy, and information—thus encompassing only material and non-material existences engaged in mutual transformation, movement, and balanced entropy tendencies (Samo Liu, 2024e).

Matter arises from non-material origins and returns thereto under informational conditions dictated by mechanics and time. In cosmic-origin philosophy, the author defines the concept of non-material existence explicitly (Samo Liu, 2024h).

Non-material existence is a cosmic-origin concept, foundational to matter and humanity. Taoism calls it Tao, Nothingness (Wu无), Yin-Yang 阴阳, and Qi炁; Buddhism calls it Emptiness 空, Causes 因, and Conditions 因缘 of causes and factors 因素; Ancient Greek philosophy calls it original existence 本原存在 (Laozi, 2019; Sakyamuni, 2020; Russell, 2017).

Influenced by information, matter emerges from non-material existence and returns to it under informational conditions. Energy is a form of non-material existence; information itself is an independent, non-material form. Currently, humanity lacks an accurate conceptual definition of information. Information is neither energy nor matter; temporarily, it can be defined as a non-material, zero-dimensional concept of "causation 因" (Yin 阴) (Samo Liu, 2025c). These represent philosophical considerations within cosmic-origin thought, awaiting scientific philosophical verification.

Modern physics, through energy and information, has inspired philosophical considerations of Yin and Yang within cosmic origins, termed basic energy and intelligent energy (Samo Liu, 2017; 2019; Liu Hongjun & Samo Liu, 2020). Intelligent energy embodies information, space, and heavenly attributes, categorized as Yin and causative, termed "Qian 乾." basic energy signifies matter and energy, categorized as Yang and conditional, termed "Kun 坤." Collectively, the universe encompasses material and non-material existence, known as "Qian Kun 乾坤."

These categorizations represent human linguistic, textual, and numeric conventions, interchangeable in labeling "Qian" as Yang and "Kun" as Yin, although conventionally "Qian Kun 乾坤" refers to Yang 阳 and Yin 阴.

Yet, Yin-Yang dynamics within "Qian Kun" remain mutable. In cosmic-origin philosophy, information is Yin, energy is Yang. During energy-matter transformations, energy becomes Yin and matter becomes Yang. In their interactive dynamics, matter serves as Yang and information as Yin. Such Yin-Yang relationships demonstrate the universe's vitality, as all universal creations from "nothingness" are living Yin-Yang integrations.

Regarding interactions among material existences, heavier (high-energy) matter is Yin; lighter (low-energy) matter is Yang. Yang always revolves around Yin, exemplified by the Moon orbiting Earth,

Earth orbiting the Sun, and galaxies orbiting black holes, extending upward to superclusters, paralleling electrons orbiting atomic nuclei at microscopic scales.

Humanity belongs to the material category and thus "Kun." Within humanity, females represent Yin 阴 (Kun 坤) while males represent Yang 阳, naturally orienting males around females, driven by biological reproduction—a natural, universal design.

The unknown knowledge of non-material existence remains a pursuit for humanity. Approximately 2,500 years ago, humans possessed perceptual, intuitive knowledge lacking scientific confirmation.

Today, having reached the zenith of material philosophy and sciences, humanity has constructed concepts of energy and information, applying them industrially. quantum mechanics and relativity's internal contradictions compel humanity to reconsider non-material existence and revisit fundamental spatial and temporal concepts.

Clearly, knowledge of energy and information falls within non-material categories, representing cosmic origins—The source of material cause, efficient cause, formal cause, and final cause. These align with Buddhism's Emptiness 空, Taoism's Nothingness 无, and Greek philosophy's foundational existence 本原存在 (Samo Liu, 2024i).

Quantum mechanics reveals matter arises through energy-information entanglements, characterized by wave-particle duality and uncertainty. Relativity equates matter and energy under light-speed conditions. Classical physics underscores matter's perpetual change, decay, and work. Thus, ancestral cosmic-origin philosophies now appear scientifically resolved (Liu Hongjun & Samo Liu, 2020; 2021a; 2021b).

Logically, Aristotle's historical suspension of cosmic-origin explorations allowed material philosophy and sciences to flourish. Yet, as humanity reaches scientific pinnacles, cosmic-origin concepts return naturally, resolving the contradictions embedded in modern physics, particularly between quantum mechanics and relativity.

Ultimately, humanity realizes that incomplete scientific knowledge reveals philosophy's profound necessity. Lacking adequate knowledge, philosophy risks profound errors. Humanity now faces existential concerns from dual-edged scientific developments—rooted fundamentally not in science itself, but in human hearts and minds, and our insufficient contemplation of cosmic origins.

Humanity's future thus hinges upon comprehensively grasping cosmic-origin philosophy, embracing peace by recognizing our unity with the cosmos, and resolving contradictions—fulfilling the profound universal intent behind humanity's creation (Samo Liu, 2025d; 2025e).

Usually, non-material knowledge and information are divided into two categories: theology and scientific philosophical metaphysics.

If material philosophy and science have significantly clarified our understanding of the material world and human society, then scientific knowledge about energy and information—already studied and applied for over 500 years—has now become our new metaphysical frontier.

Studying energy and information begins with understanding their forms and processes of existence, thus reigniting human reflection and research on space, time, and the existence within space, similar to how we approached material sciences (Samo Liu, 2025c).

"Zero (0)" is a miraculous human-created number, though it emerged last among our numerical concepts. (Jeremy Webb, 2018) It is the core of the coordinate system, the origin of all existence forms

and processes. We must fully appreciate this significant number, for it is the origin point of dialectical materialism (Samo Liu, 2025h; 2025b).

Modern physics and contemporary science have inspired humans to reconsider the cosmic origins of information and energy through the Yin-Yang dualism of Qiankun, prompting us to rethink the universe's non-material nature, marking a new beginning of exploring non-material knowledge. Such explorations, sparked by modern scientific insight, must undergo rigorous verification by science and scientific philosophy.

5.3 *Inspirations from Unknown Knowledge and Information*

Based on existing material philosophy, material sciences, and cosmic-origin philosophical logic, humans are composed of matter, which itself originates from non-material existence through motion and change. Both matter and non-matter exist, move, and transform within space, known collectively as the universal "Qiankun 乾坤," with space serving as the stage for existence (Samo Liu, 2021c).

The original or foundational existence in space is a Yin-Yang, limitless (Wuji 无极) entity, described as "light 光" in theology and physics alike. This "light" possesses Yin-Yang duality and is considered alive, though its precise form and existence process remain unknown. It defies any description by current material-scientific concepts—though the concepts of positrons and electrons in quantum mechanics may offer a starting point.

However, once existence manifests in forms expressible through human language, text, or numbers, its speed must fall below the speed of light. Conversely, any existence reaching the speed of light merges into infinite space (Samo Liu, 2025b).

Upon realizing existence as "infinite," we can comprehend why planets, galaxies, molecules, and atoms are so numerous, and why particles and quarks are so minuscule. Humans invented mathematics, enabling clear numerical descriptions regardless of quantity or size. Yet, "infinity" itself can be expressed by only one number: zero (0) (Samo Liu, 2025a; 2025b).

All existence originates, exists, moves, and transforms around the zero-coordinate point—this embodies dialectical materialism's principle of quantitative to qualitative change.

Currently, physics encapsulates cosmic creation in the "Big Bang" theory, aligning with material philosophy, cosmic-origin philosophy, and thermodynamics. When the Yin-Yang limitless existence (Wuji), called "light" by theology and physics, slows below the speed of light or splits due to certain causative conditions, heat emerges as a creative force. Thus begins the cyclical journey of material creation in the universe, generating "entropy," which might represent the observable material universe or its local portion.

Over time, with the cooling of extreme cosmic temperatures, existence initiates mutual transformations between energy and matter under mechanical and temporal conditions, striving toward equilibrium and cyclicity—though the precise cosmic-origin principles remain unclear.

Using material philosophy and scientific methodologies, humanity developed physics and chemistry, achieving modern science, nuclear weaponry, robotics, and cellular DNA research. Weapons' destructiveness escalates, robot chips shrink further, and DNA research grows ever more intricate. Humans continue discovering vast unknown knowledge about material reality and society, necessitating ongoing exploration and lifelong learning.

Nevertheless, the human psyche paradoxically resists the idea of enemies yet perceives enemies' existence, resulting psychologically in the impulse for total elimination. At material science's peak, humanity mastered universe-level energy and information—such as nuclear weapons—capable of self-annihilation. Atomic bombs, hydrogen bombs, and other catastrophic weaponry have been developed; their deployment undoubtedly threatens human survival.

Ironically, humanity has created methods and factors for its self-destruction—originating within our minds.

The paradox of humanity destroying itself seems absurd yet represents a severe existential threat that humanity must confront realistically.

Physics and modern science have reopened humanity's exploration of cosmic origins. Analyzed through cosmic-origin principles, humanity's limited understanding of universal and human origins underlies our current predicament.

From cosmic-origin analysis, humans individually and collectively generate both divine and demonic natures within themselves. Insufficient universal truth knowledge makes existential contradictions irresolvable. Without realizing that humanity was created precisely to resolve such contradictions, we might never transcend psychological barriers (Samo Liu, 2025e).

The premise of all existence is humanity's survival and existence.

Facing numerous unresolved questions and contradictions about the material universe's Qiankun, we have simultaneously reopened the door to cosmic-origin exploration, confronting vastly greater non-material universal existences. Infinite unknown knowledge awaits human exploration and resolution. Given material philosophy and science have brought humanity to this critical survival juncture, what steps should humanity now take?

VI. EXPLORING KNOWLEDGE AND INFORMATION: PHILOSOPHICAL REFLECTIONS

Many philosophers have emerged throughout human history, yet no unified definition of philosophy exists due to its inherent diversity. Indeed, everyone thinks, making everyone, in essence, a philosopher (Samo Liu, 2025a). Aristotle believed that philosophy is the leader of all disciplines. (Aristotle, 2016).

Philosophy is often mistakenly considered impractical or esoteric. However, fundamentally, philosophy represents human thinking and underpins humanity's achievement of knowledge and information. Philosophical reflection permeates human survival, existence, daily life, and work.

Aristotle's classification of philosophy into First Philosophy and Second Philosophy, and the West's labeling of engineering doctorates as PhDs ("Doctor of Philosophy"), both reflect philosophy's foundational significance.

Humans possess innate self-awareness and an instinct for hunger before they acquire language, writing, and numbers after birth. After learning these communication tools, mature humans develop sexual instincts, planning their lives, careers, learning, and daily routines through language, words, and numbers. Life's ultimate goals and everyday objectives are similarly planned and articulated, necessitating daily logical and dialectical problem-solving until death.

Human thought arises from the Yin-Yang interplay of mind and brain, involving perception and sensation. Thinking and dialectical logic are natural, existential functions inherent to living beings.

This natural cognitive capacity grants humans the unique ability to create and transmit information. Thus, language, words, and numbers emerged, empowering humanity as creators and controllers of information, uniquely intelligent beings.

The Chinese character "哲" (zhe) denotes wisdom and information. Therefore, "philosophy" (Zhexue 哲学) literally translates as the study of wisdom—the pursuit of knowledge and information. Wisdom embodies philosophical contemplation, enabling humanity's ascendancy as master of all things and ruler of the universe.

Human ancestors employed wisdom and information to ponder cosmic origins, while Aristotle initiated material philosophical thought and scientific exploration. This continuous philosophical reflection and scientific inquiry have shaped humanity's present-day achievements.

6.1 The Relationship Between Science and Philosophy

When knowledge and information from science and philosophy fail to unify, Aristotle transformed the ancestral philosophy of cosmic origins into material philosophy and material science, delegating temporarily unknown knowledge and information to theology. This allowed material philosophy and science to flourish dramatically.

Material philosophy has always guided material scientific development. Imagine the progress of scientific thought and technological advancements over the last 500 years—every breakthrough first required a philosophical framework from material philosophy, then verification through coordinate systems and mathematics, followed by experimental validation, and finally realization through industrial revolutions and technological means. The author had the privilege of being one of them.

Philosophers such as Descartes, Newton, and Leibniz created mathematical verification methods—including coordinate systems and calculus—inspired by material philosophy. Bacon and Descartes developed logical verification methods for scientific experiments. Kant formulated philosophical methods for analyzing contradictions. Schelling introduced the concept of natural divinity, and Hegel developed dialectics philosophical logic based on concepts and foundational ideas (Samo Liu, 2024i).

These philosophical logics became the foundations for classical and modern physics' remarkable growth. One cannot deny the guiding role of dialectical philosophical logic throughout the three industrial revolutions. Scientists should deeply contemplate whether today's scientific achievements would even exist without philosophy's dialectical logic. From a natural and dialectical standpoint, we must reconsider the relationship between science and philosophy. Thus, when certain scientists boldly proclaim that "philosophy is dead," we must ask: could science itself survive without philosophy?

Using this logic, philosophy and science constitute a Yin-Yang relationship—twin siblings. Philosophy is the soul of science, while science is philosophy's existence (Liu Hongjun & Samo Liu, 2020; 2021a).

Material philosophy and material science mutually support each other, guiding modern science to the pinnacle of material understanding, giving rise to quantum mechanics and relativity. Breakthroughs in material science have spurred discoveries in information and energy sciences, introducing numerous philosophical contradictions within modern physics.

These contradictions have caused anxiety and deep reflection among philosophically-minded physicists. The issue lies not within science itself but within the philosophical foundation of science—the soul of science—which has overlooked ancestral wisdom regarding cosmic origins .(Samo Liu, 2024d)

Insufficient scientific and philosophical knowledge has created these contradictions, manifesting dilemmas about human survival and existence, and producing science's "double-edged sword." To resolve the many contradictions emerging in modern science, we must use modern scientific knowledge and information to re-expand philosophical reflections on cosmic origins.

Such philosophical reflection must employ scientific philosophical methodologies and cosmic-origin philosophy to explore and expand human knowledge and information. Although humans inherently possess artistic sensibilities, scientific philosophy must remain rigorous, allowing no artistic embellishment.

New myths such as human time reversal and high-dimensional spaces, arising from modern scientific theories, must be seriously addressed by science, not casually dismissed.

6.2 Science and Theology

When philosophical knowledge fails scientific verification or when certain natural phenomena elude human understanding, metaphysics inevitably emerges as humanity's eternal exploration.

Facing an infinite material universe, an immeasurably vast yet ultimately finite existence—what we might call "infinite"—humans forever remain ignorant children, destined to perpetual exploration and learning. Fortunately, we now know that within the material universe, purely material existence constitutes merely 4.9% of all matter-space.

When metaphysics transforms into faith, theology emerges—a profound discipline arising naturally from the human heart. It represents a noble inquiry, untarnishable by human language. Humanity uses artistic contemplation to transform explorations of unknown knowledge and information into spiritual aesthetics, thereby honoring the cosmic divinity that created humanity.

The author, employing cosmic-origin philosophy, characterizes physics itself as theology. If scientific philosophy accepts this perspective, science and theology could align philosophically, collectively termed natural theology of the cosmos.

Current theological concepts, shaped by subjective human consciousness, do not reflect this philosophical category. Criticism and disdain from certain scientists and philosophers towards human-conceived notions of God raise significant questions. What does this imply?

It implies that religious communities should independently reflect upon their traditions historically, philosophically, and scientifically. Such introspection should remain free from externally imposed constraints or frameworks by scientific or philosophical authorities, who themselves lack the legitimacy to prescribe conditions.

Facing various contradictions within modern physics and science, the scientific and philosophical communities lack a unified, standardized scientific-philosophical framework. Until these internal contradictions are resolved, they hold no right to criticize humanity's profound beliefs.

6.3 The Relationship Between cosmic-origin Philosophy and Physics

Material philosophy propelled developments in material science, leading directly to achievements in classical and modern physics. Conversely, accomplishments in modern physics resolved philosophical dilemmas related to cosmic origins, reopening the gates to cosmic-origin exploration (Samo Liu, 2017; 2019; Liu Hongjun, 2020).

If the scientific community's philosophical approach accepts the scientific validity of cosmic-origin philosophy, many concepts in classical and modern physics—as well as their relationships to foundational ideas—will undergo significant revisions.

For example:

Space represents humanity's eternal unknown and sacred exploration. While humans may name space for scientific inquiry, arbitrary definitions of space must be avoided.

language, words, and numbers created by humans inherently depend on spatial concepts. The external forms of all existence express spatial form-causation. The material world may be defined as three-dimensional space, while the non-material realm may be termed non-three-dimensional space or zero-dimensional space space. Although naming conventions for spatial form-causation may vary, definitions must remain precise. Different forms of existence can be expressed using various spatial coordinate systems, always with zero as their reference origin (Samo Liu, 2025h).

Time is a sacred concept eternally pursued by humanity. While humanity can assign natural phenomena as temporal units for scientific inquiry, distortions of the concept of time are unacceptable.

Time fundamentally represents existence's self-awareness of its own existential process—a perception of thermodynamics and all mechanical processes. This irreversible thermodynamic process forms existence itself.

Human-assigned temporal units, based on natural phenomena, provide the scientific foundation for exploring existence, serving as humanity's method of measuring its own existence. Time is thus an unalterable, irreversible foundational physical unit defined by humans.

Different existences utilize varying temporal coordinate systems: celestial processes can be used "kalpa 劫", quantum mechanics use Planck time, and daily life employs familiar units like years, days, hours, and seconds—all anchored at zero as a starting point. (Samo Liu, 2025e;2025f)

Existence remains humanity's eternal object of inquiry and the source of human knowledge and information. Broadly, existence divides into two categories: causative conditions ("Yin") and factors ("Yang"). The "factors" category includes matter and energy, whereas "causative conditions" encompass mechanics and time.

Through philosophical and scientific exploration, humanity has dramatically advanced understanding of matter. Physics has notably progressed in understanding energy and made strides in comprehending information. Investigating energy and information, humanity has created nuclear weapons, invented robotics, and discovered cellular informational structures.

These developments have produced miracles alongside significant contradictions, simultaneously unlocking philosophical reflections on cosmic origins. Thus, physics has inspired reconsiderations of cosmic origins (Samo Liu, 2024g), and scientific philosophy has illuminated physical principles underlying natural philosophy (Samo Liu, 2024i).

By integrating material philosophy and cosmic-origin philosophy, the key novel viewpoints for physical thinking are as follows:

(1) *Quantum mechanics* is a great science. Analyzed through dialectical materialist logic, quantum mechanics represents humanity's philosophical culmination after over 2500 years of contradictory yet ascending philosophical inquiry. It embodies material philosophy's highest philosophical achievement toward cosmic-origin philosophy's scientific conclusion. In a series of nine articles (Samo Liu,

2024g-2025f), the author argues that there is no inherent theoretical contradiction between quantum mechanics and relativity; rather, the contradictions arise from philosophical misunderstandings. A synthesis of cosmic-origin philosophy and material philosophy can unify and resolve these contradictions, eliminating doubt about quantum mechanics' profound scientific validity.

Quantum mechanics and relativity collectively establish a scientifically philosophical natural theology (Samo Liu, 2024g).

(2) After careful examination of Einstein's great works, no evidence supports claims regarding Einstein's belief in time reversal. Instead, Einstein scientifically expressed skepticism toward humanity's assumed definitions of three-dimensional space.

Einstein remains a deeply respected, great scientist. Einstein himself was not the only one who proposed the concept of light speed. He confirmed the profound truth that the speed of light represents the dynamic limit of universal reality. This discovery led him to question material philosophy's assumptions about spatial and temporal materiality. Einstein's curved spacetime theory reflects skepticism toward the material philosophy conception of space and time. His doubts about quantum mechanics represent philosophical skepticism toward space and time concepts embedded in material philosophy.

Thus, the concept of "time reversal" is not Einstein's invention, but rather a mathematical or artistically philosophical distortion by followers lacking comprehensive scientific-philosophical guidance. The previously mentioned nine articles discussing contradictions between quantum mechanics and relativity do not criticize Einstein but praise the philosophical inspiration derived from his work.

Material philosophy's restrictive influence on scientific philosophy has become severe, necessitating new exploration within cosmic-origin philosophy.

(3) *Force* embodies universal divinity, the essential attribute through which matter and energy perceive existence, and facilitates mutual perceptions among existences (Samo Liu, 2024i). I will prove this point in the articles I will publish later.

(4) *Motion* arises from matter's inherent perception. The concept of motion emerges as an attribute only after the formation of atomic matter. Likewise, velocity, as an attribute, exclusively pertains to matter, since matter's existence is expressible via spatial coordinates. Motion can be accurately described using three-dimensional coordinate systems (Samo Liu, 2024i).

(5) *Change* characterizes both material and non-material existence fundamentally. Change originates from existences' intrinsic perception of force and time, with motion serving as one manifestation of change. All existence, being Yin-Yang dualities and embodying informational existence, inherently represents temporal processes expressible through forms, structures, and processes, inherently holding the significance of life (Samo Liu, 2024i).

(6) *Action at a distance and contact action*: Action at a distance represents the fundamental origin of matter, existence, motion, and change; whereas contact action denotes phenomena of these motions and changes in matter and existence.

(7) *Velocity, specific gravity and density as a crucial physical parameter of material existence*:

Guided by material science and philosophical frameworks, physics has established numerous material scientific parameters. Velocity is among these critical parameters.

Humans philosophically define units of time and construct three-dimensional spatial coordinate systems to specify relative positions and distances between objects. Consequently, the change in an object's position, thus determined, defines velocity.

Velocity, philosophically defined, enables scientific investigation into natural states of material existence. Any claims of curved or reversed time would fundamentally disrupt this parameter's validity, severely complicating scientific study of material states and causing conceptual chaos in physics.

Specific gravity and density are similarly critical physical parameters. Humans define spatial volume through philosophical design. The amount of matter within a unit volume constitutes specific gravity or density. Modern physics equates mass with energy under conditions approaching the speed of light; thus, specific gravity and density reflect the quantity of energy within a given volume.

Accordingly, simple mathematical calculations within three-dimensional coordinates quantify the density of "existence" within spatial units.

Modern physics informs us that within observable, calculable space, dark energy and dark matter constitute 95.1%, whereas traditional matter comprises only 4.9%. Science also confirms that dark energy and dark matter are fundamentally non-material.

These conclusions emerge from material philosophy and science methodologies. With recognition of non-material concepts and acceptance by scientific philosophy of the 95.1% ratio occupied by dark energy and dark matter, cosmic-origin philosophy inevitably becomes integral to human knowledge, prompting new philosophical reflections.

(8) Redefinition of non-material physics concepts:

The concept of non-material existence emerges from modern physics and science, informed by Daoist, Buddhist, ancient Greek philosophies, and dialectical materialism. This conceptualization awaits further scientific and philosophical validation.

Non-material existence forms a foundational concept within Aristotle's philosophical cycle of ascending cosmic-origin thought, extending material philosophical contemplation and integrating with it seamlessly.

Understanding non-material existence hinges critically upon comprehensively reassessing mass, analyzing relationships between mass, universal gravitation, and other mechanical forces.

Crucially, distinguishing material and non-material attributes of energy constitutes an essential exploration within existing human knowledge and information.

Equally vital is the exploration and analysis of "informational existence" specifically the "causative因" aspect (Yin阴) of information. Such exploration signifies a breakthrough in human understanding of space, time, and universal Qiankun乾坤, representing a divine form of existence.

(9) Physical concepts regarding information:

Information is neither matter nor energy.

In spatial philosophical terms, information exists neither as zero-dimensional nor three-dimensional. For convenience in contemplation, it is provisionally defined as a zero-dimensional existence (Samo Liu, 2025c).

Within philosophical discourse on temporal processes, time itself is information, possessing neither a spatial position nor an original concept of velocity.

Thus, classical and modern physics must fundamentally reevaluate mechanical concepts, categories, and origins. Quantum mechanics, specifically the bosons of the four fundamental forces, warrants renewed reconsideration, particularly regarding bosons associated with the weak nuclear force (Samo Liu, 2024i).

Concepts of wave-particle duality, uncertainty, and entanglement in quantum mechanics should be reexamined within the divine informational paradigm.

VII. CONCLUSION

Whether it is the philosophy of the cosmic origin or Material Philosophy, both are modes of human thought. The creation of the philosophy of the cosmic origin by our ancestors led to contradictions in thought. Aristotle entrusted the 'unknown' to metaphysics and theology, simplifying it into material philosophy, guiding material science to today. Quantum mechanics and relativity have verified the ancestral philosophy of the cosmic origin, compelling humanity to rethink issues concerning space, time, and their interrelationships. The holistic contemplation of the universe has been inspired and corroborated by modern science, and new models of cosmic origins are once again entering human thought.

Aristotle set aside human philosophical contradictions, initiating humanity's exploration into material philosophy and science, leading to nearly 500 years of unprecedented scientific and physical revolutions. Modern physics has now redirected humanity back toward cosmic-origin philosophy.

Linking Daoist, Buddhist, and ancient Greek philosophies through modern science and physics, materialist Dialectics generates renewed philosophical reflections on cosmic origins.

Dialectical materialist analysis suggests cosmic-origin philosophy can resolve theoretical contradictions between quantum mechanics and relativity in modern physics (Samo Liu, 2024g; 2024h; 2024i). The philosophical method of using Aristotle's 'known' to study the 'unknown' provides a modern physics framework, which logically requires further scientific philosophy assessment.

Subsequent discussions and analyses will further elaborate on these cosmic-origin philosophical principles, Clarify its philosophical foundations for academic discussion and critique.

Declaration of Interests:

The author declares no conflicts of interest.

Data Availability Statement:

According to publication standards and terms, data presented in this article are publicly accessible to support knowledge sharing. The author sincerely appreciates contributions from referenced works.

Solely provided funding statement: This research article received no funding support. Publication costs are borne by the author.

Ethical Approval: This article does not contain any studies with human participants performed by any of the authors.

Informed Consent: This article does not contain any studies with human participants performed by any of the authors.

REFERENCE

1. Aristotle, (2019) "Physics," translated by Zhang Zhuming, October 2019, Beijing, Commercial Press.
2. Aristotle, (2016) "Metaphysics," translated by Cheng Shihe, Taihai Publishing House, 2016.9.
3. Garrett Thomson & Marshall Missner. (2019). On Aristotle (translated by Zhang Xiaolin). Tsinghua University Press, May 2019.
4. Hiroshi Ohguri, (2015.1) "Strong Interaction and Weak Interaction" translated by Yi Ning, People's Posts and Telecommunications Press, 2015.1. Beijing.
5. Jeremy Webb, (2018) "The Void", translated by Feng Yongyong and Jin Taifeng, June 2018, The Commercial Press, Beijing.
6. Laozi (ancient)(2019) , annotated by Wang Bi (Three Kingdoms, Wei), collated and interpreted by Lou Yulie. (2019). Annotations on Laozi's Dao De Jing. Zhonghua Book Company, Beijing, December 2019.
7. Liu Hongjun, (2020). *Philosophical Reflection on the Origin of the Universe*. *Scientific Herald*, 2020, 23, 346-348. (In Chinese)
8. Liu Hongjun & Samo Liu, (2020). Reflection and Research on the Origin of the Universe. (In Chinese). Taipei Warmth Publishing.
9. Liu Hongjun & Samo Liu, (2021a). *Thoughts and Research on Human Origins*. (In Chinese). Taipei Warmth Publishing.
10. Liu Hongjun & Samo Liu, (2021b). *Zero-Dimensional Universe - The Survival Test of All Things*. (In Chinese). Taipei Warmth Publishing.
11. Liu Hongjun & Samo Liu, (2021c). *Zero-Dimensional Universe - The Absolute Space Test*. (In Chinese). Taipei Warmth Publishing.
12. Liu Hongjun & Samo Liu, (2021d). *Tao Te Ching - Universal Declaration*. (In Chinese). Taipei Warmth Publishing.
13. Liu Hongjun & Samo Liu, (2024). *Textual Research of the Universe Original Classics*. (In Chinese). Taipei Warmth Publishing.
14. Russell, B. (2017). A History of Western Philosophy (translated by Bo Yong). Taihai Publishing House, March 2017.
15. Sakyamuni (2020) (Ancient), Edited by Lai Yonghai, "Diamond Sutra and Heart Sutra" translated and annotated by Chen Qiuping; March 2020, Beijing, Zhonghua Book Company.
16. Samo Liu, (2017). *Revelation and Reflection on Mankind by Modern Physics Part I*. Open Journal of Philosophy, 2017, 7, 435-447. DOI: 10.4236/ojpp.2017.74023.
17. Samo Liu, (2019). *Revelation and Reflection on Mankind by Modern Physics Part II: Consideration on the Multidimensional Universe*. Open Journal of Philosophy, 2019, 9, 72-81. DOI: 10.4236/ojpp.2019.92007.
18. Samo Liu, (2020a). *Philosophical Reflection over the Origin of the Universe*. Philosophy Study, March 2020, Vol. 10, No. 3, 214-223. DOI: 10.17265/2159-5313/2020.03.005.
19. Samo Liu, (2020b). *The Essence of the Universe and Humankind*. Open Journal of Philosophy, 2020, 10, 316-330. DOI: 10.4236/ojpp.2020.103021.
20. Samo Liu, (2021a). *Cosmic Space in Zero Dimension: A Discussion on Spatial Questions According to M-Theory*. Open Journal of Philosophy, Vol. 11, No. 1, February 2021, 159-170. DOI: 10.4236/ojpp.2021.11012.
21. Samo Liu, (2021b). *A Second Discussion on Cosmic Space in Zero Dimension—A Discussion on Spatial Questions According to Classical Physics*. Journal of Applied Mathematics and Physics, Vol. 9, No. 4, April 2021, 556-564. DOI: 10.4236/jamp.2021.94039.
22. Samo Liu, (2021c). *The Third Discussion on Cosmic Space in Zero Dimension—According to the Correspondence between Clarke and Leibniz*. Open Journal of Philosophy, Vol. 11, No. 2, May 2021, 326-335. DOI: 10.4236/ojpp.2021.112022.

23. Samo Liu, (2024a). *Exploring the Essence of the Universe*. LJRHS, Vol. 24, Issue 5, 1-11. Great Britain Journals Press.
24. Samo Liu, (2024b). *Second Exploration of the Essence of the Universe*. LJRHS, Vol. 24, Issue 8, 1-11. Great Britain Journals Press.
25. Samo Liu, (2024c). *Third Discussion on the Origin of the Universe*. LJRHS, Vol. 24, Issue 8, 41-52. Great Britain Journals Press.
26. Samo Liu, (2024d). *A Letter to the Scientific Community*. LJRS, Vol. 24, Issue 7, 11-19. Great Britain Journals Press.
27. Samo Liu, (2024e). *The Fourth Discussion on the Origin of the Universe*. LJRS, Vol. 24, Issue 8, 1-10. Great Britain Journals Press.
28. Samo Liu, (2024f). *The Fifth Discussion on the Origin of the Universe*. LJRS, Vol. 24, Issue 8, 23-32. Great Britain Journals Press.
29. Samo Liu, (2024g). *Scientific Cosmological Ontology*. Open Journal of Philosophy, 2024, 8, 628-648. DOI: 10.4236/ojpp.2024.143043.
30. Samo Liu, (2024h). *Modern Physical Philosophy Framework*. Open Journal of Philosophy, 2024, 8, 709-729. DOI: 10.4236/ojpp.2024.143049.
31. Samo Liu, (2024i). *The Physical Principles of Natural Philosophy*. Open Journal of Philosophy, 2024, 14, 967-994, <https://doi.org/10.4236/ojpp.2024.144063>
32. Samo Liu, (2025a). *Reflection on the Science Philosophy*. Open Journal of Philosophy, 2025, 15(1), 19-40, <https://doi.org/10.4236/ojpp.2025.151003>
33. Samo Liu, (2025b). *The Pinnacle of Science or the End of Scientific Thought*, Open Journal of Philosophy, 2025, 15(1), 41-63, <https://doi.org/10.4236/ojpp.2025.151004>
34. Samo Liu, (2025c). "Space and Time", Open Journal of Philosophy, 2025, 15(1), 181-205, <https://doi.org/10.4236/ojpp.2025.151011>.
35. Samo Liu, (2025d). *Human Origin*, Open Journal of Philosophy, 2025, 15(2), 309-337, <https://www.scirp.org/journal/paperinformation?paperid=141908>
36. Samo Liu, (2025e), "Humans and Existence", Open Journal of Philosophy, 15, 884-907. doi: 10.4236/ojpp.2025.154053.
37. Samo Liu, (2025f), "A New Discourse on Philosophy", Open Journal of Philosophy, 2025, 15(3), 615-639, <https://www.scirp.org/journal/paperinformation?paperid=144617>.
38. Samo Liu, (2025h), The study of nature and form in zero, LJRS, Vol. 25, Issue 12, 41-60. Great Britain Journals Press.



Scan to know paper details and
author's profile

Concept of the "Minimum Energy Expenditure" Principle

Mukhamad I. Gulamov

ABSTRACT

In this work, based on the analysis of specific biological examples, the previously unknown principle of "minimum energy expenditure" is investigated. This principle plays a fundamental role in speciation, the formation of biodiversity, trophic chains, ecological niches, as well as in ensuring the long-term existence of a biological species, population, and individual organism. The central idea of this principle is that among many possible scenarios, the one that requires the least energy expenditure for its continued existence is chosen. This, in turn, provides the selected scenario with a minimum of entropy, that is, maximum certainty. This regularity is characteristic of all established biological objects and processes. This generalized principle applies to a wide range of biological phenomena—from low-molecular processes to the biospheres level—and is one of the fundamental properties of open systems. This principle may play a significant role in the design and construction of modern technological, artificial, and resilient biological constructs and robotss.

Keywords: principle of minimum energy expenditure, open systems, dissipative structures, speciation, biodiversity, trophic chain, ecological niches, evolutionary optimization, energy efficiency in biology, reduction of entropy.

Classification: LCC Code: QH307.2, QH541, QH501

Language: English



Great Britain
Journals Press

LJP Copyright ID: 925616
Print ISSN: 2631-8490
Online ISSN: 2631-8504

London Journal of Research in Science: Natural & Formal

Volume 25 | Issue 14 | Compilation 1.0



Concept of the "Minimum Energy Expenditure" Principle

Mukhamad I. Gulamov

ABSTRACT

In this work, based on the analysis of specific biological examples, the previously unknown principle of "minimum energy expenditure" is investigated. This principle plays a fundamental role in speciation, the formation of biodiversity, trophic chains, ecological niches, as well as in ensuring the long-term existence of a biological species, population, and individual organism. The central idea of this principle is that among many possible scenarios, the one that requires the least energy expenditure for its continued existence is chosen. This, in turn, provides the selected scenario with a minimum of entropy, that is, maximum certainty. This regularity is characteristic of all established biological objects and processes. This generalized principle applies to a wide range of biological phenomena—from low-molecular processes to the biospheres level—and is one of the fundamental properties of open systems. This principle may play a significant role in the design and construction of modern technological, artificial, and resilient biological constructs and robots.

Keywords: principle of minimum energy expenditure, open systems, dissipative structures, speciation, biodiversity, trophic chain, ecological niches, evolutionary optimization, energy efficiency in biology, reduction of entropy.

I. INTRODUCTION

In this work, we limit our consideration exclusively to the principle of minimum energy expenditure, without addressing other, albeit related, principles such as the principle of minimum free energy, the principle of minimum total potential energy, and the principle of least action. Our goal is a detailed study exclusively of the principle of minimum energy expenditure using biological examples, emphasizing its unique role in the formation of the flora and fauna of the Earth's surface.

Although the principle of minimum energy expenditure and the principle of least action may seem conceptually close, they have significant differences. The scope of the principle of least action is limited to objects and phenomena of the physical world, where it has been thoroughly studied and formalized [9, 12]. In this work, we focus on the principle of minimum energy expenditure, as it is this principle that allows for effective analysis of regularities in biological systems.

In a broad sense, the principle of least action states that physical systems evolve in such a way as to minimize a certain quantity called action. Action is defined as the time integral of the system's Lagrangian, which represents the difference between its kinetic and potential energies. This principle is universal and applicable to a wide range of physical phenomena, from classical mechanics and electrodynamics to quantum mechanics. Mathematically, the principle is expressed using variational calculus, where instead of seeking a specific trajectory of an object, a trajectory is sought that makes the action functional stationary [12].

Examples of the application of the principle of least action:

- Classical Mechanics: A body thrown in a gravitational field moves along a trajectory that minimizes action.
- Optics: Light propagates along a path that minimizes propagation time (Fermat's principle, which is a special case of the principle of least action).
- Electrodynamics: The motion of charged particles in an electromagnetic field also obeys the principle of least action.
- General Relativity: Geodesics (paths along which objects move in a gravitational field) represent paths of least action.

The principle of minimum energy expenditure is one of the fundamental principles of the biological world, underlying many natural phenomena. It plays a key role in the processes of natural selection and the evolution of the biological world [3]. Living systems, functioning as open systems and constantly exchanging matter and energy with the environment, represent dissipative structures. They maintain their internal order (low entropy) through continuous production and export of entropy to the external environment. Thus, the minimization of energy expenditure corresponds to the minimization of internal entropy generation, which means maintaining the highest degree of order in the system [10].

II. MATERIALS AND METHODS

Based on empirical observations and a comparative analysis of specific and hypothetical biological examples, this study examines the concept of the "principle of minimum energy expenditure." First, it is necessary to clarify what is meant by "energy expenditure." In this work, "energy expenditure" refers to the energy required to maintain the biological structure or phenomenon itself. This quantity is not expressed in any specific energy units. The minimum energy expenditure is primarily associated with the genetic predisposition of biological systems (species, population, organism) and the corresponding structural arrangement of open physical systems. This will become clear in the subsequent presentation of our "minimum energy expenditure" concept.

The core idea of the principle of minimum energy expenditure is that, out of a multitude of possible options for the formation of a new biological object, the emergence of a phenomenon, or the course of a natural process, nature realizes the one that requires the least energy expenditure for its further existence [6]. Unlike the principle of least action, which pertains to the minimization of action over time, the principle of minimum energy expenditure determines the initial structure and organization of a biological object or phenomenon. This constitutes their fundamental difference. Moreover, the principle of minimum energy expenditure is more broadly applicable precisely to objects and phenomena of the biological world.

The existence of any biological object implies a certain degree of order; that is, the formation of any new structure must occur with a minimal increase in disorder. The principle of minimum energy expenditure explains this as nature's striving to realize the most probable option, in which the energy costs for forming and maintaining the structure are minimal. Consequently, the evolution of the biological world is directed towards establishing and maintaining order, which is confirmed by the ascending line of development from low-molecular biological objects to the biosphere level.

It is precisely the principle of minimum energy expenditure that ensures the possibility of long-term existence for any variant of an event realized in nature. Furthermore, the minimization of energy expenditure directly leads to the minimization of entropy, which, in turn, guarantees a high degree of certainty in the evolution of natural processes. This same principle drives all biological evolutionary processes occurring under conditions that meet the requirements of the ecological field of survival [5].

The requirements of the principle of minimum energy expenditure (its qualitative and quantitative characteristics) for each biological object or phenomenon are determined by its function. For example, the energy costs for maintaining metabolism in a predator and its prey will differ significantly in accordance with their roles in the trophic chain.

Let's consider a few examples. Take the migration of migratory birds: one route passes directly over a mountain range, requiring significant energy expenditure, while another is circuitous, along the coast, where access to food is easier and strong winds are less intense. Birds, as a rule, choose the second option, minimizing the total energy costs for migration, even if it is longer. Another illustration is the two types of metabolism in bacteria. In an oxygen-rich environment, bacteria use aerobic respiration, which generates significantly more energy from a smaller volume of substrate. In an oxygen-free environment, they switch to anaerobic respiration, which produces much less energy from the same amount of food. The realization of aerobic respiration in conditions of sufficient oxygen is due to its maximum energy efficiency. Yet another example is plant growth. A plant optimally allocates its resources (energy, water, nutrients) to maximize access to light and water. This may lead to slower growth or even death of some of its parts, but overall it allows the plant to minimize energy costs for survival and reproduction.

As examples of a different kind, one can consider mutational changes leading to the appearance of, for instance, a six-legged lamb or a three-eyed child; numerous such cases are known. Such individuals are generally incapable of long-term survival or reproduction. The reason lies in an energy deficit: the energy they consume is insufficient even for maintaining basic life functions of the organism, let alone performing vital functions such as hunting or reproduction. According to the principle of minimum energy expenditure, for each biological species, the optimal structure corresponds to the "standard" (four legs, two eyes, two arms, two feet, and so on), because precisely such variants ensure minimal energy costs for existence.

Upon analyzing the correspondence of each species to its ecological niche, it becomes evident that niches are distributed in trophic chains in accordance with the principle of minimum energy expenditure. At each link of the trophic chain, species optimally conforming to this principle dominate. Moreover, the nature of "minimum energy expenditure" is specific to each level: it is distinct in the plant world, different in the herbivore link, and entirely unique among predators. Thus, each trophic level is characterized by its unique manifestation of the principle of minimum energy expenditure.

A more generalized and illustrative example reflecting the principle of minimum energy expenditure can be seen in the ecological pyramid of energy by E.P. Odum (1975) in ecological systems (see Fig. 1).

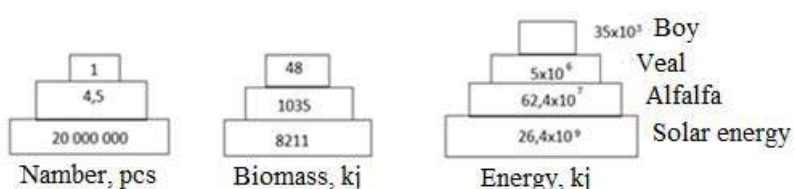


Fig. 1: Ecological Pyramids (after E.P. Odum) (not to scale)

III. RESULT

Modern evolutionary theory shows that in archaic times, the prevailing conditions and inorganic matter gave rise to the organic world, leading to the emergence of life in its biological understanding. Thus, the phylogeny of organisms, based on the principle of minimum energy expenditure,

demonstrates the directions and selective process of transforming various life forms, expressed in a general tendency towards the increasing complexity of the biological organization of living matter. Biological processes in the Earth's geographical envelope are multidirectional, saltatory, and, from an ecosystem perspective, ordered. They are subject to the logic of constant improvement and adaptation of organisms to changing habitat conditions thanks to the principle of minimum energy expenditure [3].

Informational, thermodynamic, and synergetic regularities collectively generate diversity, which can be viewed as evolutionary development. The mechanism of such development is the circulation of energy, matter, and information. This circulation occurs and will continue to occur uninterruptedly. The natural diversity of interconversions of energy, matter, and information in nature is infinite. Various biological species are, in essence, different mechanisms for converting energy from one form to another. All these transformations occur in accordance with the principle of minimum energy expenditure, which ensures the stability of their manifestation. Ultimately, this generates diversity in the real world, where this very diversity is both cause and effect [3].

Elements of biodiversity are constantly exposed to forces of attraction and pressure from surrounding environmental elements. As a result, unpredictable properties of the system manifest themselves. The action of internal forces of attraction and pressure leads to a violation of symmetry and to clustering, which, in turn, entails renewal. Interactions of any two or more elements from the entire array of Diversities of the Physical World (DPW) are always compared with one element from the multitude of All possible mentally conceivable diversities of information models of objects of ideal or physical nature (DIMIFN) in accordance with the principle of minimum energy expenditure [4] (see Fig. 2).

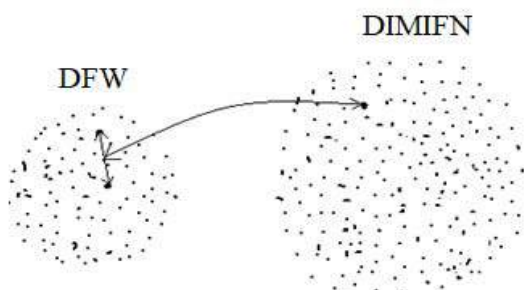


Fig. 2: Conditional representation of the relationship between two sets: DFW and DIMIFN.

Variants from the multitude of All possible mentally conceivable diversities of information models of objects of ideal or physical nature (DIMIFN) are realized in objects of the spatio-temporal continuum (Diversities of the Physical World (DFW)) through natural selection, that is, in accordance with the situation prevailing in nature within a given spatio-temporal continuum (the ecological field of survival) [4,5]. In this process, the guiding force of natural selection is the principle of minimum energy expenditure. This represents a logical continuation of the existence of physical objects from DFW that have exhausted their life cycle [4].

When a trophic chain or web is disrupted, several alternative chains or webs typically emerge. What accounts for the greater probability of a particular chain or web forming?

The probability of a particular alternative chain or web forming is determined by a variety of factors, including:

1. Resource Availability: Which species, capable of occupying the vacant niche, have the greatest access to necessary resources (food, territory, light, water, etc.)? Species that can most efficiently utilize available resources will have an advantage.
2. Species' Tolerance Ranges and Adaptability: As we have already discussed, species with wide tolerance ranges to various ecological factors (temperature, humidity, pH, etc.) and high adaptability will have a greater chance of survival and occupying the niche.
3. Competition: Which species are the strongest competitors for resources in a given situation? Competitive interactions between species will determine which species can successfully establish themselves in the new structure.
4. Predation and Other Interactions: The presence or absence of certain predators or symbionts can strongly influence the survival and distribution of species.
5. Randomness and Historical Factors: Sometimes random events (e.g., the accidental appearance of a particular species in a given location) or historical factors (e.g., which species were already present in the ecosystem before the disruption) play a role.

Ultimately, the formation of a specific trophic chain or web is determined by the complex interaction of all the aforementioned factors, with the principle of minimum energy expenditure playing a leading role.

Let us consider a hypothetical trophic structure of biodiversity (a conceptual model of a trophic web). Suppose we are given the following biodiversity structure, consisting of 13 species [6] (see Fig. 3):

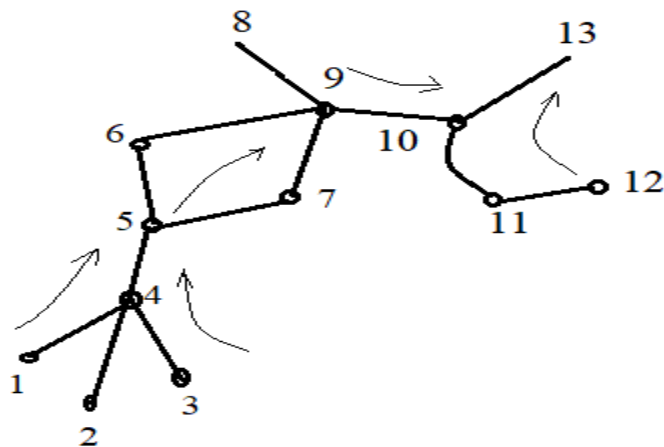


Fig. 3: Trophic chain of 13 conditional species.

Suppose that in this trophic web (Fig. 3), Species No. 7 is removed from the structure as a result of some ecological changes. What structural changes are possible in such a case?

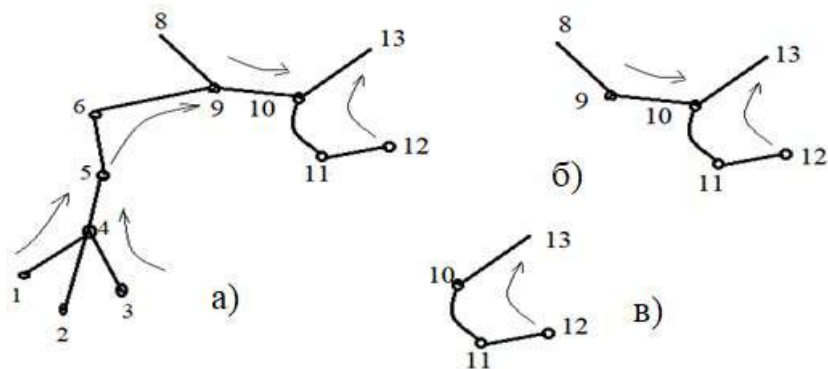


Fig. 4: Possible variants of structural changes in the trophic chain presented in Figure 3.

Depending on the survival coefficient values of species (6), (8), (9), and (10) (Fig. 3), trophic structures corresponding to variants (a), (b), or (c) (Fig. 4) may be realized [1,2,7]. In other words, the realization of various trophic structure variants is determined by a complex of factors, including (resource availability; species' tolerance ranges and adaptability; competition; predation and other interactions; randomness and historical factors). The wider the tolerance range, the higher the species' survivability. Knowing the biology of species, it is not difficult to determine their own optimal survival ranges in relation to ecological factors. In addition to this, a crucial role in the structural changes of ecosystem biodiversity is played by the universal fundamental principle of nature – the principle of minimum energy expenditure, meaning that when choosing from several possible food options, the one that requires the least energy expenditure for further existence is selected. This, in turn, is linked to the species' own optimal survival range [1]. The more complex and diverse the trophic web, the more variants of structural changes in ecosystem biodiversity.

IV. DISCUSSION

The principle of minimum energy expenditure only works on the condition that the realization of different possible variants of a physical phenomenon is not equally probable. If all possible variants of a physical phenomenon are equally probable, then discussing the principle of minimum energy expenditure is meaningless. For example, when flipping a coin, the outcome of either side is equally probable. The same applies to rolling a die (dice) in backgammon: the outcome of each face of the die is equally probable. There are many similar examples in nature.

The mathematical basis of the principle of minimum energy expenditure, which underlies any "open systems" and "dissipative structures," lies in the mathematical descriptions of the thermodynamics of systems far from equilibrium (nonlinear thermodynamics) and the methods of ecological factor interaction theory [1,2,7,10,11]. Diversity generates diversity. From existing diversity, in accordance with the principle of minimum energy expenditure, new diversity is born. Such transitions are characteristic of biological systems.

Of all possible development paths, and depending on the value of the ecological field of survival and in accordance with the principle of minimum energy expenditure, the newly formed variant of a biological object or phenomenon is realized.

V. CONCLUSION

The minimum energy expenditure is determined by the genetic predisposition of biological systems and the structural arrangement of open physical systems.

Based on the principle of minimum energy expenditure, the path or variant of biosystem development is chosen from a multitude of possible options that requires the least energy expenditure to achieve a stable state or equilibrium, which is characteristic of biological systems functioning far from thermodynamic equilibrium.

The principle of minimum energy expenditure can serve as a basis for understanding numerous processes in physics, chemistry, and biology, in which systems are formed or organized in ways that lead to optimal conditions for their existence and functioning.

The principle of minimum energy expenditure is one of the fundamental properties of open systems and lies at the foundation of the theory of natural selection.

The principle of minimum energy expenditure may play a significant role in the design and construction of modern technological, artificial, and resilient biological constructs and robots.

Glossary

1. The key idea of the principle of minimum energy expenditure is that, from the many possible options for the formation of a new biological object, the emergence of a phenomenon, or the course of a natural process in nature, the one that requires the least energy expenditure for its continued existence is realized.
2. The principle of minimum energy expenditure is explained by nature's desire to realize the most probable option, in which the energy costs for the formation and maintenance of the structure are minimal.

ACKNOWLEDGMENTS

Thank God.

Funding Source

This research did not receive any specific grants from funding agencies in the public, commercial, or non-profit sectors.

Author's Contributions

Mukhamad Isakovich Gulamov: developed the project, analyzed the literature, and prepared the manuscript.

Ethics

This material is the author's original work and has not been previously published.

Competing Interests

Since there is no conflict of interest as the sole author.

REFERENCES

1. Gulamov M.I. (1994). On the interaction of environmental factors. Tashkent. From: FAN. 97 p. [In Russian]
2. Gulamov M.I., Krasnov V.S. (2009). Theory of interaction of environmental factors. Tver (RF): Tver State University. 64 p. [In Russian]
3. Gulamov M.I. Reflections on the nature of diversity // Universum: Technical sciences: electron. scientific journal 2016. No. 4(22). URL: <http://7universum.com/ru/nature/archive/item/2489> [In Russian]

4. Gulamov M.I. On the nature of diversity renewal //Universum: Chemistry and biology: electron. scientific journal 2017. No. 10 (40). URL: <http://7universum.com/ru/nature/archive/item/5124> [In Russian]
5. Gulamov M.I. On the concept of “Ecological field of survival”// Universum: chemistry and biology: electron. scientific journal 2021. 6(84). URL: <https://7universum.com/ru/nature/archive/item/11707> [In Russian]
6. Gulamov M.I. (2022). ON QUESTION OF THE DYNAMICS OF STRUCTURAL CHANGES IN BIODIVERSITY. Journal of science. Lion, 31, 3-8. <https://doi.org/10.5281/zenodo.6627922> [In Russian]
7. Gulamov M.I. (2025). Algebra of Ecology//London Journal of Research in Science: Natural & Formal. Great Britain Journals Press Volume 25 | Issue 3 | Compilation 1.0. P. 61-104.
8. Odum, E. P. Fundamentals of Ecology. Moscow, 1975. 740 p. [In Russian]
9. Onsager, L. (1931), On the Equilibrium of Irreversible Processes. Physical Review, 37(4), 405-426.
10. Prigogine, I., & Stengers, I. (1984). Order out of chaos: Man's new dialogue with nature. Bantam Books.349 p.
11. Rubin, A.B. (1987). Biophysics. Textbook. Book 1. Moscow: Vysshaya Shkola. 320 p. [In Russian]
12. The Principle of Least Action. <https://ru.wikipedia.org/wiki/> [In Russian]



Scan to know paper details and
author's profile

Effect of Temperature, PH, and Salt on Bacteriocin Activity Produced from Different Strains of Lactic Acid Bacteria (LAB)

Dr. Mamta Sahu

Raman University

ABSTRACT

The present study was conducted to assess the effect of temperature, pH, and salt on bacteriocin activity produced from different strains of Lactic Acid Bacteria. On the basis of cultural, biochemical, physiological and morphological identification the *Lactobacillus* species were identified. Four species of *Lactobacillus* were isolated from homemade cheese, raw milk, dosa paste, sauce, and curd. *Lactobacillus* species isolated from the sampled food source include; *Lactobacillus brevis*, *Lactobacillus plantarum*, *Lactobacillus fermentum*, and *Lactobacillus casei*. The bacteriocins activity towards different levels of temperature, pH and salt was recorded. The results showed that the highest bacteriocin activity was observed at 60°C for 180 min and the lowest bacterial activity was observed at 121°C for 20 min. *L.plantarum*(P2) reported the maximum bacteriocin activity. The highest bacteriocins activity was reported at pH-6. Across different bacterial strains tested for pH stability, *L. plantarum*(P2) reported maximum bacteriocins activity. It was observed that bacteriocins produced from *L. brevis* reported highest salt tolerance. Across different bacterial strains tested for salt tolerance, *L. brevis* reported maximum bacteriocins activity. The bacteriocin produced from LAB in the current experiment show resistance to pH, heat, and different organic solvents, thus this bacteriocin opened the prospect for its utilization in preservation of food products.

Keywords: LAB, bacteriocins, temperature stability, ph stability, salt tolerance.

Classification: LCC Code: QR82, QR115, TP248.65.F66

Language: English



Great Britain
Journals Press

LJP Copyright ID: 925616

Print ISSN: 2631-8490

Online ISSN: 2631-8504

London Journal of Research in Science: Natural & Formal

Volume 25 | Issue 14 | Compilation 1.0



Effect of Temperature, PH, and Salt on Bacteriocin Activity Produced from Different Strains of Lactic Acid Bacteria (LAB)

Dr. Mamta Sahu

ABSTRACT

The present study was conducted to assess the effect of temperature, pH, and salt on bacteriocin activity produced from different strains of Lactic Acid Bacteria. On the basis of cultural, biochemical, physiological and morphological identification the *Lactobacillus* species were identified. Four species of *Lactobacillus* were isolated from homemade cheese, raw milk, dosa paste, sauce, and curd. *Lactobacillus* species isolated from the sampled food source include; *Lactobacillus brevis*, *Lactobacillus plantarum*, *Lactobacillus fermentum*, and *Lactobacillus casei*. The bacteriocins activity towards different levels of temperature, pH and salt was recorded. The results showed that the highest bacteriocin activity was observed at 60°C for 180 min and the lowest bacterial activity was observed at 121°C for 20 min. *L. plantarum*(P2) reported the maximum bacteriocin activity. The highest bacteriocins activity was reported at pH-6. Across different bacterial strains tested for pH stability, *L. plantarum*(P2) reported maximum bacteriocins activity. It was observed that bacteriocins produced from *L. brevis* reported highest salt tolerance. Across different bacterial strains tested for salt tolerance, *L. brevis* reported maximum bacteriocins activity. The bacteriocin produced from LAB in the current experiment show resistance to pH, heat, and different organic solvents, thus this bacteriocin opened the prospect for its utilization in preservation of food products.

Keywords: LAB, bacteriocins, temperature stability, ph stability, salt tolerance.

Author: Assistant Professor, Department of Microbiology Dr.C.V. Raman University, Kargi road Kota, Bilaspur (C.G.).

I. INTRODUCTION

Lactic Acid Bacteria (LAB) have been intensively used in food preservation and research across the globe has reported that LAB stimulates the nutrient level of different fermented foods and its derived products (Sameh, *et.al.*, 2016; Raman, *et.al.*, 2022). LAB improves the flavor, taste, texture, and shelf-life of different products (Korcari, *et.al.*, 2021). The LAB creates lactic acid, which makes the environment more acidic and decreases the number of pathogenic microorganisms. LAB has the ability to create organic acids, hydrogen peroxide, diacetyl, and bacteriocins which are some of the antibacterial substances. These substances are known to lessen food deterioration and the growth or proliferation of harmful bacteria. As a result, the food industry has begun to pay more attention to the utilisation of these naturally occurring chemicals as food bio-preserved agents, which currently offers a viable alternative to chemical food preservation, particularly for ready-to-use products. (Suskovic *et.al.*, 2010, Lappa, *et.al.*, 2022). Bacteriocins could also be used to prepare products that aren't being sufficiently thermally sterilized at the time of their production, as there is a risk of product becoming contaminated with pathogenic microorganisms like *Listeria monocytogenes*, which has been linked to numerous outbreaks around the world (O'Sullivan *et.al.*, 2002).

Bacteriocins are ribosomally-synthesized peptides or proteins with antimicrobial activity, produced by different groups of bacteria. Many *Lactobacillus* sp. produce bacteriocins with rather broad spectra of inhibition. Several LAB bacteriocins offer potential applications in food preservation, and the use of bacteriocins in the food industry can help to reduce the addition of chemical preservatives as well as well as the heat intensity treatments, resulting in foods that are better maintained naturally and have stronger nutritive and organoleptic qualities. This can be an alternative to satisfy the increasing consumers demands for safe, fresh-tasting, ready-to-eat, minimally-processed foods and also to develop "novel" food products (e.g. less acidic, or with a lower salt content) (Alkena *et.al.*, 2016). The inhibitory spectrum of some bacteriocins also includes food spoilage and/or food-borne pathogenic microorganisms. In the past years, a lot of works have been aimed to the detection, purification and characterization of bacteriocins, as well as to their use in food preservation strategies. However its essential to report the tolerance of bacteriocins towards different physical and chemical factors of environment. Keeping in view the role of bacteriocins, the present study was conducted to assess the effect of temperature, pH, and salt on bacteriocin activity produced from different strains of Lactic Acid Bacteria.

II. MATERIAL AND METHODOLOGY

2.1. Isolation and Identification of LAB

Homemade cheese, raw milk, dosa paste, sauce, curd, was serially diluted and spread on MRS agar medium. Plates were incubated anaerobically for 24-48 hrs at 30°. When required for the isolation of specific bacteria and incubated aerobically and anaerobically at various temperatures. A total of 13 isolates of bacterial species, namely *Aeromonas*, *Bacillus*, *Clostridium*, *Escherichia*, *Klebsiella*, *Listeria*, *Salmonella*, *Streptococcus*, *Staphylococcus*, *Enterobacter*, *Enterococcus*, and *Lactobacillus* were isolated from the sampled dairy products. On the basis of cultural, biochemical, physiological and morphological identification the *Lactobacillus* species were identified. Four species of *Lactobacillus* species were identified they include; *L.plantarum*(P2), *L. brevis*, *L.plantarum*(P1), *L. casei*, and *L. fermentum*. The morphological characteristics of the bacterial strain obtained from different food sources is given in Table-1

Table-1: Morphological characteristics of the bacterial strain obtained from different food sources.

Strain code	Cell's form	Type	Colour	Motility test	Gram staining
<i>L. brevis</i>	Rod shaped	Bacilli	Yellow	Non-motile	Gram positive
<i>L.plantarum</i>	Slender rods	Coccobacilli	Yellow	Non-Motile	Gram positive
<i>L.fermentum</i>	Rod Shaped	Cocci	Creamy White	Non-Motile	Gram positive
<i>L. casei</i>	Rod-shaped	Smooth	Opaque with pigment	Non-Motile	Gram positive

2.2. Production of Bacteriocin

The bacteriocin production from the isolated strains of LAB species (*L.plantarum* (P2), *L. brevis*, *L.plantarum*(P1), *L. casei*, and *L. fermentum*) was grown in MRS broth(Hi Media Lab, Pvt Ltd.India) with 1% incoculum and it was maintained at optimum culture condidtions for 48 hours. The cells wer removed from the growth medium afer incubation by centrifugation at 15000r/min for 15 minutes at 4°C. The obtained cell-free supernatant was adjusted to pH 6.5 using 1mol/L NaOH and it was used as crude bacteriocin.

2.3. Purification of Bacteriocin

Two methods were used for this purpose; Ammonium salt precipitation and ion-exchange chromatography (Yang *et.al.*, 2018).

2.3.1. Ammonium Salt Precipitation

Ammonium salt precipitation, various concentrations of Ammonium Sulphate (10, 20, 30, 40, 50 and 60%) was added to 10 ml of crude bacteriocin in different salt of test tubes, precipitate for 24 h at 4°C. Then the obtained mixture of bacteriocin was centrifuged at 10,000 rpm for 10 min and then the obtained precipitate was further resuspended in 25ml of 0.05m of Potassium Phosphate buffer (pH 7)(Yang *et.al.*, 1992). Further dialysis was followed in dialysis bags against 2 litres of the same buffer.

2.3.2. Ion-Exchange Chromatography

The dialyzate was used for purification by cation exchange column (DEAE cellulose column) and elution was performed by using a linear gradient from citrate phosphate buffer ranging from pH 2.6 to 7.0 (Macher *et.al.*, 1980). The bacteriocin titer was assessed (Todorov *et.al.*, 2004) of eluted samples.

2.4. Effect of Temperature, pH, and Salt on Bacteriocin Activity

In order to assess the impact of temperature, the purified bacteriocin activity was tested by incubating it at different temperatures between 60°C to 121°C and the residual activity was tested after 20 minutes, 40minutes, 120 minutes, and 150 minutes. To examine the affect the pH , the purified bacteriocin activity was tested by incubating it at different pH between 02 to 12 with sterile 1 mol/NaOH or 1 mol/L HCL. Further the effect of salt on the purified bacteriocin activity was observed by taking 400µl of the purified bacteriocin, and it was incubated at 37 °C with NaCl concentrations ranging from 10 to 40%. (Merck, Germany). Well diffusion assay was used to measure the activity.

III. RESULTS AND DISCUSSION

Four species of *Lactobacillus* were isolated from homemade cheese, raw milk, dosa paste, sauce, and curd. *Lactobacillus* species isolated from the sampled food source include; *Lactobacillus brevis*, *Lactobacillus plantarum* , *Lactobacillus fermentum*, and *Lactobacillus casei*. Table-1 and Table-2 shows the morphological, physiological and biochemical attributes of *L. brevis*, *L. plantarum* , *L. fermentum*, and *L. casei* isolated from cheese, raw milk, dosa paste, sauce, and curd. *Lactobacillus brevis* is a facultative anaerobic, hetero-fermentative species that is commonly found in fermented foods, such as beer, wine, and vegetables. It is a Gram-positive, non-spore-forming, rod-shaped bacterium that can occur singly, in pairs, or in short chains. The cells typically measure 0.7-1.0 µm in width and 2.0-4.0 µm in length, with rounded ends. *Lactobacillus plantarum* is a Gram-positive, non-motile, non-spore-forming, micro-aerophilic, and mesophilic bacterium. The cells are straight rods with rounded ends, measuring 0.9-1.2 µm in width and 3.0-8.0 µm in length, and can occur singly, in pairs, or in short chains. Some strains of *L. plantarum* can possess true catalase and manganese-containing pseudo-catalase activities, as well as nitrate- and hematin-dependent nitrite reductases. *Lactobacillus fermentum* is a Gram-positive, non-spore-forming, rod-shaped bacterium that is commonly found in fermented foods and the human gastrointestinal tract. The cells are typically 0.5-0.8 µm wide and 2.0-4.0 µm long, with rounded ends, and can occur singly, in pairs, or in short chains. *Lactobacillus casei* is a Gram-positive, non-spore-forming, rod-shaped bacterium that is widely used in the production of fermented dairy products and as a probiotic. The cells are typically 0.5-0.8 µm wide and 1.0-10.0 µm long, with rounded ends, and can occur singly, in pairs, or in short chains.

Table-2: Physiological and Biochemical characteristics of Isolated *Lactobacilli*.

Characteristics	Raw milk	Curd	Cheeses	Sauce	Dosa Batter
Species	<i>L. plantarum</i> P1	<i>L. plantarum</i> P2	<i>L. casei</i>	<i>L. brevis</i>	<i>L. fermentum</i>
Morphology	Cream colony Gram +ve Rod	Cream Colony Gram +ve Rod	Cream Colony Gram +ve Rod	White colony Gram +ve Rod	White colony Gram +ve Rod
15 °C only	+	+	+	+	-
45 °C only	-	-	-	-	-
15 and 45 °C only	+	+	+	+	+
Acid and gas from glucose	-	-	-	+	+
NH ₃ from Arginine	-	-	-	+	+
Arabinose	-	-	+	+	+
Cellobiose	+	+	-	-	+
Mannitol	+	+	-	-	+
Mannose	+	+	+	-	+
Melebiose	+	+	-	-	+
Raffinose	+	+	+	-	+
Ribose	+	+	+	+	+
Salicin	+	+	+	-	+
Lactose	-	-	-	+	+
Rhamnose	-	-	-	-	-
Sorbitol	-	-	-	-	+
Xylose	-	-	-	+	+
Trehalose	-	-	-	-	+

Due to the fact that all bacteriocin was created during the pre- and early exponential growth phases and reached a maximum level at late stationary phase, the test isolates synthesis of bacteriocin demonstrated secondary metabolic kinetics. According to certain accounts, bacteriocins are created at all times during the experimental growth phase rather than just in the late logarithmic or early stationary phases. The process of producing bacteriocin was optimised by taking into account many parameters, including carbon and nitrogen sources, pH, temperature, and salt content. The optimum parameter was then determined using an arbitrary unit. The addition of glucose (2.0%) increased the amount of bacteriocin that could be produced, while the addition of other carbon sources had no effect or had a negative impact on production. For the nitrogen source, the medium's maximum production was achieved by mixing Tryptone, yeast extract, and meat extract together. While extremely alkaline and acidic pH did not enable the formation of bacteriocin, maximum activity in composition medium was attained at initial pH ranging from 6-8, and the optimal temperature was 30°C. The bacteriocin was created at its highest level under the ideal conditions, and once it had been purified, it could be employed right away as a bio-preservative. The manufacturing of bacteriocins can be optimised to produce them more cheaply, which could eliminate the need to add chemical preservatives altogether or at least limit their use.

Table-3: Effect of Temperature on the activity (AU/ μ l) of bacteriocin produced by the isolated strains of LAB species.

Temperature	<i>L. plantarum(P1)</i>		<i>L. plantarum(P2)</i>		<i>L. casei</i>		<i>L. brevis</i>		<i>L. fermentum</i>	
	ZI (mm)	AU/ μ l	ZI (mm)	AU/ μ l	ZI (mm)	AU/ μ l	ZI (mm)	AU/ μ l	ZI (mm)	AU/ μ l
60°C for 150 min	11.0	110	15.0	150	11.0	110	13.0	130	10	100
80°C for 120 min	9.0	90	13.0	130	10.0	100	8.0	80	7.0	70
100°C for 40 min	8.0	80	12.0	120	5.0	50	7.0	70	0	0
121°C for 20 min	8.0	80	12.0	120	0	0	0	0	0	0

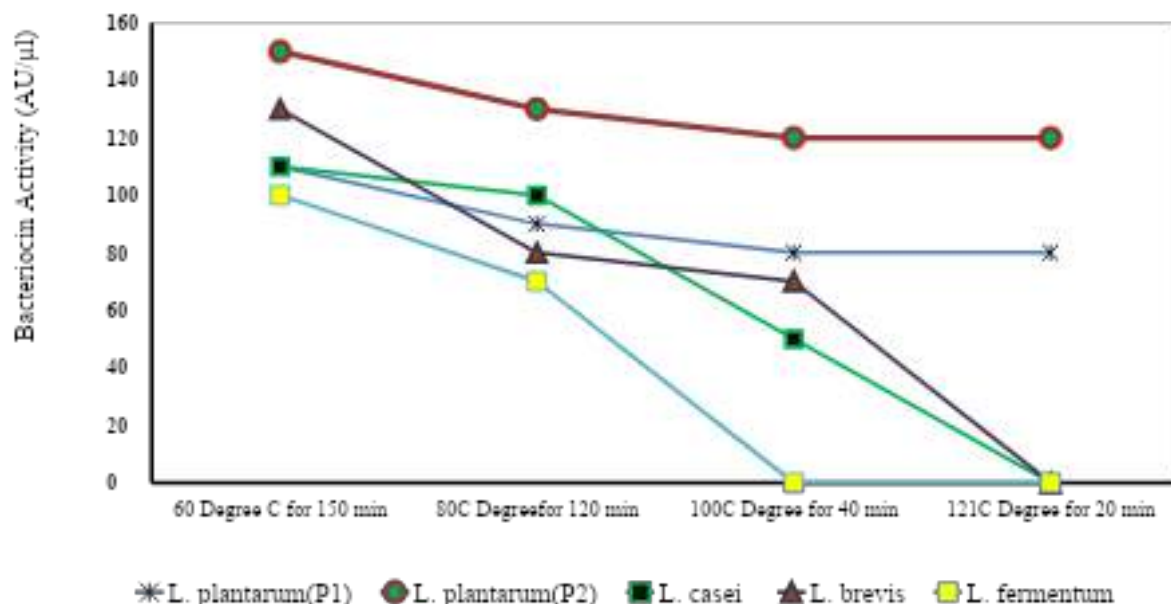


Fig-1: Thermal stability of Bacteriocin after exposure at different temperature treatment

The optimum condition for maximum bacteriocin activity was demonstrated by culturing the bacteria among various thermal ranges. Purified bacteriocin was exposed to various heat treatments: 60°C for 180 min, 80°C for 120 min, 100°C for 40 min and 121°C for 20 min (Table-3, Fig-1). The results showed that the highest bacteriocin activity was observed at 60°C for 180 min and the lowest bacterial activity was observed at 121°C for 20 min. Across different bacterial strains *L. plantarum(P2)* responded the maximum bacteriocin activity followed by *L. brevis*, *L. plantarum(P1)*, *L. casei*, and *L. fermentum*. The results report that with the increase in the temperature there was a decrease in the activity (AU/ μ l) of bacteriocins. The *L. plantarum(P2)* showed the highest thermal stability that the other bacteriocins in terms of the temperature to which they were exposed.

Table 4: Effect of pH on the activity (AU/ μ l) of bacteriocin produced by the isolated strains of LAB species.

pH	<i>L. plantarum</i> (P1)		<i>L. plantarum</i> (P2)		<i>L. casei</i>		<i>L. brevis</i>		<i>L. fermentum</i>	
	ZI (mm)	AU/ μ l	ZI (mm)	AU/ μ l	ZI (mm)	AU/ μ l	ZI (mm)	AU/ μ l	ZI (mm)	AU/ μ l
2	10	100	15	150	11	110	13	130	09	90
4	14	140	17	170	12	120	16	160	10	100
6	15	150	19	190	13	130	18	180	12	120
8	11	110	18	180	09	90	16	160	07	70
10	05	50	18	180	05	50	15	150	00	00
12	00	00	17	170	00	00	15	150	00	00

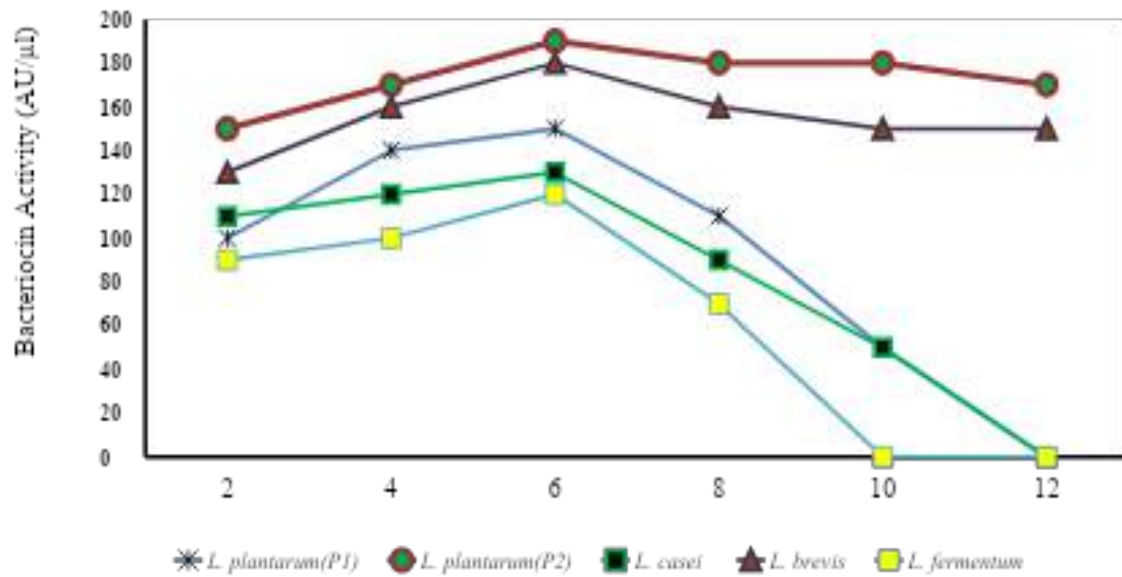


Fig-2: pH stability of Bacteriocins produced from different LAB species after exposure at different pH

The influence of pH on the activity of bacteriocins. Stability of pH of bacteriocins was observed at pH range of 2.0 to 12.0. It was observed that the bacteriocins activity report maximum stability between pH 4-6. The highest bacteriocins activity was reported at pH-6 (Table-4.18). Across different bacterial strains tested for pH stability, *L. plantarum*(P2) reported maximum bacteriocins activity followed by *L. brevis*, *L. plantarum*(P1), *L. casei*, and *L. fermentum* (Table-5, Fig-2). *L. plantarum* (P2) showed was reported to be the highest pH stable of bacteriocins after exposure at different pH. The overall results report that the pH affects the bacteriocins activity significantly.

Table-5: Effect of Salt on the activity (AU/ μ l) of bacteriocin produced by the isolated strains of LAB species.

Salt Conc.	<i>L. plantarum</i> (P1)		<i>L. plantarum</i> (P2)		<i>L. casei</i>		<i>L. brevis</i>		<i>L. fermentum</i>	
	ZI (mm)	AU/ μ l	ZI (mm)	AU/ μ l	ZI (mm)	AU/ μ l	ZI (mm)	AU/ μ l	ZI (mm)	AU/ μ l
10%	12.0	120	19	190	11.0	110	20.0	200	11.0	110
20%	10.0	100	18	180	11.0	110	19.0	190	9.0	90
30%	8.0	80	16	160	7.0	70	18.0	180	8.0	80
40%	0.0	00	16	160	5.0	50	18.0	180	6.0	60

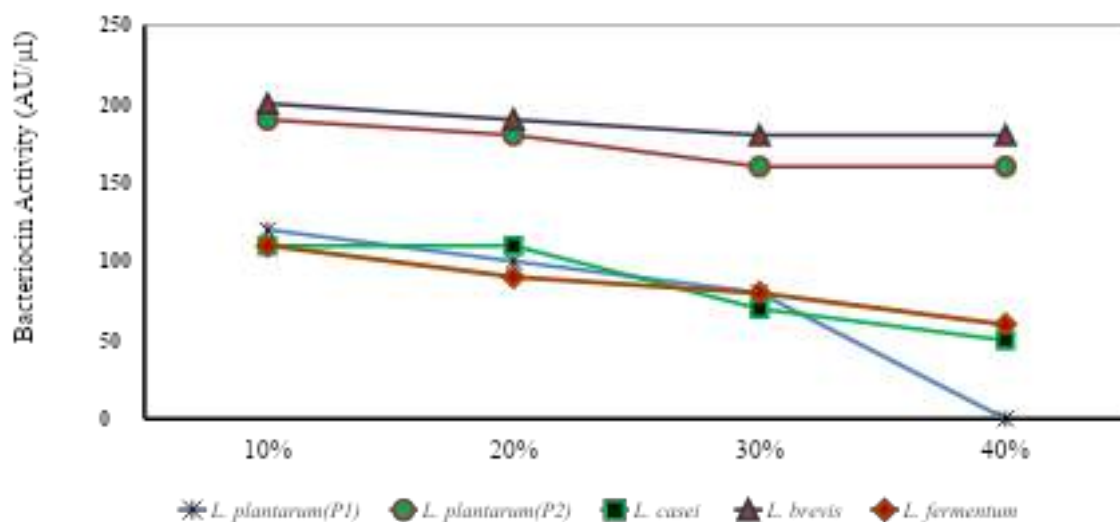


Fig. 3: Salt tolerance of Bacteriocins produced from different LAB species.

400 μ l of the purified bacteriocin were incubated at 37 °C with NaCl concentrations ranging from 10 to 40%. (Merck, Germany). Well diffusion assay was used to measure the activity. It was observed that bacteriocins produced from *L. brevis* reported highest salt tolerance. The tolerance by bacteriocin activity was recorded lowest by *L. casei*. Across different bacterial strains tested for salt tolerance, *L. brevis* reported maximum bacteriocins activity followed by *L. plantarum*(P2), *L. plantarum*(P1), *L. fermentum*, and *L. casei* (Table-5, Fig-3). The overall results show that the bacteriocin activity was highest at 20% salt concentration and lowest at 40% salt concentration.

IV. DISCUSSION

The present study examines the effect of temperature, pH and salt on the bacteriocin activity which were produced from *Lactobacillus species* isolated from Raw milk, Dosa, Curd, Sauces and Cheese. The *Lactobacillus species* were identified on the basis of morphological, biochemical and physiochemical attributes. Out of these five *Lactobacillus species*, two were identified as *L. plantarum* and coded as P1 and P2, respectively, due to their different potential in bacteriocin activity, and the other three were identified as *L. brevis*, *L. casei*, and *L. fermentum*. The bacteriocins produced by the *Lactobacillus species* in this investigation were subject to different levels of temperature, pH and salt to determine the stability of the bacteriocins for their future applications.

The *Lactobacillus* bacteriocin isolated from different samples raw milk, dosa paste, curd, sauce and cheese have thermal stability at 60°C for 150 min. The results showed that the highest bacteriocin activity was observed at 60°C for 150 min and the lowest bacterial activity was observed at 121°C for 20 min. This is significant if the bacteriocin is to be utilized as a food preservative because many food preparation processes require a heating stage. The mechanism of heat-stability of LAB bacteriocins has been reported earlier for *Plantaricin S* (Jimenez-Diaz *et.al.*, 1990), *Plantaricin A* (Daeschel *et.al.*, 1985), *Plantaricin 149* (Kato *et.al.*, 1994), *Plantaricin SA6* (Rekhif *et.al.*, 1995), *Plantaricin 423* (Van-Reenen, 1998), *Plantaricin C19* (Audisio, 1999), *Pentocin TV35b* (Okkers *et.al.*, 1999), *L. brevis* oG1 (Ogunbanwo *et.al.*, 2003), and *lactocin RN78* (Mojgani and Amirinia, 2007). Because we noted heat stability of *L. plantarum* P2 bacteriocin, the conclusions of the present study are in consistent with the findings of the papers cited above. This bacteriocin belongs to the category of bacteriocins with low molecular weight that are heat stable and retain their activity after heating at 121°C for 60 min. The bacteriocin is superior in processed foods when high heat is used because of this property. The thermal stability of other bacteriocins was not good. Additionally, Andersson (1986) noted a decrease in activity following a 15-minute heat treatment at 121°C.

The test isolates regarding bacteriocin's activity was also pH-dependent. The bacteriocin produced by *L. brevis*, *L. plantarum*(P1), *L. plantarum*(P2), *L. casei*, and *L. fermentum* showed pH stability at acidic pH (2-6). However only *L. brevis* and *L. plantarum*(P2) retained their activity at alkaline pH (8-12). *L. fermentum* have completely lost their activity from pH 10 and *L. brevis* lost its complete activity at pH 12 respectively. The overall bacteriocin activity was reported highest between pH 4-6. This was also demonstrated by Reddy *et.al.* (1984) and Abdel-Bar *et.al.* (1987) in their studies of two bacteriocins, bulgarican and lactobulgarican, isolated from *L. bulgaricus*, which had the highest activity and stability at pH 2.2 and 4.0, respectively, against a variety of pathogenic and spoilage bacteria.

In particular, pH 6 was found to have increased antibacterial activity in the bacteriocin generated by *L. brevis*, *L. plantarum*(P1), *L. plantarum*(P2), *L. casei*, and *L. fermentum*. This might be because bacteriocins' increased net charge at low pH makes it easier for the molecules to pass through the cell wall. At lower pH levels, bacteriocin solubility may also rise, aiding the diffusion of bacteriocin molecules. This concurred with earlier studies that demonstrated that the presence of NaCl enhanced the antimicrobial action of bacteriocins like nisin, leucocin F10, enterocin AS-48, and others. A modest quantity of NaCl also inhibited nisin action (Bouttefroy *et.al.*, 2000). Additionally, sodium chloride reduced the antilisterial efficacy of the antibiotics acidocin CH5 (at 1-2%; Chumchalova *et.al.*, 1998), lactocin 705, leucocins 4010 (at 2.5% NaCl; Hornbaek *et.al.*, 2004), pediocin, (at 6.5% NaCl; Jydegaard *et.al.*, 2000), curvacin (Vaerluyten). The ionic interactions between bacteriocin molecules and charged groups involved in bacteriocin binding to target cells may be interfered with by sodium chloride, which has a protective effect (Bhunia *et.al.*, 1988.) In addition, sodium chloride may cause bacteriocin structural alterations or modifications to the target cell's envelope (Lee *et.al.*, 1993) or changes in the cell envelope of the target organisms (Jydegaard *et.al.*, 2000).

The bacteriocin produced from LAB in the current experiment show resistance to pH, heat, and different organic solvents, thus this bacteriocin opened the prospect for its utilization in preservation of food products. It can also confirm that these LAB strains can be used as starting cultures for microorganisms and as bio-preservatives in a variety of fermented foods. The most typical bacteria for food fermentation and preservation are LAB. Their significance is primarily related to their safe metabolic activity as they consume accessible sugar while growing in food to produce organic acids and other metabolites (Gomashe *et.al.* 2014).

V. CONCLUSION

Lactic Acid Bacteria (LAB) can produce a range of antimicrobial compounds, such as organic acids, hydrogen peroxide, and bacteriocins, which can effectively inhibit the growth of various microorganisms. Four species of *Lactobacillus* were isolated from homemade cheese, raw milk, dosa paste, sauce, and curd. *Lactobacillus* species isolated from the sampled food source include; *Lactobacillus brevis*, *Lactobacillus plantarum*, *Lactobacillus fermentum*, and *Lactobacillus casei*. The bacteriocins activity towards different levels of temperature, pH and salt was recorded. The characterization of Bacteriocins from test isolates were studied in order to take advantage of their potential and make them viable candidates for deployment as a safe and effective biological preservative in the future. Across different LAB species the bacteriocins produced from *L. plantarum* report distinctive and comprehensive heat stability, pH instability, and salt tolerance, can be exploited as a biopreservative to increase the food items' hygienic and safety (especially processed foods). The use of *Lactobacillus* species as natural biopreservatives in food products is a promising approach to enhance food safety and extend shelf-life, thereby reducing the reliance on synthetic preservation methods.

Conflict of Interest

Author don't have any conflict of Interest regarding the publication of this manuscript

Plagiarism and AI Content

The author declares that Plagiarism of the manuscript is below 10% similarity level, and 0% AI content detected.

REFERENCES

1. Abdel-Bar, N., Harris, N.D. and Rill, R.L. (1987). Purification and properties of an antimicrobial substance produced by *Lactobacillus bulgaricus*. *J. Food Sci.* 52:411-415.
2. Alemka, A., Clyne, M., Shanahan, F., Tompkins, T., Corcionivoschi, N., & Bourke, B. (2010). Probiotic colonization of the adherent mucus layer of HT29MTXE12 cells attenuates *Campylobacter jejuni* virulence properties. *Infection and immunity*, 78(6), 2812-2822.
3. Andersson, R.E., Daeschel, M.A. and Hassan, H.M. (1988). Antibacterial activity of plantaricin SIK-83, a bacteriocin produced by *Lactobacillus plantarum*. *Biochem.* 17:61-68.
4. Audisio, M.C., Oliver, G. and Paella, M.C. 1999. Antagonistic effect of *E. faecium* J96 against human and poultry pathogenic *Salmonellae* species. *J. food Prot* 62: 751-755.
5. Bouttefroy, A., Linder, M., & Milliere, J. B. (2000). Predictive models of the combined effects of curvaticin 13, NaCl and pH on the behaviour of *Listeria monocytogenes* ATCC 15313 in broth. *Journal of Applied Microbiology*, 88(6), 919-929.
6. Chumchalova, J., Stiles, J., Josephsen, J., & Plockova, M. (2004). Characterization and purification of acidocin CH5, a bacteriocin produced by *Lactobacillus acidophilus* CH5. *Journal of Applied Microbiology*, 96(5), 1082-1089.
7. Daeschel, M.A., Mckenney, M.C. and Mcdonald (1985). Bacteriocidal activity of *Lactobacillus plantarum* C-11. *Food Microbiol.* 7:91-98.
8. Gomashe A.V. et.al., (2014). Screening and Evaluation of antibacterial activity of bacteriocin producing lab against selected bacteria causing food spoilage. *International Journal of Current Microbiology and applied Sciences*, 3(8): 658-665.
9. Hornbaek, T., Brocklehurst, T. F., & Budde, B. B. (2004). The antilisterial effect of *Leuconostoc carnosum* 4010 and leucocins 4010 in the presence of sodium chloride and sodium nitrite

examined in a structured gelatin system. *International journal of food microbiology*, 92(2), 129-140.

- 10. Jimenez-Diaz, R., Piard, J.C., Ruiz-Barba, J.L. and Desmazeaud, M.J. (1990). Isolation of a bacteriocin producing *Lactobacillus plantarum* strain from a green olive fermentation. Third symposium on lactic acid bacteria. *FEMS Microbiol Rev.* 87:91.
- 11. Jydegaard, A. M., Gravesen, A., & Knøchel, S. (2000). Growth condition-related response of *Listeria monocytogenes* 412 to bacteriocin inactivation. *Letters in Applied Microbiology*, 31(1), 68-72.
- 12. Kato, T.; Mastsuda, T.; Ogawa, E.; Ogawa, H.; Kato, H.; Doi, U.; Nakamura, R. (1994). *Plantaricin-149*, a bacteriocin produced by *Lactobacillus plantarum* NRIC 149. *J. Ferment.Bioeng.*, 77: 277-282
- 13. Korcari, D., Secchiero, R., Laureati, M., Marti, A., Cardone, G., Rabitti, N. S., ... & Fortina, M. G. (2021). Technological properties, shelf life and consumer preference of spelt-based sourdough bread using novel, selected starter cultures. *LWT*, 151, 112097.
- 14. Lappa, I. K., Kachrimanidou, V., Alexandri, M., Papadaki, A., & Kopsahelis, N. (2022). Novel Probiotic/Bacterial Cellulose Biocatalyst for the Development of Functional Dairy Beverage. *Foods*, 11(17), 2586.
- 15. Lee, S., Iwata, T., Oyagi, H., Aoyagi, H., Ohno, M., Anzai, K., ... & Sugihara, G. (1993). Effect of salts on conformational change of basic amphipathic peptides from β -structure to α -helix in the presence of phospholipid liposomes and their channel-forming ability. *Biochimica et Biophysica Acta (BBA)-Biomembranes*, 1151(1), 76-82.
- 16. Macher, B. A., & Klock, J. C. (1980). Isolation and chemical characterization of neutral glycosphingolipids of human neutrophils. *Journal of Biological Chemistry*, 255(5), 2092-2096.
- 17. Mojgani N., Sabiri G., Ashtiani M. & Torshizi M. (2009). Characterization of Bacteriocins Produced by *Lactobacillus brevis* NM 24 and *L. fermentum* NM 332 Isolated from Green Olives in Iran. *The Internet Journal of Microbiology*. 51(2), 178-184.
- 18. Ogunbanwo S.T, Sanni, A.I. & Onilude A.A. (2003). Characterization of bacteriocin produced by *Lactobacillus plantarum* F1 and *Lactobacillus brevis* OG1 *African Journal of Biotechnology*, 2(8): 219-227.
- 19. Okkers, D.J., Dicks, L.M., Sylvester, M., Joubert, J.J. and Odendaal, H.J. (1999). Characterization of pentocin TV35b, a bacteriocin like peptide isolated from *Lactobacillus pentosus* with a fungistatic effect on *Candida albicans*. *J. Appl. Microbiol.* 87:726-734.
- 20. O'Sullivan, L., Ross, R., and Hill, C. (2002). Potential of bacteriocin-producing lactic acid bacteria for improvements in food safety and quality. *Biochimie*, 84: 593–604.
- 21. Raman, J., Kim, J. S., Choi, K. R., Eun, H., Yang, D., Ko, Y. J., & Kim, S. J. (2022). Application of lactic acid bacteria (LAB) in sustainable agriculture: Advantages and limitations. *International Journal of Molecular Sciences*, 23(14), 7784.
- 22. Rekhif, N., Atrih, A., & Lefebvrexy, G. (1995). Activity of plantaricin SA6, a bacteriocin produced by *Lactobacillus plantarum* SA6 isolated from fermented sausage. *Journal of Applied Bacteriology*, 78(4), 349-358.
- 23. Sameh, A. G., Rehab, M. A. E. B., Abo, B. F. A., & Gamal, F. M. G. (2016). In vitro evaluation of probiotic potential of five lactic acid bacteria and their antimicrobial activity against some enteric and food-borne pathogens. *African Journal of Microbiology Research*, 10(12), 400-409.
- 24. Suskovic, J., Kos, B., Beganovic, J., Pavunc, A.L., Habijanic, K., and Matosec, S. (2010). Antimicrobial activity-the most improvement property of probiotic amd starter lactic acid bacteria. *Food Technol. Biotehnol.*, 48:297-307.
- 25. Todorov, S. D., van Reenen, C. A., & Dicks, L. M. T. (2004). Optimization of bacteriocin production by *Lactobacillus plantarum* ST13BR, a strain isolated from barley beer. *The Journal of general and applied microbiology*, 50(3), 149-157.

26. Van Reenen C.A., Dicks, L.M., and Chikindas M.L. (1998). Isolation, purification and partial characterization of plantaricin 423, a bacteriocin produced by *Lactobacillus plantarum*. *J. Appl. Microbiol.* 84:1131-1137
27. Yang, E., Fan, L., Yan, J., Jiang, Y., Doucette, C., Fillmore, S., & Walker, B. (2018). Influence of culture media, pH and temperature on growth and bacteriocin production of bacteriocinogenic lactic acid bacteria. *Amb Express*, 8(1), 1-14.
28. Yang, Y. C., Baker, J. A., & Ward, J. R. (1992). Decontamination of chemical warfare agents. *Chemical Reviews*, 92(8), 1729-1743.

This page is intentionally left blank



Scan to know paper details and
author's profile

Species Richness and Diversity of Soil Arthropods in Major Plantation Crops under Different Farming Practices

Shreya K. S, Girish R & Dhananjaya B. C

Nayaka University of Agricultural and Horticultural Sciences

ABSTRACT

The study examining effects of farming practices (Natural farming, Organic farming and Inorganic farming) on species richness and diversity of soil arthropods in major plantation crops (Areca nut, Coconut and Coffee) was conducted under different zones Hilly, Central Dry and Transition zone of Chikkamagaluru district, Karnataka from August 2023 to May 2024. Soil arthropods belonging to 12 different orders were collected under 5 classes viz., Entognatha, Arachnida, Insecta, Symphlan and Chilopoda. The highest numbers of individuals was observed in natural farming practice (1256) followed by organic farming (825) and least in inorganic farming (397). The highest number of soil arthropods was recorded in natural farming practice (31.90 individuals per 400g of soil) within the coconut ecosystem followed by organic farming practice 12.39 and lowest in inorganic farming practices with 5.39 individuals per 400g of soil in arecanut and coffee ecosystem, respectively. Shannon Weiner index showed highest diversity in natural farming system 2.13. Whereas, the lowest diversity was recorded in inorganic farming practices (Shannon-Wiener: 0.69).

Keywords: arthropods, abundance, diversity, natural, organic, inorganic, farming system.

Classification: LCC Code: QH541.5.S6, QL458, S589.7

Language: English



Great Britain
Journals Press

LJP Copyright ID: 925618

Print ISSN: 2631-8490

Online ISSN: 2631-8504

London Journal of Research in Science: Natural & Formal

Volume 25 | Issue 14 | Compilation 1.0



Species Richness and Diversity of Soil Arthropods in Major Plantation Crops under Different Farming Practices

Shreya K. S^a, Girish R^a & Dhananjaya B. C^b

ABSTRACT

The study examining effects of farming practices (Natural farming, Organic farming and Inorganic farming) on species richness and diversity of soil arthropods in major plantation crops (Arecanut, Coconut and Coffee) was conducted under different zones Hilly, Central Dry and Transition zone of Chikkamagaluru district, Karnataka from August 2023 to May 2024. Soil arthropods belonging to 12 different orders were collected under 5 classes viz., Entognatha, Arachnida, Insecta, Symphlan and Chilopoda. The highest numbers of individuals was observed in natural farming practice (1256) followed by organic farming (825) and least in inorganic farming (397). The highest number of soil arthropods was recorded in natural farming practice (31.90 individuals per 400g of soil) within the coconut ecosystem followed by organic farming practice 12.39 and lowest in inorganic farming practices with 5.39 individuals per 400g of soil in arecanut and coffee ecosystem, respectively. Shannon Weiner index showed highest diversity in natural farming system 2.13. Whereas, the lowest diversity was recorded in inorganic farming practices (Shannon-Wiener: 0.69). The abundance and diversity showed a significant difference between different farming practices i.e. natural, organic and inorganic farming practices in different zones. Natural farming practices followed by organic farming supported higher diversity indices and abundance of soil fauna compared to inorganic farming practices.

Keywords: arthropods, abundance, diversity, natural, organic, inorganic, farming system.

Author a: Department of Entomology, College of Agriculture, Shivamogga, Keladi Shivappa Nayaka University of Agricultural and Horticultural Sciences, Shivamogga Karnataka 577204, India.

a: Department of Soil Science, College of Agriculture, Shivamogga.

b: Keladi Shivappa Nayaka University of Agricultural and Horticultural Sciences, Shivamogga, Karnataka 577204, India.

I. INTRODUCTION

Soil arthropods, encompassing classes such as Crustacea, Arachnida, Myriapoda, and Insecta, are crucial components of soil ecosystems. These organisms are characterized by chitinous exoskeletons, segmentation and jointed appendages, enabling them to perform vital ecological functions. They contribute significantly to organic matter translocation, decomposition, nutrient cycling, and soil structure formation, all of which are essential for maintaining soil quality and health (Chethan *et al.*, 2019, Nisa *et al.*, 2017, Patil *et al.*, 2013). Diverse arthropod communities are linked to enhance ecosystem stability and resilience to disturbances, making their assessment important for effective habitat management and conservation strategies (Menta *et al.*, 2020, Nahmani *et al.*, 2005). As integral members of soil food webs, these arthropods serve as valuable indicators of soil biological activity, influencing factors such as hydrology, aeration and nutrient dynamics.

However, intensive agricultural practices pose significant threats to soil arthropod diversity and overall soil health. The conversion of natural habitats to agricultural land leads to drastic changes in soil biological and chemical properties of soil, often resulting in biodiversity loss (Rossi *et al.*, 2006, Shah, 2006, Shashidhara, 2016). These changes can negatively impact soil fauna abundance and activity due to altered temperature, moisture levels and organic matter availability (Edwards, 2004). Conventional farming methods, which heavily rely on chemical fertilizers and pesticides, disrupt natural ecosystem processes, further degrading soil quality. The widespread application of pesticides, while beneficial for crop production, has detrimental side effects, killing not only pests but also beneficial insects and other soil invertebrates, leading to environmental imbalances.

In contrast, organic and natural farming systems prioritize the enhancement of soil health and biodiversity by focusing on the management of soil organic matter and utilizing natural nutrient sources. These practices emphasize reduced soil disturbance, avoidance of synthetic chemicals, and the promotion of biodiversity through diverse planting and natural pest management strategies. Research has shown that conservation farming systems support greater arthropod abundance compared to conventional methods (Hole *et al.*, 2005). Monitoring soil arthropod diversity is critical for assessing soil stability and ensuring sustainable agricultural practices. In this context the present study was conducted to assess the abundance and diversity of various soil arthropods under different farming practices in major plantation crops.

II. MATERIALS AND METHODS

2.1 Study Area

The study was conducted in three major plantation crop ecosystems coconut, arecanut and coffee across three different zones *viz.*, hill zone (13.13°N, 75.64°E), Transition Zone (13.71°N, 75.81°E) and central dry zone (13.54°N, 76.00°E) taluks of Chikkamagaluru district. Soil samples were collected from farmers' plantations fields had been practicing natural farming, organic farming and inorganic farming for over five years. The soil samples were randomly drawn from coconut, arecanut and coffee farming systems from August 2023 to May 2024.

2.2 Sampling Site

Natural farming: This research area had a good composition of weed mulch with grasses and herbs. The practice involved the application of Jeevamritha 200 litre per acre at monthly intervals.

Organic farming: This site practiced the addition of farm yard manure/ organic manure to the soil at 2 tonnes per acre. The plantations were free from weed mulches.

Inorganic farming: The plantations were applied with inorganic fertilizers at 2 splits per year and fertilizers used were urea, DAP, potash and complex form. The plots were free from weeds and no mulching practices followed.

2.3 Sampling Procedure

The samples were drawn near the root zone within the radius of 45 cm from the plant. The surface litter and weeds were removed carefully from the sampling spot before sampling. Soil was collected by using circular core sampler measuring 12 cm diameter and 10 cm height. The core sampler was placed on the soil surface and pressed downward to a depth of 10 cm in the sampling spot. Soil sample weighing 400 g was collected in three spots randomly from each plot and were immediately transferred to aluminum cans and closed with lid. Labeling was done on each can and brought to the laboratory for further analysis.

2.4 Extraction Technique of Soil Arthropods and Processing

The soil fauna was separated from soil sample using Tullgren funnel which consisted of a funnel with mesh screen, a glass vials and a light source. The glass vials was filled with 10 ml of 75 per cent ethyl alcohol. The vials were periodically checked to keep the alcohol at desired levels. The collected soil samples were placed over the mesh fixed across wide end of each funnel. The electric bulbs were fixed at the top of the funnel setup that served as the source of light and heat energy. Light source of Tullgren funnel was switched-on for 48 hours to generate heat that led the micro-arthropods to move down passing through sieve of the funnel and get collected in glass vials. The arthropods collected were sorted using a stereo binocular microscope (35x magnification) and were identified up to order level following taxonomic keys.

2.5 Data Analysis

The recorded data on the total number of individuals arthropods species observed, in each samples were subjected to analysis of variance with square root transformation ($\sqrt{X+0.5}$). The abundance of arthropods was compared among farming practices across different zones seasons using DMRT.

Shannon- Wiener Diversity index - Diversity index were computed using PAST prog (Hammer *et al.*, 2001).

The abundance and diversity of insect community were computed using Shannon's diversity index (H) which accounts for both abundance and evenness of the species.

$$H = -\sum pi (\ln pi)$$

Where, H represents the index of species diversity in a given locality

Pi is the proportion of "ith" species in total sample and ln = Natural logarithm.

Relative abundance was determined using the following equation

$$RA (\%) = \frac{Ts}{Tp} \times 100$$

Where RA = denotes the species relative abundance (%)

Ts = total number of individuals of a species in a given area

Tp = total population of all species in the area

III. RESULTS AND DISCUSSION

3.1 Abundance of Soil Arthropods across Various Farming Practices

During the study period natural farming practices exhibited the highest abundance (1256 individuals) followed by organic farming practices (825 individuals) and lowest in inorganic farming (397 individuals). Highest individuals were recorded in class Entognatha followed by Arachnida, Insect, Symphyla and least was recorded in class Chilopoda. The majority of soil arthropods in these classes belong to orders: Diplura, Coleoptera, Hemiptera, Blattodea, Dermaptera, Diptera, Hymenoptera, Entomobryomorpha, and Scutigeromorpha and sub orders: Mesostigmata, Cryptostigmata (Table 1). These findings are similar to that of Deepika *et al.* (2020) who recorded a higher population of soil arthropods (1987 individuals) in an agricultural ecosystem with most individuals from Class Entognatha, Order Acarina, and Order Entomobryomorpha. Ojija (2016) also reported 1,719

arthropods across 63 species in grassland and woodland ecosystems. Compared to their findings, our study exhibited more abundance in natural farming followed by organic farming, which might be due to the availability of rich organic carbon, mulching practices and arthropods friendly soil and climatic conditions.

3.2 Relative Abundance of Soil Arthropods

A significant variation in the number of soil arthropods was observed among different farming practices Entognatha, Acarina, Insecta, Symphyla and Chilopoda which were most abundant in Natural farming (55.18%, 56.18%, 49.28%, 18.84% and 11.24% respectively), followed by Organic farming (33.11%, 34.98%, 32.13%, 31.88% and 40.45% respectively) and the least relative abundance observed in Inorganic farming (19.38%, 15.77%, 11.50%, 18.84% and 11.24% respectively) (Table 2). These findings align with Pahari *et al.* (2007) who reported that Acari constituted 47.04%, followed by Collembola (38.68%), while the other groups showed significantly lower dominance.

3.3 Abundance and Diversity of Soil Arthropods across Various Zones

Soil arthropod abundance varied significantly across different farming practices in various zones. In hill zone, natural farming plantation of arecanut and coffee showed the highest arthropod populations, averaging 26.70 and 20.00 per 400 g of soil, respectively. Organic farming practices recorded 17.23 and 15.09 individuals, while inorganic farming had the lowest numbers (8.15, 11.00, and 6.76 for arecanut, coconut and coffee respectively). Similar trend was observed among farming practices in transition zone and dry zone.

Overall, natural farming consistently supported the highest mean values of soil arthropods across all crops, while inorganic practices resulted the lowest abundance and diversity, highlighting the significant differences in arthropod populations linked to farming methods across zones (Table 3). In contrast to our findings Hole *et al.* (2005) found that most groups exhibited greater abundance or biomass under conservation systems than under conventional-tillage systems because the former cause fewer disturbances to their habitats, maintaining the structures that serve as shelter. Organic farming practices performed better than inorganic practices, indicating that they support higher soil arthropod populations than conventional chemical inputs. Inorganic farming practices were associated with the lowest soil arthropod counts, reflecting the negative impact of chemical inputs on soil health.

In plantation crops the species diversity of soil arthropods recorded significant differences across farming practices and zones. The highest diversity was noticed in the Natural farming practices in the Hill Zone ($H = 2.13$) in coffee followed by arecanut ($H = 2.02$). While, Organic farming practices also recorded maximum diversity in the Hill Zone ($H = 1.97$) in arecanut. Least diversity was found in inorganic farming practices ($H = 0.69$) in transition zone (Table 3). These results support the findings of Gkisakis *et al.* (2014) who observed soil arthropods, in conventional, organic and integrated olive orchards where Hilly orchards showed significantly higher seasonal arthropod diversity and evenness. Selected habitats in this study was relatively undisturbed compared to organic and inorganic farming

IV. CONCLUSION

The abundance and diversity of soil dwelling arthropods in natural farming practices showed higher diversity indices and abundance, followed by organic farming practices and least were recorded in inorganic farming practices. The present study is the first time effort to investigate the abundance and diversity of soil arthropods in natural farming practice. This study will serve as a baseline for understanding soil dwelling arthropods groups. The practices with natural and organic farming showed greater abundance and diversity, which is due to addition of large amounts of organic residue inputs,

which in turn increase the biological activity of soil arthropods due to the mulching practices followed. It also provided a more balanced and nutrient - rich environment compared to inorganic approaches potentially leading to better crop performance and soil health.

REFERENCE

1. Chethan, R., Patil, R. K., & Halappa, B. (2019). Response of soil arthropod population to different farming systems under cotton integrated with groundnut and pigeon pea crops. *Legume Research*, 42(1), 108–113.
2. Deepika, G., Kennedy, N., Rojeet, T., Mahesh, P., & Rajesh, T. (2020). Soil arthropod diversity in agricultural and horticultural ecosystem of mid hills of Meghalaya.
3. Edwards, C. A. (2004). The importance of earthworms as key representatives of the soil fauna. *Earthworm Ecology*, 2, 3–11.
4. Gkisakis, V. D., Kollaros, D., & Kabourakis, E. M. (2014). Soil arthropod biodiversity in plain and hilly olive orchard agroecosystems in Crete, Greece. *Entomology in Hellas*, 23(1), 18–28.
5. Hammer, O., Harper, D., & Ryan, P. (2001). PAST: Paleontological statistics software package for education and data analysis. *Palaeontological Electronic*, 4(1), 1–9.
6. Hole, D. G., Perkins, A. J., Wilson, J. D., Alexander, I. H., Grice, P. V., & Evans, A.D. (2005). Does organic farming benefit biodiversity? *Biological Conservation*, 122(1), 113–130.
7. Menta, C., Conti, F. D., Lozano Fondón, C., Staffilani, F., & Remelli, S. (2020). Soil arthropod responses in agroecosystem: Implications of different management and cropping systems. *Agronomy*, 10(7), 982.
8. Nahmani, J., Capowiez, Y., & Lavelle, P. (2005). Effects of metal pollution on soil macroinvertebrate burrow systems. *Biology and Fertility of Soils*, 42, 31–39.
9. Nisa, K., Wijayanti, R., & Muliawati, E. S. (2017). Diversity of arthropods in *Sacha Inchi* on dry land. *Caraka Tani: Journal of the Sustainable Agriculture*, 32, 132–141.
10. Ojija, F. (2016). Diversity and abundance of arthropods at Mbeya University of Science and Technology, Tanzania. *International Journal of Scientific & Technology Research*, 5(9), 2277–8616.
11. Pahari, D., Hazra, A. K., & Saha, G. K. (2007). Diversity and distribution of soil arthropod communities in relation to altitude and edaphic factors of different altitudinal environments of Darjeeling Himalayas. *Records of the Zoological Survey of India*, 107, 43–59.
12. Patil, R. K., Babalad, H. B., & Sanjaya, T. (2013). Soil arthropod population in organic, integrated and conventional farming. *10th National Symposium on Soil Biology and Ecology*, 96.
13. Rossi, J. P., Mathieu, J., Cooper, M., & Grimaldi, M. (2006). Soil macrofaunal biodiversity in Amazonian pastures: Matching samples with patterns. *Soil Biology and Biochemistry*, 38, 2178–2187.
14. Shah, A. H. (2006). Effect of some pesticides on soil microarthropods in apple orchard ecosystem. (M. Sc. thesis). Shere-e- Kashmir University of Agricultural Sciences & Technology, Kashmir, Shalimar, Srinagar, India.
15. Shashidhara, K. B. (2016). Studies on soil arthropods in soybean under different farming systems. (Doctoral dissertation). University of Agricultural Sciences, Dharwad, Karnataka, India.

Table 1: Abundance of Soil arthropods across different farming practices

Class	Order	Number of individuals		
		Natural farming	Organic farming	Inorganic farming
Entognatha		Collembola		
	Entomobryomorpha	201	145	64

	Poduromorpha	30	12	9
	Diplura	122	89	71
Arachnida	Mesostigmata	158	135	58
	Cryptostigmata	170	98	47
Insecta	Coleopteran	48	37	14
	Hemiptera	32	18	6
	Blattodea	22	15	6
	Dermaptera	39	21	15
	Diptera	80	39	11
	Hymenoptera	137	74	21
	Symplyla	Symplylan	170	110
Chilopoda	Scutegeromorpha	47	32	10
	Total	1256	825	397

Table 2: Relative abundance of soil arthropods across different farming practices

Class	Natural farming (RA %)	Organic farming (RA %)	Inorganic farming (RA %)
Entognatha	55.18	33.11	19.38
Arachnida	49.25	34.98	15.77
Insecta	56.38	32.13	11.50
Symplyla	49.28	31.88	18.84
Chilopoda	52.81	40.45	11.24

Note: RA – relative abundance

Table 3: Abundance and diversity of soil arthropods in plantation crops under different farming practices

Crops	Farming practices	Hill zone		Transition zone		Central Dry zone		Mean abundance
		Abundance	H ^o	Abundance	H ^o	Abundance	H ^o	
Areca nut	Natural	26.70 (5.21 ^a)	1.81	21.15 (4.65 ^a)	2.02	17.84 (4.28 ^a)	1.69	21.9 (4.73 ^b)
	Organic	17.23 (4.21 ^b)	1.97	12.0 (3.53 ^b)	1.72	7.96 (2.90 ^b)	1.61	12.39 (3.59 ^c)
	Inorganic	8.15 (2.94 ^d)	0.69	5.85 (2.51 ^d)	0.81	3.50 (2.00 ^d)	0.90	5.83 (2.52 ^d)
*Coconut	Natural	-	-	22.44 (4.78 ^a)	1.91	18.93 (4.40 ^a)	1.77	31.90 (5.69 ^a)
	Organic	-	-	9.0 (3.08 ^c)	1.71	6.67 (2.67 ^{bc})	1.68	7.8 (2.89 ^d)
	Inorganic	11.0	0.78	6.29	0.85	4.58	0.81	7.2

		(3.39 ^{cd})		(2.60 ^c)		(2.25 ^{cd})		(2.79 ^d)
**Coffee	Natural	20.0 (4.52 ^b)	2.13	16.00 (4.06 ^a)	1.86	-	-	18.00 (4.30 ^b)
	Organic	15.0 (3.9 ^c)	1.79	12.63 (3.62 ^b)	1.75	7.18 (2.77 ^{bc})	1.58	11.63 (3.48 ^c)
	Inorganic	6.76 (2.69 ^e)	0.85	5.4 (2.42 ^{cd})	0.91	4.03 (2.12 ^{bc})	0.72	5.3 (2.43 ^d)
S.Em±		0.12		0.10		0.1		0.10
CD at 5%		0.38		0.31		0.30		0.33

Note: Figures in parentheses are $\sqrt{X+0.5}$ transformed values. Means followed by the same letter do not differ significantly by DMRT ($P = 0.05$)

H^o = Shannon – weiner diversity index

*Coconut plantation observed only in inorganic plantation. In hill zone non-availability of plantation with organic and natural farming practice.

** Coffee plantation observed only in organic and inorganic plantation. In central dry zone Non availability of plantation with natural farming practice

Great Britain Journal Press Membership

For Authors, subscribers, Boards and organizations



Great Britain Journals Press membership is an elite community of scholars, researchers, scientists, professionals and institutions associated with all the major disciplines. Great Britain memberships are for individuals, research institutions, and universities. Authors, subscribers, Editorial Board members, Advisory Board members, and organizations are all part of member network.

Read more and apply for membership here:
<https://journalspress.com/journals/membership>



For Authors



For Institutions



For Subscribers

Author Membership provide access to scientific innovation, next generation tools, access to conferences/seminars/symposiums/webinars, networking opportunities, and privileged benefits. Authors may submit research manuscript or paper without being an existing member of GBJP. Once a non-member author submits a research paper he/she becomes a part of "Provisional Author Membership".

Society flourish when two institutions "Come together." Organizations, research institutes, and universities can join GBJP Subscription membership or privileged "Fellow Membership" membership facilitating researchers to publish their work with us, become peer reviewers and join us on Advisory Board.

Subscribe to distinguished STM (scientific, technical, and medical) publisher. Subscription membership is available for individuals universities and institutions (print & online). Subscribers can access journals from our libraries, published in different formats like Printed Hardcopy, Interactive PDFs, EPUBs, eBooks, indexable documents and the author managed dynamic live web page articles, LaTeX, PDFs etc.



GO GREEN AND HELP
SAVE THE ENVIRONMENT

JOURNAL AVAILABLE IN

PRINTED VERSION, INTERACTIVE PDFS, EPUBS, EBOOKS, INDEXABLE DOCUMENTS AND THE AUTHOR MANAGED DYNAMIC LIVE WEB PAGE ARTICLES, LATEX, PDFS, RESTRUCTURED TEXT, TEXTILE, HTML, DOCBOOK, MEDIAWIKI MARKUP, TWIKI MARKUP, OPML, EMACS ORG-MODE & OTHER



SCAN TO KNOW MORE



support@journalspress.com
www.journalspress.com



*THIS JOURNAL SUPPORT AUGMENTED REALITY APPS AND SOFTWARES